Selective Catalytic Reduction of NO_x under Lean-Burn Conditions using Supported Metal Oxide Catalysts

A thesis submitted to the ***University of Pune***

for the award of

Doctor of Philosophy *in* ***Chemistry***

by

Neelam Jagtap

Under the guidance of

Dr. M. K. Dongare

Catalysis & Inorganic Chemistry Division

National Chemical Laboratory

Pune - 411 008, India

November, 2009

राष्ट्रीय रासायनिक प्रयोगशाला
(वैज्ञानिक तथा औद्योगिक अनुसंधान परिषद)
डॉ. होमी भाभा मार्ग पुणे - 411 008. भारत
NATIONAL CHEMICAL LABORATORY
(Council of Scientific & Industrial Research)
Dr. Homi Bhabha Road, Pune - 411 008. India.

Certificate of the Guide

Certified that the work incorporated in the thesis, ***"Selective Catalytic Reduction of NO_x under Lean-Burn Conditions using Supported Metal Oxide Catalysts"*** submitted by ***Neelam Jagtap,*** for the Degree of ***Doctor of Philosophy,*** was carried out by the candidate under my supervision in the Catalysis & Inorganic Chemistry Division, National Chemical Laboratory, Pune – 411 008, India. Such material as has been obtained from other sources has been duly acknowledged in the thesis.

(**Dr. M. K. Dongare**) Date:
Research Guide

Communication Channels
NCL Level DID : 2590
NCL Board No. : +91-20-25902000
EPABX : +91-20-25893300
+91-20-25893400
FAX
Director's Office : +91-20-25893355
COA's Office : +91-20-25893619
COS&P's Office : +91-20-25893008
WEBSITE
www.ncl-india.org

Declaration by the Candidate

I, hereby declare that the thesis entitled ***"Selective Catalytic Reduction of NO_x under Lean-Burn Conditions using Supported Metal Oxide Catalysts"*** submitted by me for the degree of ***Doctor of Philosophy*** to the ***University of Pune***, is the record of work carried out by me at ***Catalysis & Inorganic Chemistry Division, National Chemical Laboratory*** under the guidance of ***Dr. M. K. Dongare*** and has not formed the basis for the award of any degree or diploma to this or any other University. I further declare that the material obtained from other sources has been duly acknowledged in the thesis.

(Neelam Jagtap) Date:

Signature of the Candidate

dedicated to my mom.....

the best mother a daughter could have…

Acknowledgements

Several people have been instrumental in the completion of this thesis work & I take this opportunity to express my gratitude towards them.

It gives me immense pleasure to sincerely acknowledge my research guide ***Dr. M.K. Dongare*** *for his invaluable guidance and support given throughout the course of this investigation. Where others see obstacles he sees opportunities, and where others see failure he sees potential. His constant encouragement and insight have led to the successful completion of this work. He will always continue to be an inspiring influence for the rest of my life.*

I take this opportunity to express my deepest sense of gratitude and indebtedness to ***Dr. S.B. Umbarkar*** *for her guidance and suggestions throughout my research work. Without her patience and moral support it would have been difficult for me to complete this work. Her friendly nature ensured that I never felt any hesitations in approaching her for scientific discussions. I shall remain grateful to her forever.*

I extend my thanks to Dr. Veda Ramaswamy, Dr. C.V.V. Satyanarayana, Dr. C.S. Gopinath, Dr. T. Raja, Dr. A.V. Ramaswamy and all other scientific & non-scientific staff of Catalysis Division, National Chemical Laboratory, Pune for the help they rendered during my tenure as a research student.

I would like to extend a very special thank you to three individuals, Mr. Madhu from the Catalysis Division, Mr. S.B. Kale from the Glass Blowing Section and Mr. Prashant Mane from Organic Chemistry Division for helping me in their own ways during my stay at N.C.L.

My sincere thanks to Dr. S. Sivaram, Director, National Chemical Laboratory, Pune for providing the infrastructure to carry out the research work and utilize the facilities.

The financial assistance in the form of Senior Research Fellow from Council of Scientific & Industrial Research, New Delhi, is duly acknowledged.

Special thanks to my postgraduate teacher Dr. (Mrs.) R. Kashalkar who introduced me to the field of research. Without her initiative all this would not have happened.

I attribute very little of my success to myself, because it is the people around me who give me the ability to do what I do.

I take this opportunity to thank my friends in the laboratory, Rajni and Trupti, for their cheerful co-operation and affection. I will cherish the happy moments we shared together for a long time to come. I also thank Rokhsareh, Samadhan, Swati, Tejas and Vaibhav for their co-operation and help.

It is a pleasure to thank Vijayaraj, M. Sankar, Selvakannan, Thiru for their timely assistance and friendly support.

I owe my deepest gratitude to my mom & dad, for their unfailing love that has helped me throughout my life. I will always be indebted to them for their understanding attitude, even when I spent endless hours in the lab. Dad, thank you for the constant faith that you have shown in me. Mom, you have been my constant source of inspiration. Nothing makes me more driven than you to say that you are proud of me.

I have no words to express my gratitude to my brothers Hemant & Girish, who are my source of strength. Thanks a lot for being so understanding & supportive throughout the course of this thesis period. Their unstinted love & support is warmly acknowledged.

I take this opportunity to thank Romi, who has been more of a friend than a sister-in-law and for bringing Tanishka in our lives, who has been a constant source of happiness ever since she has arrived.

I express my sincere thanks to my in-laws for their love, support and understanding in the last one year without which the completion of the thesis would not have been possible.

And then, I thank the Almighty for giving me the strength and fortitude it took to complete this project. Without His blessings none of this would have been possible.

Finally, I thank Murugan for being my best friend and worst critic for all these years and for being there for me in times of need. This thesis is as much your accomplishment as it is mine.

Neelam Jagtap

Contents

Chapter 1:	**Introduction**		**1**
1.1	Introduction to Catalysis		**2**
1.2	Origin and types of nitrogen oxides (NO_x)		**6**
	a)	Thermal NO_x	**7**
	b)	Fuel NO_x	**7**
	c)	Prompt NO_x	**8**
1.3	Effects of NO_x on public health and environment		**8**
1.4	Emission Legislation Norms		**9**
1.5	Emission Control Strategies		**11**
1.6	NO_x emission and its control from automobile engines		**12**
1.7	Lean-NO_x control technologies		**16**
1.7.1	Direct NO decomposition		**16**
1.7.2	NO_x storage Reduction (NSR)		**17**
1.7.3	Selective Catalytic Reduction of NO_x		**21**
	a)	With NH_3/urea as reductant	**21**
	b)	With hydrocarbons as reductants	**24**
	i)	Zeolite based catalysts	**24**
	ii)	Platinum group metal catalysts	**26**
	iii)	Base Metal Oxide catalyst	**27**
1.8	Scope and objectives of the thesis		**29**
1.8.1	Thesis outline		**29**
1.9	References		**32**
Chapter 2:	**Support Modification to Improve the Sulphur Tolerance of Ag/Al_2O_3 for SCR of NO_x with Propene under Lean-Burn Conditions**		**38**
2.1	Introduction		**39**
2.2	Experimental section		**41**
2.2.1	Catalyst Preparation		**41**
2.2.2	Characterization		**42**
	a)	Powder X-ray diffraction studies	**42**
	b)	Nitrogen adsorption studies	**42**

		c) EDAX analysis	**42**
		d) FT-IR of adsorbed pyridine	**42**
		e) FT-IR	**43**
		f) In-situ Diffuse Reflectance FT-IR Studies (DRIFTS)	**43**
	2.2.3	Catalytic Activity Tests	**43**
2.3		Results and Discussion	**44**
	2.3.1	Structural and Textural properties	**44**
	2.3.2	Pyridine adsorption study	**45**
	2.3.3	Catalytic activity	**48**
		a) Influence of addition of SiO_2 and TiO_2 to AgAl on the catalytic activity	**48**
		b) Influence of addition of SO_2 on the catalytic activity	**50**
		c) Influence of water addition	**51**
		d) FT-IR study of spent catalysts	**55**
		e) In-situ DRIFTS study	**56**
2.4		Conclusions	**62**
2.5		References	**63**
Chapter 3:		**Effect of Magnesia Modification on the Low Temperature Catalytic Activity and Sulphur Tolerance of Ag/Al_2O_3 System**	**65**
3.1		Introduction	**66**
3.2		Experimental Section	**68**
	3.2.1	Materials	**68**
	3.2.2	Catalyst preparation	**68**
	3.2.3	Catalyst characterization	**68**
		a) Powder X-ray diffraction studies	**68**
		b) Nitrogen adsorption studies	**69**
		c) NH_3 temperature programmed desorption (TPD) studies	**69**
		d) In situ Diffuse Reflectance FT-IR studies (DRIFTS)	**69**
	3.2.4	Catalytic activity measurement	**69**
3.3		Results and Discussion	**70**
	3.3.1	Structural and Textural properties	**70**
	3.3.2	NH_3 TPD studies	**72**

3.3.3 Catalytic activity study **72**

a) Catalytic performance of AgMgAl in the absence of SO_2 **72**

b) Catalytic performance of AgAl and Ag7MgAl in the presence of SO_2 **77**

3.3.4 In situ DRIFTS study **78**

3.4 Conclusions **82**

3.5 References **84**

Chapter 4: NO Reduction under Diesel Exhaust Conditions over Au/Al_2O_3 **86**

4.1 Introduction **87**

4.2 Experimental Section **88**

4.2.1 Catalyst Preparation **88**

4.2.2 Catalytic activity measurements **88**

4.2.3 Catalysts characterization **89**

4.3 Results and Discussion **89**

4.3.1 HC-SCR of NO over 1 wt% Au/Al_2O_3 and 2 wt% Ag/Al_2O_3 **89**

4.3.2 In-situ Infrared studies **92**

a) Infrared spectra over Au/Al_2O_3 under $NO+CO+C_3H_6+O_2$ **92**

b) Effect of addition of decane **92**

c) Effect of addition of hydrogen and decane **94**

4.3.3 Ex-situ XPS measurements **99**

4.4 Conclusions **103**

4.5 References **104**

Chapter 5: Summary and Conclusions **106**

List of publications **111**

Presentations **112**

Chapter 1: Introduction

General review and literature survey

Chapter 1: Introduction

1.1. Introduction to Catalysis

Catalysis is a tremendously challenging and highly multidisciplinary field which can be defined as a "science of accelerating a chemical reaction for converting desired raw materials to desired products using a substance which participates in the reaction but is not consumed in the process." The substance that speeds up the chemical reaction is termed as a *catalyst* which can be recovered and recycled and is of immense importance in the field of chemistry and biology. Catalysts have become so well known because of their wider applications that even a common man is using this terminology in day-to-day life for many other phenomenon of accelerating the process. One example is that of an automotive catalytic converter, which represents a very successful application of catalysis for the removal of pollutant gases from automobile exhausts. The word catalysis came from two Greek words, the prefix, *cata* meaning down, and the verb *lysein* meaning to split or break. A catalyst accelerates a chemical reaction. It does so by forming bonds with the reacting molecules, and by allowing these to react to a product, which detaches from the catalyst, and leaves it unaltered such that it is available for the next reaction. Catalysis is a widely occurring process in nature. For example, living matter relies on enzymes which catalyze numerous biological transformations and involve complex and large molecular weight structures that are evolved in nature over millions of years to carry out particular reactions very selectively. Man-made catalysts are relatively simple. Historically important examples are the production of H_2SO_4 using V_2O_5 and the production of ammonia using iron-based catalysts [1]. The ammonia synthesis process using iron catalyst is considered as one of the most important discovery of the century as it changed the whole scenario in agricultural production and contributed in major way to solve the global food production problem. Research on the mode of operation and the synthesis of catalysts, including an improved understanding of thermodynamics due to the pioneering works of Ostwald and Van't Hoff, paved the way for a rational approach in developing more sophisticated and superior catalysts [2]. J. J. Berzelius defined a catalyst in 1836 as a compound, which increases the rate of a chemical reaction, but which is not consumed by the reaction. *'Many bodies have the property*

of exerting on other bodies an action which is very different from chemical affinity. By means of this action they produce decomposition in bodies and form new compounds into the composition of which they do not enter. This new power, hitherto unknown, is common both in organic and inorganic nature. I shall call it catalytic power. I shall also call catalysis the decomposition of bodies by this force' [3]. This definition allows for the possibility that small amounts of the catalyst are lost in the reaction or that the catalytic activity is slowly lost. However, the catalyst affects only the ***rate of the reaction***, it changes neither the thermodynamics of the reaction nor the equilibrium composition. Many years later in 1895 Ostwald came up with a definition "*A catalyst is a substance that changes the rate of a chemical reaction without itself appearing into the products*" according to which a catalyst could also slow down a reaction. Nowadays, the definition in use is "*A catalyst is a substance which increases the rate at which a chemical reaction approaches equilibrium without becoming itself permanently involved.*" The effect of the catalyst is purely kinetic; a catalyst offers an alternative path for the reaction which is energetically much more favorable than the uncatalyzed reaction (Figure 1.1).

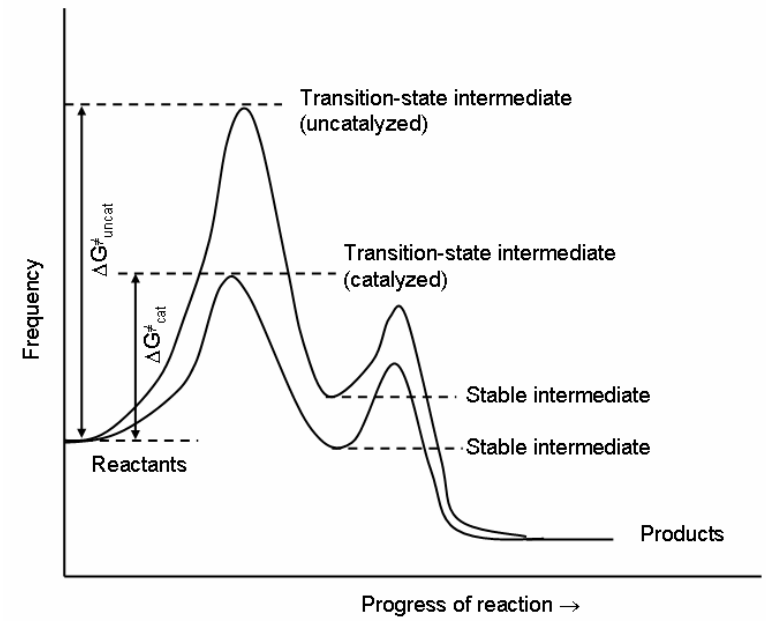

Figure 1.1 *Effect of the catalysts on a thermodynamically favorable reaction*

The basic principle of all catalysts is that they lower the activation energy by offering an alternative reaction path [4]. A catalyst decreases the activation energy of

a reaction ($\Delta G^{\neq}$ is lowered), thereby increasing the rate of the reaction, but has no effect on the chemical equilibrium of the reaction (ΔG remains the same). The action of a catalyst can be very specific, which under ideal conditions, results in selective formation of the desired product and avoids side reactions. Further advantages of the use of catalytic reagents are reduced time and energy requirements, which results in an overall process with increased environmental sustainability. A catalyst can be poisoned when another compound binds to it irreversibly or chemically alters it. This effectively destroys the usefulness of the catalyst. Catalysis plays a key role in production of such a wide variety of products, having applications in food, clothing, drugs, plastics, agrochemicals, detergents, fuels etc. [5]. In addition to these, it plays an ever-expanding role in the balance of ecology and environment by providing cleaner alternative routes for stoichiometric technologies [6], by conversion of polluting emissions to harmless streams. Thus the importance of catalysis to society is obviously based on its great economic impact in the production of broad range of commodity products that improve our standard of living and quality of life. Usually, catalysts are categorized depending on the physical form in which they are used.

There are mainly three types of catalysis processes: biocatalysis, homogeneous catalysis, and heterogeneous catalysis. In biocatalysis the catalyst is a biologically active molecule like enzyme. Enzymes are protein molecules, the structure of which results in a very shape-specific active site. Having shapes that are optimally suited to guide the reactant molecules in the optimum configuration for reaction, enzymes are highly specific and efficient catalysts. For example, the enzyme catalase catalyzes the decomposition of hydrogen peroxide into water and oxygen at an incredibly high rate of up to 10^7 hydrogen peroxide molecules per second [7].

$$2H_2O_2 \xrightarrow{Catalase} H_2O + O_2$$

In homogeneous catalysis, the catalyst and the reactants are in the same phase. Example of homogenous catalysis is the catalytic carbonylation of methanol to acetic acid by $[Rh(CO)_2I_2]^-$ complexes in solution [8].

$$CH_3OH + CO \longrightarrow CH_3COOH$$

In heterogeneous catalysis, the reactants, products and the catalysts are in different phases. The solids catalyze reactions of molecules in gas or solution. Commonly, the catalyst is a porous high surface area material supporting an active metal. These reactions usually occur at the surface of the catalyst. In heterogeneous processes, the catalytic sites are part of an insoluble inorganic solid or are distributed on the surface of an insoluble support like silica, alumina or carbon. To use the often-expensive materials (e.g. platinum, rhodium etc) in an economical way, catalysts are usually nanometer-sized particles supported on an inert, porous structure. Example of heterogeneous catalysis is the selective oxidation of ethylene to ethylene epoxide, an important intermediate towards ethylene glycol (antifreeze) and various polyethers and polyurethanes. The catalyst used is silver promoted by small amounts of chlorine, exhibiting a selectivity of 90% with about 10% of ethylene ending up as CO_2 [9]. Heterogeneous catalysts are considered to be the workhorses of the chemical and petrochemical industry. One of the advantages of heterogeneous catalysis is the easy separation of the catalyst from the reaction mixture. This allows easy purification of the product and facile reuse of the catalytic material. Hence, most of the industrial catalysts are heterogeneous in nature. It is estimated that 85-90% of all chemical processes are run catalytically, with a ratio of applications of heterogeneous to homogeneous catalysis of approximately 3:1 [10].

"Environmental catalysis" an upcoming sub-branch of catalysis has been recently defined as "*the development of catalysts to either decompose environmentally unacceptable compounds or provide alternative catalytic syntheses of important compounds without formation of environmentally unacceptable by-products."* Environmental catalysis encompasses the study of catalysts and catalytic reactions that impact the environment and provides an effective solution for the removal of various types of pollutants. The removal of NO_x, CO and unburnt hydrocarbons from the exhaust of gasoline internal combustion engines is one of the finest examples of application of environmental catalysis. The development of three-way catalysts (TWCs), which is being used over the past four decades and its success in the effective abatement of the above mentioned pollutants from the exhausts of gasoline engine is an example of remarkable achievement in the field of environmental catalysis. However, the present three way catalytic converter is not effective in removal of NO_x from automobile engine exhausts such as diesel engine or gasoline engine operating under lean burn condition (higher air: fuel ratio), which are

becoming more popular because of their higher fuel efficiency. The following sections give the details of the background and present status of the research and development work being carried out on NO_x abatement catalysis.

1.2. Origin and types of nitrogen oxides (NO_x)

Nitrogen oxides (NO_x) are simple molecules that are naturally present in the atmosphere. NO_x is a collective term used when referring to nitrogen oxides. Several nitrogen oxides exist and Table 1.1 lists these compounds with their general properties.

Table 1.1 *Oxides of nitrogen (NO_x)*

Name	**Properties**
Nitric oxide, NO	Colorless, odorless gas
Nitrogen dioxide, NO_2	Pungent, non-flammable, reddish brown gas
Nitrous oxide, N_2O	Colorless, slightly sweet odor
Nitrogen trioxide, N_2O_3	Unstable at room temperature
Nitrogen pentoxide, N_2O_5	Colorless solid

The natural sources of these oxides include nitrogen fixation by lightening, volcanic activity and microbial activity. The main oxides of nitrogen present in the atmosphere are nitric oxide (NO), nitrogen dioxide (NO_2) and nitrous oxide (N_2O). Nitrous oxide occurs in much smaller quantities than the other two, but it is a powerful greenhouse gas and exhibits a higher global warming power (300 times more) than CO_2. For a long time there was little concern about these nitrogen oxides. However, the levels of NO_x have now increased to an extent that they have become an extremely important family of air pollutants. The increase in NO_x emissions is mainly due to the significant rise in anthropogenic (human) activities. These are mainly formed due to the combustion of fossil fuels such as coal and petroleum in power plants and many industrial sites where thermal energy is produced, and also from the use of gasoline and diesel in automobiles [11].

At ambient temperatures, oxygen and nitrogen do not react with each other to form NO because the reaction has an extremely high activation energy.

$$N_2 + O_2 \longrightarrow 2NO \qquad \Delta H^o = 180.6 KJ/mol \qquad (1)$$

However, in an internal combustion engine, because of the high temperature the reaction between nitrogen and oxygen from air to yield nitrogen oxides is thermodynamically favored. Once formed, a part of NO reacts with air to form NO_2.

$$NO + \tfrac{1}{2}O_2 \longrightarrow NO_2 \qquad \Delta H^o = -113 KJ/mol \qquad (2)$$

NO_x emitted from engine exhaust typically consists of a mixture of 95% NO and 5% NO_2 [12]. There are three mechanisms of NO_x formation during the combustion process – *thermal, fuel and prompt* NO_x [13].

(a) Thermal NO_x

Formed by fixation of atmospheric nitrogen and its formation is thermodynamically favored by high flame temperature and atomic oxygen concentration [reaction (1)]. The formation of thermal NO_x occurs at 1300 K and takes place according to the mechanism established by Zeldovich [13] involving $N^{\bullet}$ and $O^{\bullet}$ radicals:

$$N_2 + O^{\bullet} \longrightarrow NO + N^{\bullet} \qquad (3)$$

$$N^{\bullet} + O_2 \longrightarrow NO + O^{\bullet} \qquad (4)$$

The rate of NO formation is essentially controlled by reaction (3) and increases exponentially with temperature. The Zeldovich mechanism dominates NO formation under most engine conditions [14]. The formation of thermal NO_x in an engine can be controlled by lowering the combustion temperature by operating the engine under excess air (fuel-lean) conditions but most of these approaches are not very effective [14].

(b) Fuel NO_x

Formed by oxidation of organic nitrogen (eg. pyridine, quinoline and amine type compounds) present in fuels such as coal and heavy oils. During the combustion process these nitrogen containing organics decompose into compounds such as HCN, NH_3 or free radicals such as $NH^{\bullet}$ and $CN^{\bullet}$. All of these compounds ultimately form

NO_x [15]. In contrast to thermal NO_x, fuel NO_x formation is relatively independent of temperature at normal combustion temperatures and is insensitive to the nature of the organic nitrogen compound [14]. The amount of fuel NO_x formed depends on the amount of nitrogen-containing compounds in the original fuel. For example, fuel oil contains 0.1% to 0.5% nitrogen while coal could contain up to 1.6% nitrogen. Nowadays, fuel NO_x formation is less significant because the nitrogen content in gasoline and diesel has fallen significantly over the last 10 years. Fuel NO_x concentration can be limited by decreasing the concentration of bound nitrogen in the fuel or by operating the burner in fuel-rich condition.

(c) Prompt NO_x

Formed by the reaction of hydrocarbon fragments with nitrogen radicals to form intermediates such as HCN and H_2CN. These intermediates can be further oxidized to NO in the lean zone of the flame. NO can further react with oxygen to form NO_2 or N_2O.

$$NO + \tfrac{1}{2}O_2 \longrightarrow NO_2 \qquad \Delta H^o = -113 KJ/mol \qquad (2)$$

$$2NO \longrightarrow N_2O + \tfrac{1}{2}O_2 \qquad \Delta H^o = -99 KJ/mol \qquad (5)$$

Prompt NO_x formation is proportional to the number of carbon atoms present per unit volume and is independent of the nature of the parent hydrocarbon. The quantity of HCN formed increases with the concentration of hydrocarbon radicals. Prompt NO_x can be formed in a significant quantity at low-temperature, fuel-rich conditions and where residence times are short. Prompt NO_x can be reduced by operating at lower temperatures and highly oxidizing combustion conditions.

1.3. Effects of NO_x on public health and environment

Nitrogen oxides emitted in atmosphere are considered to be a serious health hazard for humans and are known to have severe negative effect on the environment. Sustained levels of NO exposure cause detrimental effect on both physiological and pathological processes in humans. NO exposure over a period of time results in direct tissue toxicity and contribute to the vascular collapse associated with septic shock, whereas chronic expression of NO is associated with various carcinomas and

inflammatory conditions including juvenile diabetes, multiple sclerosis, arthritis and ulcerative colitis [16]. In significant concentrations, nitrogen dioxide is highly toxic causing severe lung damage with a delayed effect. NO_2 can severely irritate the mucous membrane. When in contact with body moisture, nitrous and nitric acids are formed and attack the walls of the alveoli in the lungs leading to respiratory problems. NO_2 can react with haemoglobin by forming meta- haemoglobin that causes several pathologies in children. Other health effects of too high NO_2 concentration in the air include shortness of breath and chest pains. Nitrogen oxides play an important role in the photochemistry of the troposphre and the stratosphre. Nitric oxide is easily oxidised to NO_2 by ozone or hydroperoxide radicals ($HOO^{\bullet}$).

$$NO + O_3 \longrightarrow NO_2 + O_2 \quad (6)$$

$$NO + HOO^{\bullet} \longrightarrow NO_2 + OH^{\bullet} \quad (7)$$

NO_2 can then react with hydroxy radicals to form nitric acid thus contributing to acidification [17].

$$NO_2 + OH^{\bullet} \longrightarrow HNO_3 \quad (8)$$

NO_x and volatile organic compounds react photochemically in the lower atmosphere to produce peroxyacetyl nitrate (PAN), peroxybenzoyl nitrate (PBN), and other trace oxidizing agents eventually leading to the formation of smog. For all these reasons, in the last few decades, the emission of NO_x in the atmosphere has been regulated in most of the countries worldwide by restrictive legislations.

1.4. Emission Legislation Norms

In view of the noxious effects of NO_x on human health and environment, emission legislation norms were introduced. The Kyoto Protocol is an international agreement linked to the United Nations Framework Convention on Climate Change. The major feature of the Kyoto Protocol is that it sets binding targets for 37 industrialized countries and the European community for reducing greenhouse gas (GHG) emissions. Recognizing that developed countries are principally responsible for the high levels of GHG emissions in the atmosphere as a result of more than 150

years of industrial activity, the Protocol places a heavier burden on developed nations for the reduction of GHG emissions [18]. In November 1999, another protocol, "The Gothenburg Protocol" was adapted to Abate Acidification, Eutrophication and Ground-level Ozone. The Protocol sets emission limitations for 2010 for four pollutants: sulphur, NO_x, VOCs and ammonia. It has been estimated that once the Protocol is implemented, Europe's sulphur emissions should be cut by at least 63%, NO_x emissions by 41%, VOC emissions by 40% and ammonia emissions by 17% compared to 1990. The Protocol also sets tight limit values for specific emission sources (e.g. combustion plant, electricity production, dry cleaning, cars and lorries) and requires best available techniques to be used to keep emissions down [19].

Emission regulations in Europe were formulated by the United Nations Economic Commission for Europe (UN-ECE). The European Union has been upgrading emission norms at an interval of 4-5 years. They have progressively tightened their emission norms from *pre-Euro* stages in the eighties to *Euro III* standards which are in place since the year 2000. European Union took up *Euro IV* norms in the year 2005 and the latest that have been implemented are the *Euro V* norms since September 2009. Based on European norms, India has adopted Bharat Stage Norms since the year 2000. Table 1.2 shows the emission standards for European countries whereas Table 1.3 and 1.4 show Bharat Stage norms for different kind of vehicles.

Table 1.2 *European Emission Norms and the year of implementation*

Emission standard	**CO (g/km)**		**HC (g/km)**		**NO_x (g/km)**		**PM (g/km)[a]**	
	Petrol	**Diesel**	**Petrol**	**Diesel**	**Petrol**	**Diesel**	**Petrol**	**Diesel**
Euro II (1996)	0.5	0.7/0.9	-	-	-		-	0.08-0.1
Euro III (2000)	-	0.56	0.2	-	0.15	0.5	-	0.05
Euro IV (2005)	-	0.3	0.1	-	0.08	0.25	-	0.025
Euro V (2009)	-	-	0.05	0.05	0.08	0.08	0.0025	0.0025

[a] Particulate matter

Table 1.3 *Emission norms for 2 and 3 wheelers in India [20]*

Vehicle	Pollutants	Year 2005	From 2008 but not later than 2010
		Bharat stage II (eq. Euro II) (g/km)	**Bharat stage III (eq. Euro III) (g/km)**
2-wheelers	CO	1.50	1.0
	HC + NO_x	1.50	1.0
3-wheelers (Petrol)	CO	2.25	1.25
	HC + NO_x	2.20	1.25
3-wheelers (Diesel)	CO	1.00	0.50
	HC + NO_x	0.85	0.50
	PM	0.10	0.50

Table 1.4 *Emission norms for 4 wheelers in India [20]*

Vehicle	Pollutants	Year 2005	From 2010[a]	From 2010[b]
		Bharat stage II (eq. Euro II) (g/km)	**Bharat stage III (eq. Euro III) (g/km)**	**Bharat stage IV (eq. Euro IV) (g/km)**
Cars (Petrol)	CO	2.2	2.3	1.0
	HC + NO_x	0.5	0.35	0.18
	PM	-	-	-
Cars (Diesel)	CO	1.0	0.64	0.50
	HC + NO_x	0.7	0.56	0.30
	PM	0.08	0.50	0.025

[a] Applicable in the Metros and major cities since April 2005.

[b] To be applicable in the Metros from April 2010 and applicable in Europe since 2005.

1.5. Emission Control Strategies

There are several techniques developed to control NO_x emissions. These can be classified in three categories: pre-combustion control techniques, combustion control techniques and post-combustion control techniques [13, 21, 22]. Pre-combustion control techniques involve removing nitrogen, which is organically bound in the fuel, through a hydrotreating process [23]. Combustion control technique is a primary treatment method for controlling NO_x emissions. In this method, efforts are

made to minimize the level of NO_x formed during the combustion process. Combustion control techniques involve modifying the combustion process and/or equipment to inhibit the formation of NO_x and this is usually achieved by lowering the combustion temperature (below 1573 K) to minimize the NO_x formation through atmospheric nitrogen fixation [13, 21]. As mentioned above, lower temperatures of flame limit the thermal NO_x formation. Injection of steam or water into the combustion chamber, flue-gas recirculation, low NO_x burners, use of low nitrogen fuels and catalytic combustion approaches are used in this method resulting in reduction of NO_x emissions. Precombustion procedures are not very expensive, but a drawback of these techniques is sometimes they enhance N_2O formation [24]. The main disadvantage of these methods is the low NO_x conversion (<50%) compared to post-combustion techniques (100%) [21, 23, 25]. On the other hand, post-combustion control techniques involve injection of chemicals in specific temperature windows, in presence or absence of catalysts, to convert NO_x to N_2. Post-combustion methods are secondary measures for the treatment of the flue gas already containing NO_x. According to the environment in which they are applied secondary methods for NO_x control can be separated in wet and dry methods. The wet methods or chemical scrubbing are chemical oxidation/absorption processes that are applied to small NO_x sources and have disadvantages such as high cost and waste generation in the form of dissolved nitrates and nitrites [21, 26]. The dry methods include catalytic and non-catalytic process. An example of non-catalytic methods is the selective non-catalytic reduction (SNCR), developed by Exxon [27]. It is a homogenous gas phase reduction process in which NO_x is selectively reduced by NH_3 to N_2. This process requires low capital investment however its operational temperature window (1123-1323 K) is very narrow and difficult to operate in larger facilities [13, 21, 22]. In comparison to the non-catalytic solutions, catalytic methods offer lower operating temperatures and are the primary method to control gas emissions.

1.6. NO_x emission and its control from automobile engines

The introduction of automobiles in the market offered unlimited flexibility and mobility to the general public. In the last 70 years the world vehicle fleet has increased from about 40 million vehicles to over 700 million; this figure is projected to increase to 920 million by the year 2010 [28]. However the use of automobiles has resulted in increased emission of various air pollutants like NO_x, CO and unburnt

hydrocarbons (HCs). The negative impact of these pollutants on the environment and health is well documented [29] and therefore air pollution generated from mobile sources is a problem of general interest. In general, the emissions from automobile engines depend on air/fuel ratio [30]. Air-fuel ratio (AFR) is the mass ratio of air to fuel present during combustion. When all the available oxygen is used to burn the fuel and all the fuel is burnt completely within a vehicle's combustion chamber, the mixture is chemically balanced and this AFR is called the stoichiometric mixture (Figure 1.2). For gasoline fuel, the stoichiometric air/fuel mixture is approximately 14.7 times the mass of air to fuel. Any mixture less than 14.7 is considered to be a rich mixture, any more than 14.7 is a lean mixture. When the engine is operated rich of stoichiometric, the CO and HC emissions are highest while the NO_x emissions are lowest. This is because complete burning of gasoline is prevented by the deficiency in O_2. The level of NO_x is reduced because the adiabatic flame temperature is reduced.

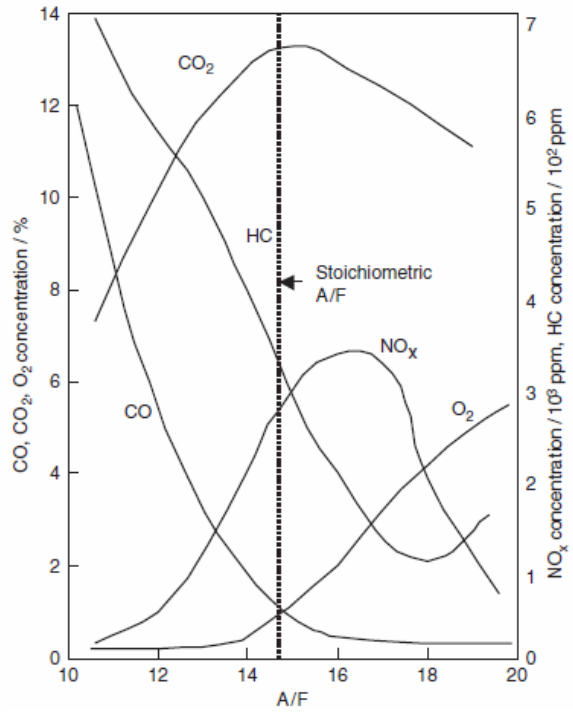

Figure 1.2 *Engine emissions as a function of air-to-fuel ratio*

Tuning of the engine to lean feed, the CO and HC are reduced because nearly complete combustion takes place. Again, the NO_x is reduced because the operating temperature is decreased. Just lean of stoichiometric operation, the NO_x is at maximum, since the adiabatic flame temperature is highest. At stoichiometric,

adiabatic flame temperature is lowered because of the heat of vaporization of the liquid fuel gasoline. Within the region of operation of the spark-ignited engine, a significant amount of NO_x, CO and HCs are emitted in the atmosphere. As discussed in section 1.3 NO_x and HCs undergo photochemical reactions in sunlight leading to the formation of smog and ozone whereas CO is a direct poison to humans.

The need to control these emissions was recognized as early as 1909 [31]. Emission controlling legislative norms was accordingly introduced in the U.S. in 1970 (Clean Air Act), in Europe (European Emission norms in 1992), in Japan and in India (Bharat Stage Norms) and these have become more stringent over the years. The problem of the emission of these pollutants from the exhaust gases of stoichiometric gasoline engines has been solved using the "three-way catalyst" (TWCs), which simultaneously convert NO_x, CO and HCs into N_2, CO_2 and H_2O. These perform three functions at a time and hence the name. The three-way catalysts are based on the platinum group metal (Pt, Pd and Rh) supported on high surface area γ-Al_2O_3 washcoated on a ceramic or metallic honeycomb. The γ-Al_2O_3 is sometimes stabilized with La_2O_3 or BaO. The reactions that take place on the TWCs are summarized in Table 1.5 [32]. Due to the higher price of Pt as compared to Pd, the former has been substituted by Pd and a Pd/Rh catalyst and been used for commercial automotive applications [33, 34]. Due to the increasing fuel cost and better fuel economy, lean-burn engines have become the main options for vehicles. Diesel engine and lean burn gasoline fuelled cars operate in large excess of oxygen, thus resulting in decreased fuel consumption.

Table 1.5 *Reactions occurring on the automotive exhaust catalysts*

Process	**Reaction**
Oxidation	$2CO + O_2 \rightarrow 2CO_2$
	$HC + O_2 \rightarrow CO_2 + H_2O$[a]
Reduction/three-way	$2CO + 2NO \rightarrow 2CO_2 + N_2$
	$HC + NO \rightarrow CO_2 + H_2O + N_2$[a]
	$2H_2 + 2NO \rightarrow 2H_2O + N_2$
WGS	$CO + H_2O \rightarrow CO_2 + H_2$
Steam reforming	$HC + H_2O \rightarrow CO_2 + H_2$[a]

[a] Unbalanced reaction.

The higher fuel efficiency of diesel engines as compared to spark-ignited engine can be explained on the basis of working of these engines. In spark-ignited engine, air and fuel are mixed before introduction in the cylinder. The air to fuel mixture is kept constant and the mixture is chosen to be stoichiometric, i.e., about 14.6 on an air-to-fuel weight basis [35]. A commonly used measure for the air-to-fuel ratio is the parameter λ, which is defined as the ratio of available air to air required for complete combustion. In the case of stoichiometric mixture, λ equals unity. The air-fuel mixture is compressed in the cylinder and ignited by a spark plug. The maximum compression ratio in spark-ignited engine is maintained at about 10 so as to avoid self-ignition of the gasoline-air mixture. In diesel engines, only the air is compressed. Just before the piston reaches its upper position, diesel is sprayed into the compressed air. The amount of fuel injected depends on the engine load. Since the amount of air in the cylinder is constant, λ varies much more than in spark-ignited engines, between 1.1 and 6. In diesel engines, ignition is not induced by a spark; compression of air in the cylinder results in a sharp temperature increase, causing self-ignition of the fuel. Therefore, the maximum cylinder pressure is not determined by the fuel properties but by material constraints, and a higher compression ratio can be used. The higher compression ratio, higher air-to-fuel ratio and the lack of "pumping losses" which occur in spark-ignited engines make diesel engines more fuel efficient than the spark-ignited engines. The optimum use of the fuel consequently results in lower emission of CO_2, CO and HCs. Unfortunately the TWCs which so effectively remove NO_x, CO and HCs from spark-ignited engines are ineffective for the removal of NO_x from the exhausts of lean-burn engines. The presence of large excess of oxygen entails that the concentration of CO and NO_x [2] is lower and therefore the reaction between CO and NO_x (see Table 1.5), essential in the three-way catalysis process, does not take place to the required extent. Thus, the removal of NO_x from the exhaust of lean-burn engines is a major challenge in environmental catalysis and lot of efforts have been taken in the last few decades both academically and industrially to develop lean NO_x technology. The following section discusses the various lean NO_x technologies used for the abatement of NO_x with a special emphasis on hydrocarbon selective catalytic reduction of NO_x.

1.7. Lean-NO_x control technologies

Along with the concern in the pollutants of NO_x, CO and HC, the care about the emission of CO_2 is also increasing. Lean burn engines, which emit less CO_2 as compared to their stoichiometric spark ignited gasoline counterparts, are becoming more popular. However, the three way catalysts are not capable of reducing NO_x from the exhaust of such engines. Therefore worldwide efforts have been taken to develop suitable catalysts for the reduction of NO_x under lean conditions. In the following section lean-NO_x technologies such as NO decomposition, NO_x Storage Reduction (NSR) and Selective Catalytic Reduction (SCR) with different reducing agents (NH_3/urea and hydrocarbons) are discussed.

1.7.1. Direct NO decomposition

This method is the simplest and most desirable because addition of a reducing agent is not required. In the catalytic decomposition, NO is directly decomposed into N_2 and O_2 according to the reaction,

$$NO \longrightarrow \tfrac{1}{2} N_2 + \tfrac{1}{2} O_2 \qquad (9)$$

The above reaction is thermodynamically favorable at temperatures below 1173 K but is kinetically limited because of the high activation energy of 364 kJ/mol in the absence of a catalyst [36]. Therefore, a catalyst is needed to lower the activation energy, which in turn would facilitate the reaction. Cu-ZSM-5 was reported to be the most active catalyst for the decomposition of NO_x. However its activity was seriously inhibited in the presence of excess O_2 because the active species Cu^+ is easily oxidized to Cu^{2+} in this environment. In addition, the presence of H_2O and SO_2, which are invariably present in the diesel exhausts, were found to poison the catalysts [37]. Therefore their use for the decomposition of NO_x from lean-burn engines is impractical. Perovskite-type oxides have also been investigated for this reaction and were for some time considered as potential candidates for NO decomposition [38, 39]. The advantages of these catalysts are their extreme thermal stability but unfortunately, the surface areas of these catalysts are low [40]. Ishihara *et al.* [41] investigated the NO decomposition activity over $LaMnO_3$ by substitution of La and Mn and found $La_{0.7}Ba_{0.3}Mn_{0.8}In_{0.2}O_3$ to be the most active catalyst. It was found that the substitution

of Mn with Cu in $La_{0.7}Ba_{0.3}Mn_{0.8}In_{0.2}O_3$ is effective for increasing NO decomposition activity. NO direct decomposition proceeds on the perovskite oxide of $La_{0.7}Ba_{0.3}Mn_{0.6}In_{0.2}Cu_{0.2}O_3$ under coexistence of O_2, H_2O, and SO_2 [42]. However these catalysts were found to be active only at high temperatures (1223 K), which make it difficult to apply under actual exhaust conditions. Goralski and Schneider [43] carried out free energy minimization calculations to determine the thermodynamic feasibility of NO_x decomposition catalyst in stoichiometric and lean gas mixtures over a range of temperatures and compositions. Although some interesting results were obtained, they concluded that lean-burn NO_x control for automobiles based on the idea of NO_x decomposition is not a feasible approach for practical application.

1.7.2. NO_x storage Reduction (NSR)

The NO_x storage reduction method (NSR) also referred to as NO_x adsorbers or lean NO_x traps (LNTs) was developed and commercialized by Toyato researchers in 1990 [44-48]. This method is regarded as one of the most promising solutions for the control of NO_x emission from lean-burn and light duty diesel engines. In this approach an additional reducing agent is not required to be added either. A typical NSR catalyst consists of precious metal as active site (e.g. platinum and rhodium), alkaline-earth metals or alkaline metals as NO_x storage site (usually barium oxide) and a high surface area support for highly dispersing these sites (e.g. alumina). The Pt-Ba/Al_2O_3 catalytic system is a representative of this class of catalyst. The key features of this approach are the presence of a NO_x storage compound (usually BaO which provide high NO_x storage capacity) and the use of cyclic changes in the feed composition from lean to rich conditions, but with the latter period being usually 50–100 times shorter than the lean period. The NO_x storing process over a Pt-Ba/Al_2O_3 catalyst is illustrated in reactions (10) and (11) and the NO_x release/reduction processes in reactions (12) and (13). Figure 1.3 illustrates the reaction mechanism of NO_x storage and reduction [49].

$$NO + O_2 \xrightarrow{Pt} NO_2 \quad (10)$$

$$NO_2 + BaO \longrightarrow Ba(NO_3)_2 \quad (11)$$

$$Ba(NO_3)_2 \xrightarrow{HC,CO,H_2} BaO + NO_x \quad (12)$$

$$BaO + NO_x \xrightarrow{HC,CO,H_2} N_2 + CO_2 + H_2O \quad (13)$$

In lean-burn conditions, where oxygen exists in high concentration in exhaust gases, NO_x is oxidized by oxygen to NO_2 over the platinum site and stored on the barium oxide as barium nitrate. When the engine is switched to rich burn condition the hydrocarbons, hydrogen and CO react with the stored NO_x to yield nitrogen, water and carbon dioxide. However because of its sulphur sensitivity, this technology has been commercialized only in Japan where low sulphur gasoline (10 ppm or less) is available. In fact, the major drawback of the NSR catalyst is its sensitivity to SO_x (SO_2 and SO_3) poisoning. In the presence of SO_x, the NO_x adsorption sites are occupied by sulphur species causing a decrease in the number of available sites for NO_x adsorption. Two types for the causes of sulfur poisoning of NSR catalysts [50] have been identified:

(i) SO_2 in the exhaust gas is oxidized on precious metals and then reacts with alumina to form aluminum sulfate ($Al_2(SO_4)_3$). $Al_2(SO_4)_3$ covers the surface of Al_2O_3 or plugs the micro-pores of Al_2O_3.

(ii) SO_x reacts with the NO_x storage components (BaO) to form barium sulfate ($BaSO_4$). Since the surface sulfates are thermally more stable and difficult to decompose compared to nitrates [51, 52], their gradual accumulation leads to the deactivation of the catalyst. As time passes, NO_x storage capacity gradually drops, and the catalyst loses activity.

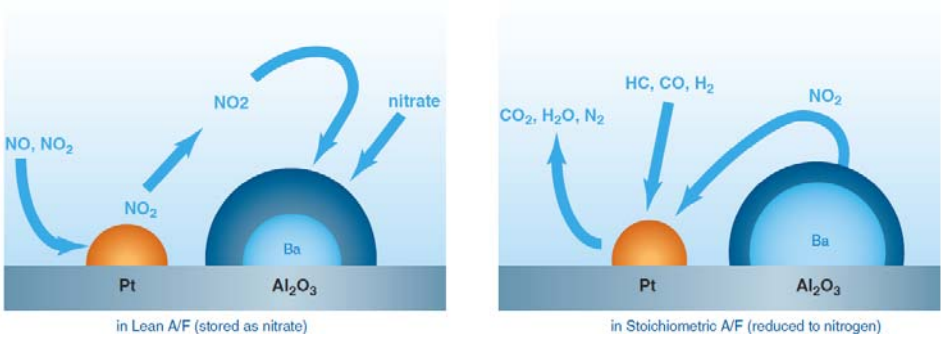

Figure 1.3 *Possible mechanism of NO_x storage and reduction over NSR catalyst*

It has been pointed out that the deactivation proceeds more rapidly when SO_2 is present under rich conditions than under lean conditions or continuous SO_2 exposure [53, 54]. It was suggested that sulfur is adsorbed on platinum sites during the

rich period, then oxidized to sulfate during the lean period. This sulfate is trapped in the vicinity of the platinum particles, blocking the sites that are important in the initial steps of NO_x storage. During the lean phase, the sulfates are formed throughout the catalyst and not specifically at the platinum sites, thus having less effect on the performance of the material. To improve SO_x durability of NSR catalyst, a variety of approaches had been tried, such as additives, supports and nature of substrates (monoliths-ceramic or metallic either hexagonal or cubic). The effect of the addition of transition metal elements to $Pt/Ba/Al_2O_3$ catalyst was investigated for improving SO_x durability [55, 56]. NO_x reducing activity of the catalyst was improved by some additives, and the highest activity was gained upon Fe-compound addition after aging test containing SO_2. However, the addition of a Cu-compound had a negative effect on the NSR catalysis. The effect of different Fe loading to $Pt/Ba/Al_2O_3$ system on SO_x desorption performance under oxidizing conditions was studied and it was found that the Fe-compound promotes the SO_2 desorption from the NSR catalyst. Addition of Fe inhibits the growth in size of $BaSO_4$ particles under oxidizing condition in the presence of SO_2 and facilitates the decomposition of $BaSO_4$ particles and the sulfur desorption when exposed to reducing conditions. Researchers working at Toyota have also addressed the problem of sulfur poisoning of NSR catalysts. The work includes the addition of TiO_2 to the support material to promote the decomposition of sulfate at the interface of the TiO_2 and Al_2O_3. The presence of TiO_2 suppresses the sulfate formation by the enhancement of sulfur desorption from the support without reducing the NO_x storage capacity significantly [57]. Duprez *et al* have also reported improvement in durability of the catalyst against sulfur poisoning after TiO_2 addition [58]. TiO_2 is an acidic material, and sulfates on TiO_2 are less stable than on alumina. Therefore, TiO_2 particle dispersed on the alumina-based catalyst promotes the decomposition and removal of sulfates under reducing condition. The SO_x desorption is facilitated more by smaller particle size of TiO_2, which could be dispersed highly in the catalyst. Recently, ZrO_2-TiO_2 (ZT) mixed oxide as a support for K-compounds was found to improve the NO_x removal activity [59]. A relative high ability for NO_x removal above 773 K was obtained with 60-80 wt% ZrO_2 content, particularly with 70%. The SO_2 aging studies on these catalysts showed that the catalyst with ZT70 retained the highest amount of active potassium which did not get sulphated nor formed a solid phase with the support material. The high activity was attributed to the acidity of support, which was confirmed by NH_3 temperature programmed desorption

(TPD) measurement. Another serious problem of NSR catalysts is its thermal deterioration. The formation of $Al_2(SO_4)_3$ and $BaSO_4$ species during the rich phase of the cycle leads to deactivation of the catalyst. In order to regain the activity, periodic regeneration at higher temperature of about 923 K are needed. This causes severe fuel penalty and lowers drivability of the car. The time required for this high-temperature treatment may be as long as 60–120s. Furthermore, H_2S forms as the main product of sulphate reduction. The high hydrothermal stability is required to avoid catalyst deactivation during this periodic treatment and during full load operations of engines. A main effect typically observed after severe hydrothermal treatment is a reduction in the activity of NO_x removal at low temperature. A good activity below 473 K is very important for overall catalytic converter performances, because the temperature of the emissions in typical procedures for checking auto-exhaust emissions is below 473 K for over 50–60% of the testing time. Also the high temperature treatment causes Pt sintering and formation of platinum oxide. As a result, fewer sites become available for NO and O_2 adsorption and the rate of catalytic steps such as NO oxidation decreases [60, 61]. Thermal aging also leads to the decrease of the surface area, which has a negative effect on the NO_x storage efficiency of the catalyst. However, the loss of barium-containing NO_x storage components after the high temperature treatment due to the reaction with Al_2O_3 imposes a more noticeable influence on the NO_x storage capacity [62, 63]. Imagawa *et al* [64] have reported improvement in the thermal durability of ZrO_2-TiO_2 supports by the addition of alumina. At high temperature, ZrO_2-TiO_2 particles agglomerate easily. As a result, the surface area of the ZrO_2-TiO_2 decreases, causing degradation of NSR activity. The addition of alumina to ZrO_2-TiO_2 leads to the formation of nano-level composite between alumina and ZrO_2-TiO_2, which resulted in the improvement of thermal durability of the ZrO_2-TiO_2 support. Addition of alumina inhibits the sintering of ZrO_2-TiO_2 particle in high temperature region as a result of which the NO_x storage amount of the alumina-zirconia-titania nano-composite was higher than that of the catalyst of ZrO_2-TiO_2 after SO_x aging test. Recent advances in the composition of these NSR catalysts are the introduction of titania nanoparticles and Rh/ZrO_2 components to improve the regeneration during the periodic high-temperature treatment in rich conditions [6, 10], but the question of resistance to deactivation by SO_2 and hydrothermal stability are not solved. It is thus necessary to develop new materials, which combine a very high

hydrothermal stability, a good activity at low temperature and a good resistance to deactivation by SO_2.

1.7.3. Selective Catalytic Reduction of NO_x

(a) With NH_3/urea as reductant

The selective catalytic reduction of nitrogen oxides with ammonia (NH_3-SCR) under lean conditions is a well established industrial catalytic technology since 1970s for the clean up of flue-gas from stationary sources [65, 66]. The special feature of this reaction is that a stoichiometric dosage of ammonia is sufficient for total NO_x conversion. This technology has also been applied for the reduction of NO_x from heavy-duty diesel vehicles by the substitution of ammonia with the less toxic urea [67, 68] in Europe. The basic reactions that take place on the catalyst with NH_3 as the reductant can be shown as:

Selective or desired reactions,

$$4NO + 4NH_3 + O_2 \longrightarrow 4N_2 + 6H_2O \quad (14)$$

$$2NO_2 + 4NH_3 + O_2 \longrightarrow 3N_2 + 6H_2O \quad (15)$$

A small fraction of the SO_2 produced, in the boiler by oxidation of sulphur in the fuel, is oxidized to SO_3 over the SCR catalyst. This causes problems of corrosion and deposit of ammonium sulphate [$(NH_4)_2SO_4$] and ammonium bisulphate (NH_4HSO_4).

Non selective reactions,

$$2SO_2 + O_2 \longrightarrow 2SO_3 \quad (16)$$

$$4NH_3 + 5O_2 \longrightarrow 4NO + 6H_2O \quad (17)$$

$$4NH_3 + 3O_2 \longrightarrow N_2 + 6H_2O \quad (18)$$

The commercial catalyst used in stationary sources is based on homogeneous mixtures of titanium dioxide, tungsten oxide (or molybdenum trioxide) and vanadium pentoxide supported on a monolith or wire screen plate [69, 70]. V_2O_5, WO_3 and MoO_3 are the active components. Anatase TiO_2 is used as high surface area carrier to

support the active components. Vanadia is responsible for the reduction of NO_x and also for the undesired oxidation of SO_2 to SO_3. Accordingly, the vanadia content is generally kept low and is below 1% (w/w) in high sulphur applications. WO_3 (or MoO_3) is employed in larger amounts (10 and 6% (w/w) for WO_3 and MoO_3, respectively); they act as "chemical" and "structural" promoters by enlarging the temperature window of the SCR reaction, limiting the oxidation of SO_2, and improving the mechanical, structural, and morphological properties of the catalysts. It has also been reported that WO_3 and MoO_3 make the catalyst more poison-resistant [71]. During a commercial SCR process over V_2O_5-WO_3-TiO_2 systems, the composition of the flue gas must be monitored permanently and the quantity of NH_3 reductant added must be tightly controlled to minimize slip into the exhaust stream. In general, SCR removes between 60 to 85% of NO_x using 0.6 to 0.9 mol NH_3 for 1 mol of NO_x and leaves 1 to 5 ppm of unreacted NH_3 (referred to as NH_3 slip- an undesired secondary emission since ammonia is an irritating and toxic gas and cannot be released in the exhaust line and therefore its emissions are also the object of regulations as NO_x). Among the particular advantages to use NH_3 as reducing agent is the high selectivity of NH_3 reaction with NO in the presence of oxygen and the promotional effect of oxygen on the kinetics of this reaction. However, the toxicity of vanadium and ammonia slip which result in the formation of $(NH_4)_2SO_4$ and NH_4HSO_4 leading to the plugging and corrosion of the SCR equipment are the major drawbacks of this technology. Other metal oxide catalysts studied for the NH_3-SCR reaction include metal-containing clays and layered materials [72-74] supported on active carbon [75] and micro- and meso- porous materials [76-78] but none of these have exhibited the long term stability (over 10 years) under practical conditions required for a commercial catalyst.

NH_3-SCR technology for high-duty diesel (HDD) vehicles has also been developed to the commercialization stage and is available in European market since 2001. For mobile source applications, the preferred reductant source is aqueous urea, which hydrolyses to produce ammonia in the exhaust stream according to the reaction:

$$CO(NH_2)_2 + H_2O \longrightarrow 2NH_3 + CO_2 \qquad (19)$$

Apart from the hydrolysis step, the SCR-urea process is similar to that of stationary sources. For the use of urea-SCR in diesel powered cars the catalyst must be active in the presence of excess of oxygen at very high space velocities (500,000 per hour), at low reaction temperatures (the temperature of the emissions in typical diesel cycles used in testing is in the range of 120 °C-200 °C for over 50% of the testing time) and should be resistant to poisons such as sulphur. Since TiO_2-supported V_2O_5, promoted with WO_3 used in NH_3-SCR fulfill these requirements, the same have been used since 2005 for HD diesel vehicles in Europe. However, the operating conditions in a mobile diesel engine (such as heavy duty trucks or passenger cars) are very different than those in stationary sources. Engine load and speed vary often and abruptly, which directly changes the volumetric flow and temperature of the exhaust gas as well as the NO_x emissions. Therefore the SCR system for vehicle applications would require precise calibration of the amount of urea injected as a function of the quantity of NO_x emitted by the engine, exhaust temperature and catalyst characteristics. Industrial liquid urea, known as "Adblue" is an aqueous solution of 32.5 wt% urea solution. Adblue is corrosive and requires stable materials for the components like tank, pipes, injector etc. Another characteristic of this solution is its proneness to crystallization and polymerization. When parts of the exhaust system are constantly welted by Adblue on the same spot, undesired urea crystals or polymers may form if the exhaust line temperature is lower than 573 K. This phenomenon will result in uncontrolled ammonia production when the crystals or polymers melt or sublime after being heated at significantly higher temperatures (T > 623 K). This may result in ammonia release. To overcome all these problems a sophisticated system is required for the use of urea-SCR which would consist of a control unit to monitor the quantity of urea injected, a tank to store the Adblue solution, an urea injector to atomize the Adblue, a mixing device to ensure homogenous distribution of NH_3 in the exhaust gas at the SCR catalyst inlet, a hydrolysis catalyst to improve the urea conversion to NH_3, the SCR catalyst for NO_x conversion, a oxidation catalyst to prevent NH_3 release in the exhaust line and a NO_x sensor to control the NH_3 quantities injected and to allow diagnosis of the NH_3-SCR system. Moreover this whole system must be located under the vehicle floor, in the exhaust line for architecture purpose, since there is no other place for this large set-up to fit. Furthermore, the transportation and storage of ammonia is not very cost-effective. So, although urea-SCR has been used in heavy-duty vehicles with limited success, its use in diesel powered passenger

cars or light-duty vehicles is not practical due to the complications of maintaining an on-board source of ammonia. That is why a powerful stimulus for research is the discovery that SCR can be carried out using hydrocarbons as reducing agents.

(b) With hydrocarbons as reductants

The conventional three-way catalyst (TWC) is very effective in the removal of NO_x from gasoline engines, but diesel engines exhaust gas contains a large excess of oxygen and under these conditions the three-way catalysts are ineffective. A solution is represented by the reduction of NO_x with urea as discussed in the above section, but some technical issues arise due to handling of a storage tank onboard and the difficult control of the amount of urea added to the exhaust gas, depending on the working conditions of the engine [13]. A typical composition of the exhaust emitted from lean-burn engines contains about 0.05% NO_x, 5%–10% O_2, 10% H_2O, and 0.05%–0.1% unburnt hydrocarbons [79]. Hydrocarbon SCR (HC-SCR) exploits this unburned hydrocarbons contained in the exhaust gas combined with the addition of extra diesel fuel. Thus this method is a more suitable solution for cars and trucks and has subsequently attracted the most attention. To date, many kinds of catalysts, including zeolite, noble metals and metal oxides have been investigated for HC-SCR. This section gives a summary of the various catalytic formulations used for this reaction.

(i) Zeolite based catalysts

Quite a few zeolite based catalysts have been reported for lean-NO_x reduction by the HC-SCR process. Among those reported in the literature, Cu/ZSM-5 zeolite is probably the most studied catalyst for high temperature applications, whereas Pt/ZSM-5 is for low temperature applications. In most lean-NO_x catalysts, zeolites are used as catalyst support on which the active metals are ion exchanged. Among many different zeolites, the ZSM-5 zeolites with high silica content have been preferentially used for lean-NO_x catalysts. Cu-ZSM-5 was the first catalyst reported by Held *et al*. [80] and Iwamoto *et al*. [81, 82] to show good catalytic activity for the reduction of NO under lean conditions by a variety of hydrocarbons including C_2H_4, C_3H_6 and C_3H_8. The temperature at which highest NO reduction is obtained depends on the type of reductant used. Over Cu-ZSM-5, for example, maxima in activity were reported at 523, 598 and 573 K for C_2H_4, C_3H_6 and C_3H_8 respectively [81, 83-85]. The rate of the NO reduction reaction goes through a maximum with temperature and above the

optimum temperature the loss in activity is observed due to the unselective oxidation of hydrocarbon with O_2. The overall activity of Cu-ZSM-5 was also found to depend on the exchange level of copper [83, 84]. The catalytic activity increased with the extent of Cu exchange, reached a maximum at an exchange level of 80-100%, and then decreased slightly at higher levels. The major drawback of Cu/ZSM-5 based catalysts is their poor activity in the presence of water. The deactivation is attributed to the redistribution of Cu species in the zeolitic structure, high dispersion of Cu ions in Al_2O_3 leading to the formation of inactive CuO aggregates on the external surface of the zeolite crystallites [85] and the formation of a $CuAl_2O_4$ compound [86]. Hydrothermal de-alumination of the zeolite framework has been a major issue in the deactivation of the catalyst. It appears that deactivation is mainly caused by migration of Cu^{2+} ions to locations inside ZSM-5 where their reduction to Cu^{1+} is more difficult and also to the decrease in the number of bridging hydroxyls (zeolitic Brönsted acid sites), which are required for the activation of hydrocarbons [87]. A substantial enhancement in the $DeNO_x$ SCR activity of Cu-ZSM-5 catalyst in the presence of water has been reported by Argonne National Laboratory [88, 89]. The Cu-exchanged ZSM-5 zeolite crystals were coated with fine CeO_2 nanoparticles by ion-exchange method. The addition of CeO_2 promoted the reducibility of Cu ions and also increased the resistance for destruction of the zeolite structure. In addition the coating of the catalyst lowers the maximum activity temperature range by about 423 K of the HC-SCR reaction compared to the metal-zeolite only. In continuation of the same work, the CeO_2 coated Cu-ZSM-5 catalyst was impregnated with small amount of Rh and tested for the selective catalytic reduction of NO with C_3H_6 in the presence/absence of 10% H_2O and 50 ppm SO_2 [90]. Under dry conditions, addition of CeO_2 decreased the maximum NO conversion as compared to the CeO_2 free Cu-ZSM-5 catalyst but shifted the whole temperature window by about 373 K to lower temperatures especially at lower space velocities. Addition of water in the feed had no inhibiting effect on the NO_x reduction activity. However in the presence of 50 ppm SO_2 the beneficial effect of CeO_2 coating was nullified at lower reaction temperature and higher space velocities. Besides Cu-ZSM-5 a variety of different ions have been exchanged in zeolites [91, 92] and tested for the SCR of NO_x under lean conditions. Pt- exchanged zeolites have been tested with C_2H_4 as the reductant and it was found that the Pt-containing catalyst was more active at temperatures below 573 K and exhibited better thermal stability than corresponding Cu-containing one [93].

However these are found to be less selective to N_2 and a substantial amount of N_2O production was seen on these catalysts. Besides the nature and amount of exchanged metal, the framework type and the Si/Al ratio also affected the catalytic property. Accordingly zeolites with different framework types such as ZSM-5, Y type and ferrierite (FER) have been investigated in the SCR of NO_x. Li and Armor [94, 95] compared a number of Co-exchanged zeolites using methane as the reducing agent and found Co-ZSM-5 to be the most active one. Co-Y showed the poorest catalyst activity for this reaction although it had a two to three-fold higher cobalt exchange capacity than the other zeolites studied. This same group later reported [96] that a Co-exchanged ferrierite (Si/Al = 8) showed a two-fold increase in activity compared to Co-ZSM-5. In agreement, Hall *et al*. [97] also observed the ability of Co-ferrierite to effectively activate CH, as a selective NO reductant, and reported higher NO reduction rates over this catalyst when methane was compared with isobutene. Many other zeolite systems containing palladium, gallium, indium, cerium, silver, nickel, manganese, rhodium and H-form zeolites have been evaluated for the reduction of nitrogen monoxide [98, 99]. Although, metal exchanged zeolites are active catalysts for the selective reduction of NO by hydrocarbons in the presence of excess O_2, a review of the papers on this topic showed that there are major limitations for its utilization for commercial applications, mainly due to the limited temperature range of catalytic activity, inhibiting effect of water, its low hydrothermal stability, and reported vulnerability to poisoning by SO_2 under realistic exhaust compositions. In conclusion, if zeolite based catalysts are to be used in automotive application their hydrothermal resistance along with their resistance to poisons such as SO_2 must be dramatically increased. Thus, the search for better lean-NO_x catalysts, which requires both more stable supports and more active catalytic material continues.

(ii) Platinum group metal catalysts

The selective catalytic reduction with hydrocarbons is a promising method for the removal of NO_x from the exhaust of lean-burn engines. Zeolite based catalysts have the disadvantage of insufficient hydrothermal stability whereas the base metal catalysts such as copper and nickel do not have good thermal durability and these are sensitive to poisoning by SO_2 [100, 101]. Supported noble metals catalysts, in particular platinum group metals (PGM), were found to be very active in the reduction of NO_x in presence of excess of O_2 and initially extensive work was carried out on

ruthenium and iridium. However the oxides of these metals are very volatile at high temperatures, which eventually led to metal loss, and therefore could not be used in automotive catalysts [102, 103]. However platinum, palladium and rhodium showed good activity at relatively low temperatures (lower than 573 K) [104], more resistance to poisoning against SO_2 [105], and higher tolerance towards steam [106] compared to the metal oxide catalysts. This low temperature activity characteristic is of critical importance, since a major percentage of the automotive exhaust emissions is released during the initial heating period of the engine ('cold start' problem). The role of Pt and Pd is to oxidize CO and HCs whereas that of Rh is to reduce NO_x. Amongst the three noble metals, platinum is the most active at low temperatures and therefore widely studied. The performance of supported platinum catalysts depends on several factors such as the amount of metal loading and dispersion [107, 108], nature of the support [109, 110], method of catalyst preparation [111], nature of hydrocarbon used as reductant [112], presence of promoters [113], combination with other catalytic materials [114], etc. The support seems to play an important role in the reaction mechanism via hydrocarbon activation. This effect is more pronounced when using olefins rather than saturated hydrocarbons as reducing agents [105, 114]. However, Pt-based catalysts are characterized by low selectivity towards N_2 (substantial amount of N_2O is formed) and narrow temperature window of operation [12, 25]. Although Rh catalysts show higher selectivity towards N_2, the drawback is that their activity decreases significantly for higher oxygen feed concentrations and these require higher operating temperatures compared to Pt [110].

(iii) Base Metal Oxide catalyst

Numerous catalytic formulations, as discussed above, have been tested since the discovery of HC-SCR for the catalytic reduction of NO_x under lean conditions. Although transition metal containing zeolites show high activity these suffer from poor hydrothermal stability. On the other hand, supported noble metals, especially Pt/Al_2O_3 exhibit high activity at low temperatures and enhanced resistance to SO_2 and water vapor but these are active only in a narrow temperature range and exhibit low selectivity for N_2. In this context, base metal oxide catalysts have shown considerable promise since these too show high activity and moderate tolerance to SO_x and water vapor, especially at higher temperatures. Many base oxides/metals (e.g. Al_2O_3, TiO_2, ZrO_2, MgO and these oxides promoted by, e.g. Co, Ni, Cu, Fe, Sn, Ga, In, Ag,) have

been reported to be active catalysts for HC-SCR [115-117]. Amongst these, Ag/Al_2O_3 is thought to be the most promising candidate for practical use and hence have received wide attention. The effect of amount of Ag loading (1–10 wt%) on the catalytic performance was tested [118-121] and it was found that optimum silver loading was in between 1-3 wt% [122-125] whereas increased metal loading resulted in lower selectivity due to the fact that metallic Ag species favors propene oxidation, thus, decreasing its selectivity for NO_x reduction [120]. Besides limited activity, catalysts with higher Ag loadings were found to produce significant amounts of N_2O [119, 121, 123, 126, 127]. In a review on SCR of NO_x with hydrocarbons it is suggested that different Ag loadings result in different catalytic phases, which are related to different reaction pathways [126]. Mechanistic studies have proved that NO decomposition-type mechanism takes place on the high loading material [126] whereas in the case of low loading Ag/Al_2O_3, NO_2 formation and its subsequent reduction to form N_2 was proposed for the NO reduction over the Ag^+ phase. Another important parameter for SCR of NO_x with hydrocarbons over Ag-based catalysts is the type of reductant. Various reductants have been tested including alkanes, alkenes [126, 128] and several oxygenates [120]. In practice, academic studies have focused on the use of C_2-C_3 alkenes and alkanes as reductants [116], as these molecules are found in car exhaust gases and usually give high conversions of NO_x in the presence of excess of O_2. When oxygenated hydrocarbons, such as ethanol, 2-propanol and acetone are used instead of propene, high NO_x conversions (95–100%) are observed at significantly lower temperatures (573 K) [119, 120]. However, depending on the temperature, substantial amounts of several by-products such as N_2O, HCN, NH_3, CH_3CN are formed, which in terms of health danger are much less desirable than nitrogen oxide [119, 120, 129]. Thus, oxygen-containing hydrocarbon species are not considered viable reductants with silver, until selectivity to N_2 is improved. Although Ag/Al_2O_3 catalytic system has shown promising activity in the NO_x reduction it still has major drawbacks that need to be addressed. The main drawback of this system is the poor SO_x resistance (at lower temperatures) and narrow temperature window at which high NO_x conversion is achieved. The influence of SO_2 on the catalytic activity has been investigated in details and mechanistic studies have proven that the deactivation is caused due to the formation of silver and alumina sulphate species [126 and references therein]. Another drawback of this system is low activity in the low temperature range (423-573 K), which is typical of lean-burn engine exhausts.

However, an added impetus to this area of research is the discovery that addition of small amount of H_2 to the HC-SCR feed over Ag/γ-alumina catalysts improves the NO_x reduction at lower temperature (hydrogen effect) [130 and references therein], which has further attracted the researcher working on this system for exploiting the potential of this catalyst for commercial applications.

1.8. Scope and objectives of the thesis

Since Ag/Al_2O_3 has shown potential for its utility for SCR of NO_x using hydrocarbon as reductant, there is a scope for improvement in the catalytic activity of this catalyst particularly, its sulfur tolerance and hydrothermal stability. Therefore the objective of the present thesis was to improve the performance of this catalyst for SCR of NO_x using hydrocarbons at lower temperature, improve its sulfur tolerance and hydrothermal stability. To achieve this objective we have modified the alumina support by doping with Si and Ti as well as for sulfur tolerance as well as the nature of basic alumina support is changed by incorporation of MgO in the structure. By modifying the alumina support the sulfur tolerance has been considerably improved as well as the low temperature activity also been also increased showing the potential of this catalyst composition for SCR of NO_x under lean condition. The effect of these dopings and MgO additions have been characterized by various techniques and mechanistic aspects of these improvements have been also investigated by *in-situ* FTIR study to follow the reaction pathways. Similarly Au/Al_2O_3 catalyst system also has been investigated in detail for SCR of NO_x under lean condition and this catalyst system also showed promising results. However the mechanistic aspects of this catalyst studied using *in-situ* FTIR showed slightly different behavior than Ag/Al_2O_3.

1.8.1. Thesis outline

This section gives the chapter wise distribution of the work done during the Ph.D. tenure.

Chapter 1: An overall perspective of the origin and types of nitrogen oxides, its effect on the public health and environment, the various emission control strategies and NO_x emission control from automobiles have been discussed in this chapter. The different lean technologies used for the abatement of NO_x (catalytic decomposition of NO_x, NO_x storage reduction and selective catalytic reduction of NO_x using

NH_3/urea/hydrocarbon as reductants) have been discussed. The use of "three-way catalysts" in stoichiometric engines and their ineffectiveness in the reduction of NO_x in gasoline and diesel engines, which work under lean-burn conditions, have been mentioned. Finally the objective of the present work undertaken with the emphasis on the selective catalytic reduction of NO with hydrocarbons as reductant is mentioned.

Chapter 2: This chapter describes the synthesis of Ag/Al_2O_3 catalyst and its support modification to improve the sulfur tolerance in the selective catalytic reduction (SCR) of NO with propene as the reductant under lean-burn conditions. The catalysts were tested for the SCR of NO and SO_2 tolerance in the presence/absence of water in the feed. The catalysts were characterized by different physico-chemical techniques before and after the reaction. Mechanistic studies were carried out to study the deactivation phenomenon caused by the presence of SO_2 in the reaction feed mixture.

Chapter 3: In this chapter the effect of Mg addition on the catalytic activity and SO_2 tolerance of Ag/Al_2O_3 system for C_3H_6 SCR has been studied. A series of Ag-Mg/Al_2O_3 catalysts were prepared by impregnation method with 2% Ag loading. The Mg content was varied from 5.5 wt% to 17 wt%. These samples were tested for the selective catalytic reduction of NO with propene in the presence of excess oxygen under dry conditions. The sample with best activity was tested for sulfur tolerance under dry conditions in the presence of 20 ppm SO_2. *In-situ* DRIFTS experiments were carried out to study the mechanism of deactivation of the catalysts in the presence of SO_2.

Chapter 4: In this chapter, results of SCR of NO by hydrocarbon using 1% Au/Al_2O_3 will be presented. The gold supported on alumina (1 wt%) was prepared by urea deposition precipitation method and compared with silver supported on alumina (2 wt% Ag) for the selective catalytic reduction of NO by hydrocarbons under diesel exhausts conditions. The reaction feed consisted of 300 ppm NO, 300 ppm CO, 300 ppm C_3H_6, 100 ppm $C_{10}H_{22}$, 2000 ppm H_2 (when present), 10% O_2, 10% CO_2, 5% H_2O and balance He. The effect of addition of H_2 to the feed on the catalytic activity as a function of temperature was also studied. Infrared experiments were carried out to study the various adsorbed species formed on the catalyst surface in the presence/absence of H_2.

Chapter 5: This chapter presents the summary and conclusions of the thesis work.

1.9. References

1. H. D. Gesser, *Applied Chemistry: A textbook for Engineers and Technologists,* Kluwer Academic/Plenum Publishers, New York.
2. R. A. van Santen, P. W. N. M. van Leeuwen, J. A. Moulijn, B. A. Averill, *Catalysis: An Integrated Approach, 2nd* edition, Elsevier, Amsterdam, **1999**.
3. J. J. Berzelius, *Edinburgh New Philosophical Journal,* XXI, **1836**, pp. 223.
4. a) B. Cornils, W. A. Herrmann, Eds. *Applied Homogeneous Catalysis with Organometallic Compounds,* VCH, Weinhein, **1996**; (b) R. Noyori, *Asymmetric Catalysis in Organic Synthesis,* Wiley, New York, **1994**.
5. G. W. Parshall, *Homogeneous Catalysis,* John Wiley, New York, **1980**.
6. R. A. Sheldon, *Chem. Ind*. (**1992)** 903.
7. D. S. Goodsell *"Catalase" Molecule of the Month. RCSB Protein Data Bank,* http://www.rcsb.org/pdb/static.do? p=education discussion/molecule of the month/pdb57 1. html
8. Catalysis and Surface Science, ed. Heinz Heinemann and Gabor A. Somorjai, Marcel Dekker Inc. New York.
9. I. Chorkendroff, J. W. Niemantsverdriet *Concepts of Modern Catalysis and Kinetics* Wiley-VCH **(2003)**.
10. B. Cornils, W. A. Herrmann, *J. Catal*. 216 **(2003)** 23.
11. H. Schneider, U. Scharf, A. Wokaun, A. Baiker, *J. Catal.* 147 **(1994)** 545.
12. A. Fritz, V. Pitchon, *Appl. Catal. B* 13 **(1997)** 1.
13. H. Bosch, F. Janssen, *Catal. Today* 2 **(1988)** 369.
14. F. Garin, *Appl. Catal. A* 222 **(2001)** 183.
15. R. J. Heinsohn, R. L. Kabel *Sources and Control of Air Pollution,* New York, Prentice-Hall, **1990** pp. 308.
16. B. S. Tylor, Y. M. Kion, Q. I. Wang, R. A. Sharpio, T. R. Billiar, D. A. Geller *Arch. Surg.* 1 **(1997)** 1177.
17. S. E. Manahan, *Fundamentals of Environmental Chemistry,* 2nd Ed. Boca Raton, FL: Lewis Publishers, **2001** pp. 554.
18. http://unfccc.int/kyoto_protocol/items/2830.php
19. J. W Erisman, P. Greenfelt, M. Sutton *Environ Int.* 29 **(2003)** 311.
20. Auto Fuel Report, Chapter 12 Proposed vehicular emission norms for new

vehicles, pp. 183.

21. Z. R. Ismagilov, M. A. Kerzhentsev, *Catal. Rev.-Sci. Eng.* 32 **(1990)** 51.
22. C. A. Latta, *Plant Engineering* 9 **(1998)** 1.
23. M. Wojciechowska, S. Lomnicki, *Clean Products and Process* 1 **(1999)** 237.
24. J. N. Armor, *Catal. Today* 26 **(1995)** 147.
25. V. I. Pârvulescu, P. Grange, B. Delmon, *Catal. Today* 46 **(1998)** 233.
26. S. E. Maisuls, *Multiphase Catalysts for Selective Catalytic Reduction of NO_x with Hydrocarbons*. University of Twente, Ph.D. Thesis **(2000)**.
27. E. R. Altwicker, L. W. Canter, S. S. Cha, K. T. Chuang, D. H. F. Liu, G. Ramachandran, R. K. Raufer, P. C. Reist, A. R. Sanger, A. Turk, C. P. Wagner, *Air Pollution,* D.H.F Liu, B.G. Liptak, eds. *Environmental Engineer's Handbook*. Boca Raton: CRC Press LLC. **1999** pp. 1.
28. T. Johnson, *The Environmental Benchmark for Heavy-Duty Applications,* Keynote Lecture at ASME **(2002)** Spring Technical Conference.
29. M. L. Church, B. J. Cooper, P. J. Willson, *SAE Paper 890815* **(1989)** 1.
30. J. Kummer, Catalysts for Automobile Emission Control, Prog. Energy Combust Sci. 6 **(1980)** 177.
31. M. Frankel, *J. Soc. Chem. Ind.* 28 **(1909)** 692.
32. K. C. Taylor, *Automobile Catalytic Converters,* Eds. : J. R. Anderson, M. Boudart, Catalysis-Science and Technology, Springer, Berlin, **(1984)**, Chapter 2, pp. 119.
33. Y. Lui, J. Dettling, *SAE 930249* **(1993)** Warrendale, Pa.: SAE International.
34. J. Dettling, Y. Lui *SAE 9200294* **(1992)** Warrendale, Pa.: SAE International.
35. J. P. A. Neeft, M. Makkee, J. A. Moulijn, *Fuel Proc. Technol.* 47 **(1996)** 1.
36. H. Glick, J. J. Klein, W. Squire, *J. Chem. Phys.* 27 **(1957)** 850.
37. M. Iwamoto, H. Yahiro, S. Shundo, Y. Yu, N. Mizuno, *Appl. Catal.* 69 **(1991)** 15.
38. C. Tofan, D. Klvana, J. Kirchnerova, *Appl. Catal. B* 36 **(2002)** 311.
39. Y. Wu, Z. Zhao, Y. Liu, X. Yang, *J. Mol. Catal. A* 155 **(2000)** 89.
40. M. Iwamoto, H. Yahiro, *Catal. Today* 22 **(1994)** 5.
41. T. Ishihara, M. Ando, K. Sada, K. Takiishi, K. Yamada, H. Nishiguchi, Y. Takita, *J. Catal.* 220 **(2003)** 104.
42. T. Ishihara, K. Anami, K. Takiishi, K. Yamada, H. Nishiguchi, Y. Takita,

Chem. Lett. 32 **(2003)** 1176.

43. C. T. Goralski, W. F. Schneider, *Appl. Catal. B* 37 **(2002)** 263.
44. N. Miyoshi, S. Matsumoto, K. Katoh, T. Tanaka, J. Harada, N. Takahashi, K. Yokota, M. Sugiura, K. Kasahara, *SAE Technical Paper 950809* **(1995)**.
45. N. Takahashi, H. Shinjoh, T. Iijima, T. Suzuki, K. Yamazaki, K. Yokota, *Catal Today* 27 **(1996)** 63.
46. S. Matsumoto, *Catal Today* 29 **(1996)** 43.
47. S. Matsumoto *Cat. Tech.* 4 **(2000)** 102.
48. M. Takeuchi, S. Matsumoto *Top Catal.* 28 **(2004)** 151.
49. M. Misono, T. Inui, *Catal. Today* 51 **(1999)** 369.
50. S. Matsumoto, Y. Ikeda, H. Suzuki, M. Ogai, N. Miyoshi, *Appl. Catal. B* 25 **(2000)** 115.
51. P. Engström, A. Amberntsson, M. Skoglundh, E. Fridell, G. Smedler, *Appl. Catal. B* 22 **(1999)** L241.
52. A. Amberntsson, M. Skoglundh, M. Jonsson, E. Fridell, *Catal. Today* 73 **(2002)** 279.
53. E. Fridell, H. Persson, L. Olsson, B. Westerberg, A. Ambertson, M. Skoglundh, *Top. Catal.* 16/17 **(2001)** 133.
54. E. Fridell, A. Amberntsson, L. Olsson, A. W. Grant, M. Skoglundh, *Top. Catal.* 30/31 **(2004)** 143.
55. K. Yamazaki, T. Suzuki, N. Takahashi, K. Yokota, M. Sugiura, *Appl. Catal. B* 30 **(2001)** 459.
56. K. Yamazaki, N. Takahashi, H. Shinjoh, M. Sugiura, *Appl. Catal. B* 53**(2004)** 1.
57. S. Matsumoto, Y. Ikeda, H. Suzuki, M. Ogai, N. Miyoshi *Appl. Catal. B* 25 **(2000)** 115.
58. D. Duprez, *Catal. Today* 112 **(2006)** 17.
59. N. Takahashi, A. Suda, I. Hachisuka, M. Sugiura, H. Sobukawa, H. Shinjoh, *Appl. Catal. B* 72 **(2007)** 187.

60 G. W. Graham, H.-W. Jen, W. Chun, H. P. Sun, X. Q. Pan, R.W. McCabe, *Catal. Lett.* 93 **(2004)** 129.

61. D. Uy, A. E. O'Neill, J. Li, W. L. H. Watkins, *Catal. Lett.* 95 **(2004)** 191.
62. M. Eberhardt, R. Riedel, U. Göbel, J. Theis, E.S. Los, *Topics Catal.* 30/31

(2004) 135.

63. G. W. Graham, H.-W. Jen, J.R. Theis, R. W. McCabe, *Catal. Lett.* 93 **(2004)** 3.
64. H. Imagawa, T. Tanaka, N. Takahashi, S. Matsunaga, H. Shinjoh, TOCAT5, PI-430, Tokyo, Japan **(2006)**.
65. B. H. Engler, *Chem. Ing. Tech.* 63 **(1991)** 298.
66. N. Haug, B. Scharer, 51 **(1991)** 389.
67. M. Devadas, G. Piazzesi, O. Kröcher, A. Wokaun, *International Symposium on Air Pollution Abatement Catalysis,* Krakow, Poland, September 21-25, **(2005)**.
68. M. Devadas, O. Kröcher, M. Elsener, A. Wokaun, N. Söger, M. Pfeifer, Y. Demel, L. Mussmann, *Appl. Catal. B* 67 **(2006)** 187.
69. K. Kartte, H. Nonnenmaker, *US Patent No. 3 279 884* **(1966)**.
70. F. Nakajima, M. Tacheuci, S. Matsuda, S. Uno, T. Mori, Y. Watanabe, M. Inamuri, *US Patent No. 4 085 193* **(1978)**.
71. *C. H Satterfield. Heterogeneous Catalysis in Industrial Practice.* 2nd edition. Hill 7 McGraw, **(1991)**.
72. (a) E. M. Serwicka *Polish J. Chem.* 75 **(2001)** 307. (b) E. M. Serwicka, B. Krzysztof *Catal. Today* 90 **(2004)** 85.
73. A. De Stefanis, A. A. G. Tomlinson *Catal. Today* 114 **(2006)** 126.
74. A. Vaccari, *Appl. Clay Science* 14 **(1999)** 161.
75. M. Yoshikawa, A. Yasutake, I. Mochida *Appl. Catal. A* 173 **(1998)** 239.
76. G. Centi, S. Perathoner *Appl. Catal. A* 132 **(1995)** 179.
77. S. C. Larsen In *Application of Zeolites in Environmental Catalysis,* V.H. Grassian, ed., CRC Press LLC, Boca Raton, Fla, USA, **(2005)** pp. 269.
78. H.-Y. Chen, Q. Sun, B. Wen, *Catal. Today* 96 **(2004)** 1.
79. H. H. Kung, M.C. Kung, *Catal. Today* 30 **(1996)** 5.
80. W. Held, A. Konig, T. Richter, L. Ruppee, *SAE paper 900496* **1990)**.
81. M. Iwamoto, H. Hamada, *Catal. Today* 10 **(1991)** 57.
82. M. Iwamoto, H. Yahiro, S. Shundo, Y. Yu-U, N. Mizuno, Shokubai, *Catalyst* 32 **(1990)** 430.
83. S. Sato, Y. Yu, H. Yahiro, N. Mizuno, M. lwamoto, *Appl. Catal.* 70 **(1991)** Ll.
84. M. lwamoto, N. Mizuno, *Proc. Inst. Mech. Eng. Part D: J. Automobil Eng.* 207 **(1993)** 23.
85. S. A. Gomez, A. Campero, A. Martinez-Hernandez, G. A. Fuentes, *Appl.*

Catal. A 197 **(2000)** 157.

86. J. Y. Yan, G.-D. Lei, W. M. H. Sachtler, H. H. Kung, *J. Catal.* 161 **(1996)** 43.
87. R. A. Grinsted, H.-W. Jen, C. N. Montreuil, M. J. Rokosz, M. Shelef, *Zeolites* 13 **(1993)** 602.
88. M. K. Neylon, M. J. Castagnola, N. B. Castagnola, C. L. Marshall, *Catal. Today* 96 **(2004)** 53.
89. M. J. Castagnola, M. K. Neylon, C. L. Marshall, *Catal. Today* 96 **(2004)** 61.
90. V. G. Komvokis, E.F. Iliopoulou, I.A. Vasalos, K.S. Triantafyllidis, C.L. Marshall, *Appl. Catal. A* 325 **(2007)** 345.
91. E. A. Lombardo, G. A. Sill, J. L d'Itri, W. K. Hall. *J. Catal* 173 **(1998)** 440.
92. A. J. Desai, V. I. Kovalchuk, E. A. Lombardo, J. L d'Itri, *J. Catal* 184 **(1999)** 396.
93. H. Hirabayashi, H. Yahiro, N. Mizuno, M. lwamoto, *Chem. Lett.* 22 **(1992)** 35.
94. Y. Li, J. N. Armor, *Appl. Catal. B* 1 **(1992)** L31.
95. Y. Li, J. N. Armor, *Stud. Surf. Sci. Catal.* 81 **(1994)** 103.
96. Y. Li, J. N. Armor, *Appl. Catal. B* 3 **(1993)** Ll.
97. F. Witzel, G. A. Sill, W. K. Hall, *J. Catal.* 149 **(1994)** 229.
98. G. Delahay, B. Coq, *Zeolites for Cleaner Technologies,* Eds. : M. Guisnet, J.P. Gilson, Imperial College Press: London, **2002**.
99. Y. Traa, B. Burger, J. Weitkamp, *Micropor. Mesopor. Mater.* 30 **(1999)** 3.
100. G. J. Barnes, *Am. Chem. Soc. Ads. Chem. Ser.* **(1975)** 143.
101. Y. Yao, *J. Catal.* 36 **(1975)** 226.
102. M. Shelef, H. S. Gandhi, *Platinum Met. Rev.* 18 **(1974)** 2.
103. A. G. Graham, S. E. Wanke, *J. Catal.* 68 **(1981)** 1.
104. (a) Z. Liu, S. I. Woo, *Catal. Rev.* 48 **(2006)** 43; (b) S. Roy, M. S. Hegde, G. Madras, *Applied Energy* 86 **(2009)** 2283.
105. G. Zhang, T. Yamaguchi, H. Kawakami, T. Suzuki, *Appl. Catal. B* 1 **(1992)** L15.
106. M. Iwamoto, H. Yahiro, H. K. Shin, M. Watanabe, J. Guo, M. Konno, T. Chikahisa, T. Murayama, *Appl. Catal. B* 5 **(1994)** L1.
107. J. M. Garcia-Cortes, J. Perez-Ramirez, J. N. Rouzaud, A. R. Vaccaro, M. J. Illan-Gomez, C. Salinas-Martinez de Lecea, *J. Catal.* 218 **(2003)** 111.
108. R. Burch, P. J. Millington, A. P. Walker, *Appl. Catal. B* 4 **(1994)** 65.

109. H. H. Ingelsten, M. Skoglundh, E. Fridell, *Appl. Catal. B* 41 **(2003)** 287.
110. A. Kotsifa, D. I. Kondarides, X. E. Verykios, *Appl. Catal. B* 80 **(2008)** 260.
111. E. Seker, E. Gulari, *J. Catal.* 194 **(2000)** 4.
112. R. Burch, T. C. Watling, *Catal. Lett.* 43 **(1997)** 19.
113. I. V. Yentekakis, V. Tellou, G. Botzolaki, I. A. Rapakousios, *Appl. Catal.* B 56 **(2005)** 229.
114. G. Corro, J. L. G. Fierro, R. Montiel, F. Banuelos, *J. Mol. Catal. A* 228 **(2005)** 275.
115. H. Hamada, Y. Kintaichi, M. Sasaki, T. Ito, *Appl. Catal.* 75 **(1991)** L1.
116. Y. Kintaichi, H. Hamada, M. Tabata, T. Yoshinari, M. Sasaki, T. Ito, *Catal. Lett.* 6 **(1990)** 239.
117. K. A. Bethke, D. Alt, M. C. Kung, *Catal. Lett.* 25 **(1994)** 37.
118. T. N. Angelidis, S. Christoforou, A. Bongovianni, N. Kruse, *Appl. Catal. B* 39 **(2002)** 197.
119. A. Martínez-Arias, M. Fernádez-García, A. Iglesias-Juez, J. A. Anderson, J. C. Conesa, J. Soria, *Appl. Catal. B* 28 **(2000)** 29.
120. T. Miyadera, *Appl. Catal. B* 2 **(1993)** 199.
121. F. C. Meunier, J. P. Breen, V. Zuzaniuk, M. Olsson, J. R. H. Ross, *J. Catal.* 187 **(1999)** 493.
122. T. E. Hoost, R. J. Kudla, K. M. Kollins, M. S. Chattha, *Appl. Catal. B* 13 **(1997)** 59.
123. K. A. Bethke, H. H. Kung, *J. Catal.* 172 **(1997)** 93.
124. M. C. Kung, K. A. Bethke, J. Yan, J.-H. Lee, H. H. Kung, *Appl. Surf. Sci.* 121-122 **(1997)** 261.
125. T. Miyadera, *Appl. Catal. B* 13 **(1997)** 157.
126. R. Burch, J. P. Breen, F. C. Meunier, *Appl. Catal. B* 39 **(2002)** 283.
127. F. C. Meunier, R. Ukropec, C. Stapleton, J. R. H. Ross, *Appl. Catal. B* 30 **(2001)** 163.
128. K. Shimizu, A. Satsuma, T. Hattori, *Appl. Catal. B* 25 **(2000)** 239.
129. E. Seker, J. Cavataio, E. Gulari, P. Lorpongpaiboon, S. Osuwan, *Appl. Catal. A* 183 **(1999)** 121.
130. J. P. Breen, R. Burch, C. Hardacre, C. J. Hill, B. Krutzsch, B. Bandl-Konrad, E. Jobson, L. Cider, P. G. Blakeman, L. J. Peace, M. V. Twigg, M. Preis, M.

Gottschling, *Appl. Catal. B* 70 **(2007)** 36.

Chapter 2: Support Modification to Improve the Sulphur Tolerance of Ag/Al_2O_3 for SCR of NO_x with Propene under Lean-Burn Conditions

Impregnation of small quantities of SiO_2 or TiO_2 improved the sulphur tolerance of Ag/Al_2O_3 catalysts during the SCR of NO_x using propene under lean conditions. FTIR study showed the sulfation of silver and aluminum sites in Ag/Al_2O_3 catalyst whereas, its formation is drastically suppressed in the case of Ag/Al_2O_3 doped with SiO_2 or TiO_2.

Chapter 2: Support Modification to Improve the Sulphur Tolerance of Ag/Al_2O_3 for SCR of NO_x with Propene under Lean-Burn Conditions

2.1. Introduction

Removal of NO_x from the exhaust gases of lean-burn and diesel engines is a major challenge to fulfill future restrictive standard emissions. Hydrocarbon selective catalytic reduction (HC-SCR) of NO_x is a powerful technology for the removal of nitrogen oxides, carbon monoxide and unburned hydrocarbon from automotive emissions except under a large excess of oxygen. In such conditions, a narrow operating window is usually reported for the conversion of NO_x accompanied with a significant production of nitrous oxide [1]. Numerous studies dealt with this topic over a wide variety of catalytic systems such as metal oxides [2], zeolites [3-4] and noble metal supported alumina [5], which have been found to be active for this reaction depending on the running temperature. Out of these, Ag/Al_2O_3 is one of the most active and selective for the SCR of NO_x to N_2. The main advantage of this system is its inherent thermal and hydrothermal stability [6], and its wide operating window observed for the selective conversion of NO to nitrogen particularly in presence of heavy hydrocarbons and hydrogen [7].

The lean-burn engine exhausts typically contain water and SO_2. The presence of water is usually known to cause deactivation of the catalyst. However this deactivation is known to be reversible upon removal of water from the feed. Deactivation of the catalyst due to SO_2 in the exhaust gases is one of the major limitations of this catalyst system for its practical applications and has been correlated to the formation of sulphate species on the catalyst surface. Therefore it becomes essential that the catalysts should be stable and active in the presence of water vapor and SO_2. Most researchers have demonstrated the effect of SO_2 [8-10] and $SO_2 + H_2O$ [11, 12] on Ag/Al_2O_3 system. Meunier and Ross [8] reported the effects of SO_2 on the lean $DeNO_x$ activity of 1.2 wt% Ag/Al_2O_3 with C_3H_6. The sample was rapidly and permanently deactivated after exposure to 100 ppm SO_2 at 759 K, which was attributed to the formation of surface silver sulfate species. Jen [9] also found that the NO_x conversion dropped over 2 wt% Ag/Al_2O_3 catalysts from 62% to 28% when the

catalyst was tested with a mixture of propene and propane in presence of 18 ppm SO_2. In contrast, Park *et al.* [10] who studied the effect of SO_2 on the activity of Ag/Al_2O_3 with various Ag loadings on a C_3H_6-SCR for NO concluded that the improvement in the NO_x conversion was due to the formation of Ag_2SO_4 phase. These authors observed correlatively an enhancement of -NCO species formation and the suppression of propene oxidation compared to Ag_2O. The decrease of catalytic performance in presence of SO_2 was mainly due to the poisoning of alumina active sites, which are also responsible for NO reduction to N_2. It was concluded that the addition of SO_2 enhanced the performance of silver sites, but hindered the NO reduction function of alumina sites. In another study, Abe *et al*. [11] reported excellent NO_x reduction and SO_2 tolerance with ethanol as the reductant above 700 K in presence of 10% O_2, 10% H_2O, and 30–80 ppm SO_2 on Ag/Al_2O_3 with higher silver loading (4.6%). The authors suggested that silver sulfate should be catalytically active for NO_x reduction at temperatures above 700 K. Sumiya *et al.* [12] have also reported high NO_x conversion (80%) with ethanol for a 4 wt% Ag/Al_2O_3 even after 10% H_2O and 30 ppm SO_2 were introduced. Angelidis *et al.* [13] have reported a promotional effect on the catalytic reduction of NO_x over 5 wt% Ag/Al_2O_3 upon addition of 25-100 ppm SO_2 at 753 K in presence of excess oxygen and a mixture of propane/propene. The promotional effect was clear over long-term experiments up to 15 h and the catalyst activity was stabilized earlier in presence of SO_2. The authors attributed the promotional effect to the formation of hydrocarbon oxygenates, sulphur accumulation on the catalyst surface and change in the $DeNO_x$ reaction mechanism. The additive effect of noble metals for NO reduction by hydrocarbons has also been reported in the literature [14, 15]. Lee *et al.* [14] found that addition of Pd improved the water tolerance of Co-FER system in the SCR of NO_x by CH_4. The improved water tolerance was attributed to the role of Pd in the oxidation of NO to NO_2, an intermediate in the NO reduction and enhanced NO adsorption on the catalyst surface. In another study, the addition of 0.01 wt% Pd into a 5 wt% Ag/Al_2O_3 system increased the reaction activity of NO at low temperatures. However the catalytic activity drastically decreased in presence of SO_2 due to Ag_2SO_4 phase, the formation of which was enhanced by Pd [15]. *In situ* DRIFTS results suggested that Pd addition catalyzed the partial oxidation of C_3H_6 into a surface enolic species, which are reactive towards NO_3^- to form a surface -NCO species. In presence of SO_2, the formation of these intermediate species was inhibited, hence the decrease in activity

[15]. Incorporation of SiO_2 in this system increased the sulphur tolerance of the Ag-Pd/Al_2O_3 system. Addition of SiO_2 enhanced the formation of the intermediate species (NO_3^-, enolic and –NCO species) and hence the high activity in the NO_x reduction when the gas feed contained SO_2 [16].

From the above discussion it is clear that the main reason for the deactivation of SCR catalysts is the sulphation of the active metal (Ag, Pd etc) and the support (Al_2O_3). One way of improving the sulphur durability of alumina based SCR catalyst is by modification of the support so as to make it more sulphur tolerant. One strategy is to facilitate the decomposition of sulphates by adding certain materials to the catalyst like SiO_2 or TiO_2. SiO_2 and TiO_2 were chosen as the additives because these are weakly sulphating supports and it is well known that the sulphates of SiO_2 and TiO_2 decompose at lower temperatures than those of Al_2O_3 [17, 18]. With the aim of improving the sulphur tolerance of the Ag/Al_2O_3 based system, in the present work, 2 wt% Ag/Al_2O_3 catalysts was prepared by wet impregnation method and the Al_2O_3 support was modified by incorporation of SiO_2 or TiO_2. The influence of these additives on the nature of adsorbates by *in situ* spectroscopic measurements (using DRIFT) with further comparison of catalytic performances in terms of NO conversion to nitrogen was carefully examined in order to investigate the possible intermediates or strongly adsorbed species which may cause inhibiting effects.

2.2. Experimental Section

2.2.1. Catalyst Preparation

Alumina-supported silver catalyst (2 wt% Ag, labeled as AgAl) was prepared by impregnation of commercially available boehmite (AlOOH) with aqueous silver nitrate solution. The sample was dried overnight at 373 K and calcined in air at 773 K for 6 h. For the preparation of 1 wt% SiO_2 incorporated AgAl, 0.347 g $Si(OC_2H_5)_4$ was dissolved in isopropyl alcohol. This solution was added to boehmite (14.3 g) dispersed in isopropyl alcohol under constant stirring. The solution was evaporated and the sample dried overnight at 373 K. To this dried sample aqueous silver nitrate solution (0.315 g) was added, stirred on a hot plate and dried overnight at 373 K and subsequently calcined in air at 773 K for 6 h. The above procedure was repeated for the preparation of TiO_2 incorporated Al_2O_3 sample with $Ti(OC_4H_9)_4$ (0.439 g) as the titanium source followed by Ag impregnation. The material was dried at 373 K and subsequently calcined at 773 K for 6 h. The final samples were labeled as AgSiAl and

AgTiAl respectively. In order to study the effect of amount of additive on the SCR of NO_x, additional two samples with 2 wt % of SiO_2 and TiO_2 were prepared by the method discussed above and were labeled as Ag2SiAl and Ag2TiAl respectively.

2.2.2. Characterization

(a) Powder X-ray diffraction studies

The powder X-ray diffraction data of the samples was collected on a Rigaku Miniflex diffractometer equipped with a Ni filtered Cu Kα radiation (λ = 1.5406 Å, 30 kV, 15 mA) radiation. The data was collected in the 2θ range 20-80° with a step size of 0.02° and scan rate of 4° min^{-1}.

(b) Nitrogen adsorption studies

The BET surface area of the calcined samples was determined by N_2 sorption at 77 K using NOVA 1200 (Quanta Chrome) equipment. Prior to N_2 adsorption, the materials were evacuated at 573 K under vacuum. The specific surface area, S_{BET}, was determined according to the BET equation.

(c) EDAX analysis

The analysis was carried out using Quanta 200 3D with EDAX at 30 kV.

(d) FT-IR of adsorbed pyridine

The nature of the surface acid sites was studied by FTIR of adsorbed pyridine at room temperature. The FT-IR spectra of chemisorbed pyridine (Py-IR) were obtained in a high temperature cell (Spectra-Tech) fitted with a Zn-Se window (Shimadzu 8000 FTIR spectrophotometer). The temperature in the cell was varied from 303 to 698 K. The sample (30 mg) was finely crushed and placed in a sample holder. Prior to pyridine adsorption, the sample was out gassed for 2 h at 698 K under N_2 flow to remove adsorbed moisture. The cell was cooled to room temperature stepwise and the spectra of neat catalyst were recorded (250 scans resolution 4 cm^{-1}) at different temperatures. The sample was dosed with two successive pulses of pyridine (10 μl each). Spectrum was recorded at room temperature after an equilibration time of 30 min. The temperature-programmed desorption of pyridine was studied at 298, 373, 473, 573 and 673 K after equilibration for 30 min after

attaining the temperature. The spectrum of the neat sample was subtracted from the pyridine adsorbed sample.

(e) FT-IR

The FT-IR spectra were recorded in transmittance mode with a Thermo-Nicolet FT-IR spectrometer**.** The spectrometer was equipped with an XT-KBr beam splitter and MCT/A detector. The sample was diluted with KBr (1:100 wt/wt) and the spectra recorded at room temperature in ambient air using 100 scans with a resolution of 4 cm^{-1}.

(f) In-situ Diffuse Reflectance FT-IR Studies (DRIFTS)

The diffuse reflectance FT-IR measurements were carried out under a flow of He in the instrument described in section *2.2.2 (d)*. About (30 mg) of finely crushed sample was placed in a sample holder and pretreated at 698 K for 2 h in He flow to remove adsorbed moisture. The spectrum of neat catalyst was recorded (400 scans with resolution 4 cm^{-1}) at 623 K prior to the experiment under He flow. The reported spectra are difference spectra of adsorbed species and neat catalyst.

2.2.3. Catalytic Activity Tests

The SCR of NO by propene was carried out at atmospheric pressure in quartz tubular down flow reactor (inner diameter 4 mm). Catalyst powder (750 mg, particle size < 180 μm) was placed in the reactor and a thermocouple was inserted in the center of the catalyst bed to measure the temperature. Prior to the reaction the catalyst was activated at 773 K for 3 h in He flow. The typical reactant gas mixture consisting of NO (1000 ppm), C_3H_6 (2000 ppm) CO_2 (10%) and O_2 (5%), 0 or 5% H_2O, 0 or 20 ppm SO_2 gas and balance He were fed from independent mass flow controllers. The online analysis of the effluent gases was carried out by monitoring the relative masses m/z = 30 (NO), 28 (N_2), 44 (N_2O, CO_2), 41 (C_3H_6) and 46 (NO_2) as function of time using a mass spectrometer, a chemiluminescence's NO_x analyzer and a micro GC (Varian CP 4900) equipped with a molecular sieve 5Å and a Porapaq Q column. The total flow of the inlet gas was set at 250 mL min^{-1} to obtain a gas hourly space velocity (GHSV) of 20000 h^{-1} (W/F =0.05 g h L^{-1}). In these studies NO and C_3H_6 conversions were calculated as follows:

$$\text{NO conversion (\%)} = \frac{[NO_x]_{inlet} - [NO_x]_{outlet}}{[NO_x]_{inlet}} \times 100$$

$$C_3H_6 \text{ conversion (\%)} = \frac{[C_3H_6]_{inlet} - [C_3H_6]_{outlet}}{[C_3H_6]_{inlet}} \times 100$$

2.3. Results and Discussion

2.3.1. Structural and Textural properties

Table 2.1 shows the BET surface area of all the samples prepared in this study and changes after 20 ppm SO_2 exposure under dry atmosphere. For comparison, the surface area of γ-Al_2O_3 is also included. Upon introduction of Ag in the γ-Al_2O_3 support and the addition of 1 wt% SiO_2 or TiO_2 to AgAl catalyst, the surface area decreased. This is due to the blocking of the pores of γ-Al_2O_3 after impregnation of the support with other metal oxides resulting in the decrease in surface area. Subsequent decrease in specific surface area is also noticeable for used catalysts. Similar tendencies were earlier reported and ascribed to blockage of the pores by the accumulated sulphur [19]. Figure 2.1 shows the XRD pattern of the fresh sample (Figure 2.1A) and those recorded after exposure to the gas stream containing 20 ppm SO_2 at 623 K (Figure 2.1B). The diffraction pattern of fresh AgAl, AgSiAl and AgTiAl (Figure 2.1A) show characteristic X-ray lines of γ-Al_2O_3 located at 2θ = 36.7, 46.0, 60.7 and 66.9 degree (JCPDS: 29-0063). No peak due to bulk metallic Ag or Ag_2O species were observed indicating that the Ag is well dispersed over the support and is amorphous due to low silver loading (2 wt% Ag). Additionally, no peak corresponding to SiO_2 phase or TiO_2 was seen in AgSiAl and AgTiAl respectively. This showed that the structural property of γ-Al_2O_3 support was maintained even after incorporation of SiO_2 or TiO_2. Figure 2.1B shows the XRD patterns of the used catalysts exposed to 20 ppm SO_2 in the reaction feed at 623 K. All the samples exhibit the characteristic peaks of γ-Al_2O_3 and no X-ray line corresponding to bulk Ag_2SO_4 was observed in the diffraction patterns of any of the samples.

Table 2.1 *Changes in specific surface area of the catalysts before and after SO_2 exposure under dry atmosphere (in the absence of water)*

Samples	**Surface area (Fresh catalysts) (m^2 g^{-1})**	**Surface area (After exposure to 20 ppm SO_2)**	**Relative loss in specific surface area**	**Sulphur content, wt% (After exposure to 20 ppm SO_2)***
γ- Al_2O_3	237	-	-	-
AgAl	216	198	0.08	0.14
AgSiAl	192	190	0.01	0.05
AgTiAl	190	186	0.02	0.00

* By EDAX analysis

2.3.2. Pyridine adsorption study

Nature of acidity was determined by FTIR of adsorbed pyridine and the results are shown in Figure 2.2. IR bands appear at 1441, 1482, 1583, 1592 and 1613 cm^{-1} with a weak contribution at 1551 cm^{-1} in spectra recorded at room temperature on AgAl, AgSiAl and AgTiAl. As observed, no significant shift related to changes in charge disturbance in the pyridine ring due to adsorption on stronger acidic sites occurs according to the nature of the additive [20]. Only slight changes are observed in the relative intensity of the bands at 1592 and 1583 cm^{-1}. Previous characterization of Pt/Al_2O_3 by pyridine adsorption corroborates our observations on AgAl with the existence of six contributions, which essentially characterize pyridine adsorption on Lewis acid sites [21]. Previous adsorption studies carried out on silica-alumina catalysts [20-22] showed that pyridine adsorbed on Lewis acid site (LAS) essentially gives characteristic infrared bands at 1450 (ν_{19b}) and 1610 cm^{-1} (ν_{8a}) whereas pyridine adsorbed on Brønsted acid sites (BAS) shows characteristic bands at 1545 (ν_{19b}) and 1630 (ν_{8a}) cm^{-1} Additionally, the IR bands at 1482, 1583 and 1592 cm^{-1} can be assigned to weak adsorption of pyridine via hydrogen bonding. Clearly, no significant increase in the relative intensity of the 1551 cm^{-1} band characteristic of pyridinium ions on Brønsted sites is observed particularly after SiO_2 incorporation. Hence, infrared spectra of all the samples show the predominance of LAS on γ-Al_2O_3.

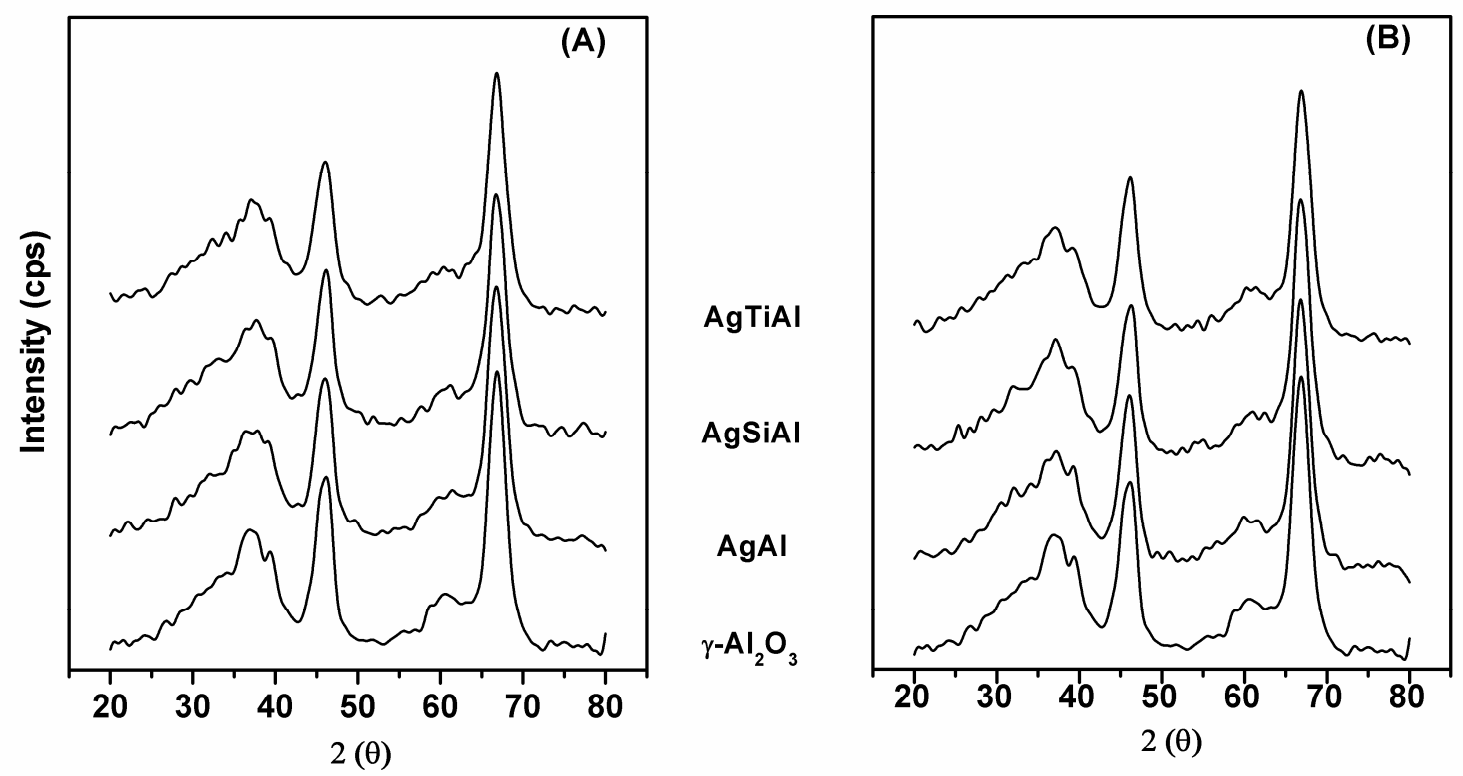

Figure 2.1 *(A) X-ray diffraction pattern of fresh γ-Al_2O_3 and the different samples before the reaction and (B) of fresh γ-Al_2O_3 and the samples after the reaction with 20 ppm SO_2 in the feed. Reaction conditions: 1000 ppm NO, 2000 ppm C_3H_6, 10 % CO_2, 5 %O_2, 0 or 20 ppm SO_2, He balance, Temp. 623 K*

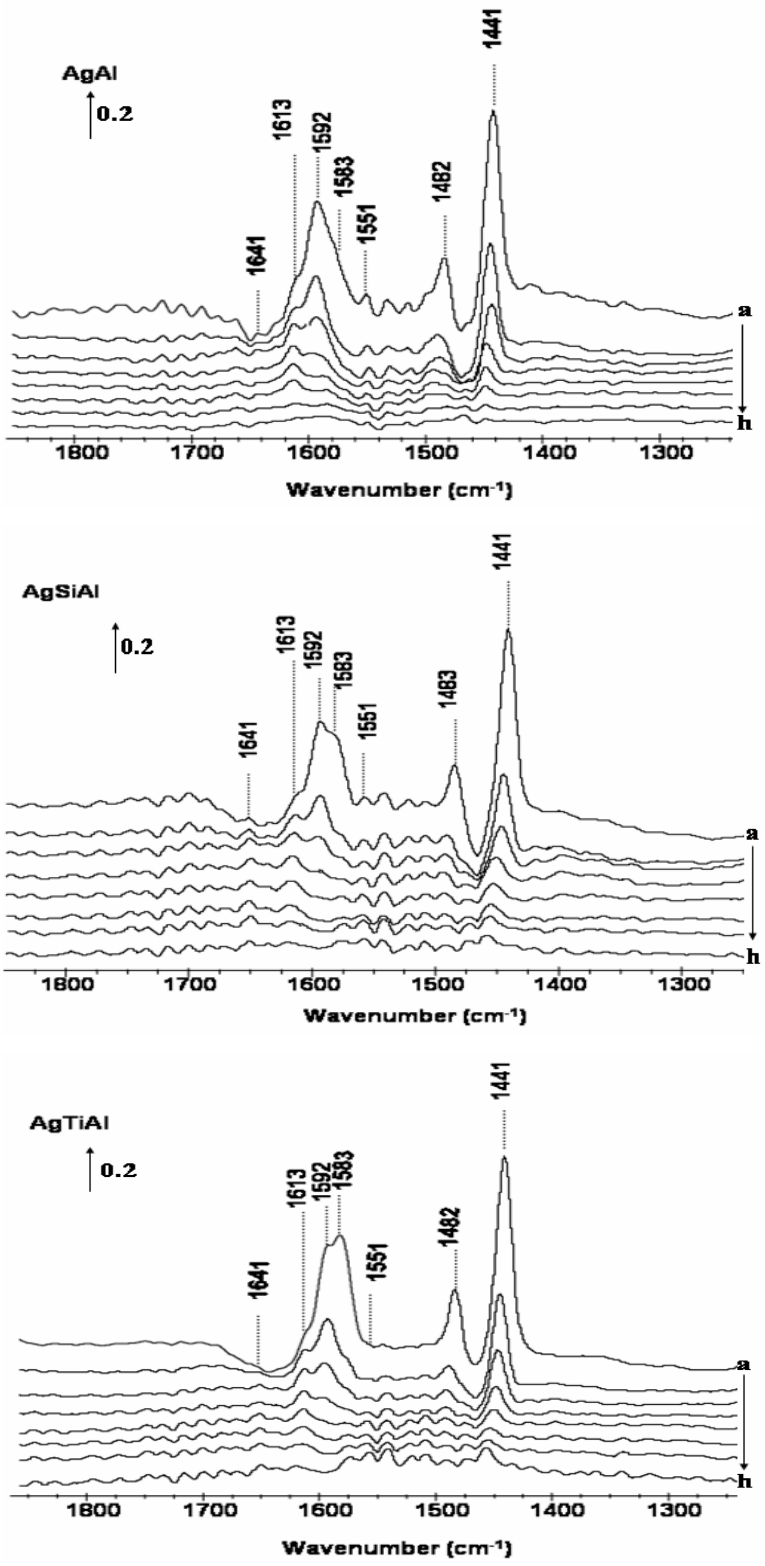

Figure 2.2 *FT-IR spectra of pyridine adsorbed on the samples followed by evacuation at: (a) 298 K, (b) 373 K, (c) 423 K, (d) 473 K, (e) 523 K, (f) 573 K, (g) 623 K and (h) 673 K*

In all the three samples the IR band at 1592 cm^{-1} completely disappears on heating at 473 K, indicating its attribution to weakly interacting species. From Figure 2.2 it can be seen that, the shoulder at 1613 cm^{-1} and the band at 1441 cm^{-1} disappears after heating AgAl at 623 K. In contrast over AgSiAl and AgTiAl the shoulder at 1613 cm^{-1} is clearly visible even after heating at 623 K and the band at 1441 cm^{-1} is seen after heating at 673 K. These features indicate the presence of stronger LAS on AgSiAl and AgTiAl compared to AgAl. These general features are in good agreement with pyridine adsorption studies reported earlier on Ag/Al_2O_3 and Ag/TiO_2-Al_2O_3 [23]. These authors reported the presence of stronger LAS on Ag/TiO_2-Al_2O_3 than on Ag/Al_2O_3.

2.3.3. Catalytic activity

(a) Influence of addition of SiO_2 and TiO_2 to AgAl on the catalytic activity

The SCR of NO using propene over Ag/Al_2O_3 and Si/Ti doped catalysts at various temperatures showed only N_2 formation and a complete oxidation of propene into CO_2. CO formation was not observed under dry conditions. It is worthwhile to mention here that no undesirable side product (NO_2) was formed. The overall steady-state conversions of NO and C_3H_6 at different temperatures are shown in Figure 2.3, which account for competitive oxidation of C_3H_6 by NO and O_2 according to the following set of reactions:

$$C_3H_6 + 9NO \rightarrow 3CO_2 + 3H_2O + \tfrac{9}{2}N_2$$

$$C_3H_6 + \tfrac{9}{2}O_2 \rightarrow 3CO_2 + 3H_2O$$

As indicated in Figure 2.3, amongst the three catalysts prepared, AgAl showed the highest NO conversion (44 %) at lower temperature (623 K). At this temperature the NO conversion on AgSiAl and AgTiAl was 36 and 38 % respectively showing lower overall activities for NO conversion. Similar trend is observed in the case of propene conversion with maximum conversion (20%) on AgAl and least propene conversion on AgTiAl (13% at 623 K). Subsequent comparisons indicate that reaction (2) predominates in the overall temperature range of this study but the relative contribution of the direct oxidation of propene by oxygen on the overall propene conversion accentuates with a rise in temperature. However, it seems obvious that the

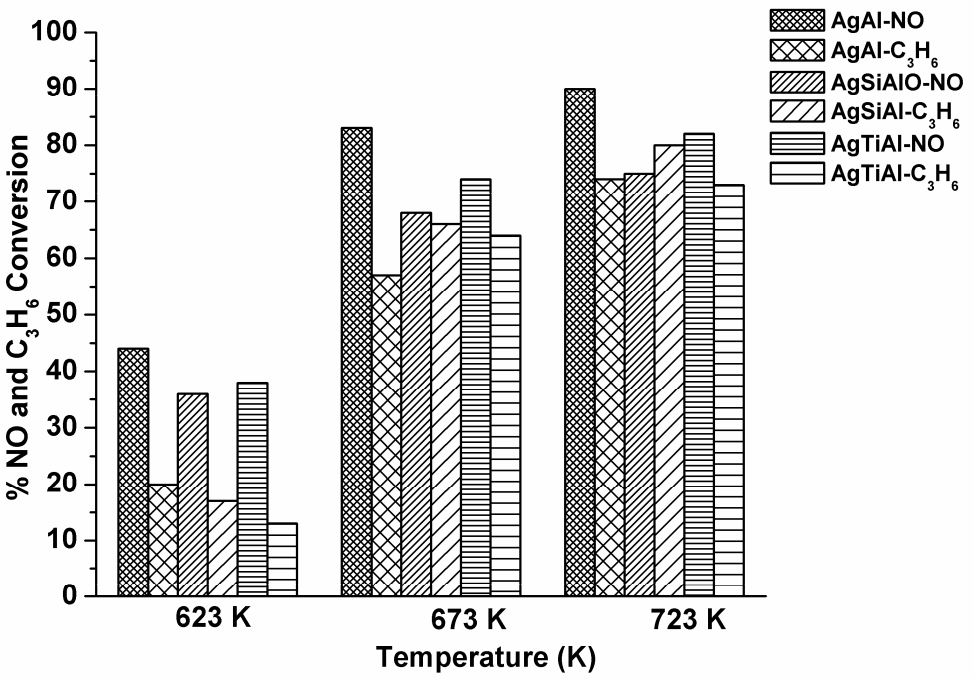

Figure 2.3 *Conversion of NO and C_3H_6 as a function of temperature on AgAl, AgSiAl and AgTiAl in the absence of SO_2. Gas composition: 1000 ppm NO, 2000 ppm C_3H_6, 5 %O_2, 10 % CO_2, He balance*

competition is more in favor of reaction (2) than reaction (1) on AgAl than on AgSiAl and AgTiAl highlighting the promotional effect of Si and Ti on the selectivity behavior. The influence of the amount of additive on the catalytic performances has been examined. AgAl catalysts with 2 wt% SiO_2 (Ag2SiAl) and TiO_2 (Ag2TiAl) were prepared and tested for the SCR of NO (Figure 2.4). Addition of 2 wt% SiO_2 and TiO_2 resulted in lower NO conversion as compared to AgAl. When conversion of NO at the same temperature (623 K) was compared the following trend was observed: AgAl (44%) > AgSiAl (36%) ~ AgTiAl (38%) > Ag2SiAl (19%) ~ Ag2TiAl (23%). Such a comparison highlights a detrimental effect of increasing amount of SiO_2 and TiO_2 on the overall conversion of NO. On the other hand a selectivity enhancement with a greater ability of the catalyst to activate the C_3H_6/NO reaction at the expense of the C_3H_6/O_2 reaction is evident. Such observations could be tentatively explained on the basis of previous investigations, which mentioned the involvement of ad-NO_x species on alumina [8, 24] and the participation of Lewis acid sites for the production of

oxygenates, both species being considered as intermediate in the $DeNO_x$ reactions [23]. Hence, the above-mentioned experimental observations probably suggest that an optimal amount of Si and Ti additives would determine the overall performances of Si- and Ti-modified catalysts in the C_3H_6/NO reaction with a detrimental effect at high Ti and Si coverage due to a loss of accessible alumina active sites at the surface partially compensated by an improvement of the acidic properties after Si and Ti incorporation.

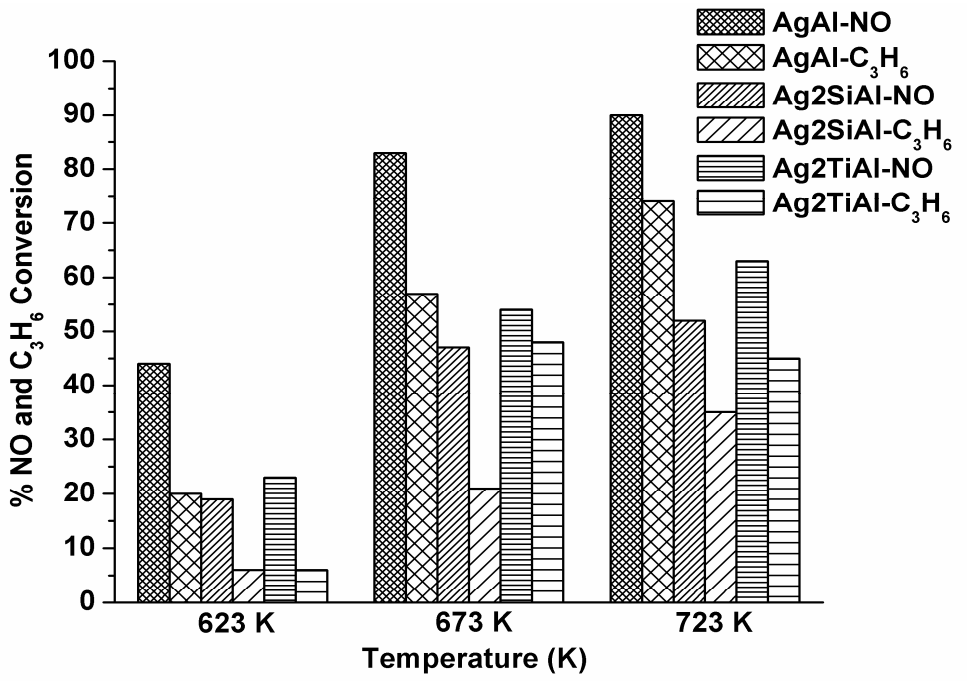

Figure 2.4 *Effect of amount of additive on the conversion of NO and C_3H_6 as a function of temperature. Gas composition: 1000 ppm NO, 2000 ppm C_3H_6, 5 %O_2, 10 % CO_2, He balance*

(b) Influence of addition of SO_2 on the catalytic activity

All the catalysts in the first series were tested in presence of 20 ppm SO_2 in the absence of water. Figure 2.5 shows the effect of SO_2, H_2O and H_2O+SO_2 on the catalytic activity at 623 K. It is clearly seen that SO_2 strongly inhibits the NO conversion on AgAl (in the absence of water), decreasing from 44% to 21%. On the other hand, SO_2 does not decrease the conversion of NO significantly on AgSiAl and AgTiAl (Figure 2.3). This result underlines the fact that incorporation of Si and Ti has increased the sulphur tolerance of AgAl system. Such an improvement could be partly

related to changes in the competitive adsorption of NO_x and SO_x by modifying the acidic properties. In addition, it is noticed that the deactivation in case of AgAl is also reflected in the loss in the specific surface area (see Table 2.1) of used catalysts due to sulphur accumulation. This sulphur accumulation on Ag/Al_2O_3 was also confirmed by chemical analysis of sulphur content of the used catalysts using EDAX technique (Table 2.1). In case of AgSiAl and AgTiAl catalysts no sulphur accumulation was observed in chemical analysis. Previous investigations on the effect of SO_2 on catalyst performances for SCR sometimes lead to controversial observations with reversible or irreversible deactivation and also beneficial effects depending on the catalyst compositions and the nature of hydrocarbons. Angelidis *et al.* [13] has reported that when 5 wt%Ag/Al_2O_3 is used as catalyst no deactivation due to SO_2 is observed when propene is used as reducing agent as against propane which shows total deactivation in presence of SO_2. Similar tendencies were also reported on Ga_2O_3-Al_2O_3 depending on the method of catalyst preparation [19]. Surprisingly the sol-gel method developed for such a preparation leads to a beneficial effect of SO_2 while co-precipitation and impregnation led to detrimental effects. In fact, Haneda *et al.* [19] discussed their results in terms of stabilization of sulphate species inducing a negative effect and the creation of Brønsted acid sites, which could activate the conversion of C_3H_6. In case of NSR catalyst also Imagawa *et al*. [25] have shown that doping of TiO_2 to nanocomposite of Al_2O_3 and ZrO_2-TiO_2 as support has improved the sulphur tolerance of the catalyst considerably which is attributed to the formation of the Al_2O_3-TiO_2 solid solution after addition of TiO_2 to the nanocomposite [25]. Our results obtained on AgAl and AgSiAl and AgTiAl could be discussed in the light of those previous statements. As a matter of fact, changes in the selectivity observed on modified-AgAl with a preferential inhibiting effect can be correlated to lower extent of deactivation due to sulphate accumulation which emphasizes the fact that the oxidation of SO_2 to SO_3 is a pre-requisite step for sulphate formation [26]. Further spectroscopic investigations were performed in order to investigate changes in surface properties due to accumulation of S- and N-containing adsorbed species.

(c) Influence of water addition

The influence of H_2O and simultaneous addition of H_2O+SO_2 in the feed on the NO conversion to N_2 over the three samples is illustrated in Figure 2.5. For these

tests, prior to the introduction of H_2O in the feed, the inlet composition was checked at 423 K. The catalyst was then heated to 623 K at 10 K min^{-1} in a water containing flow (5%). After stabilization, the conversion was recorded and then SO_2 was introduced in the feed gas. The activity of the catalyst in the presence of H_2O+SO_2 was monitored for 12 h and then the conversion was recorded. In the presence of water in the feed, AgAl gave a maximum of 38% NO conversion; AgSiAl gave 50% NO conversion whereas AgTiAl gave 25% NO conversion to nitrogen.

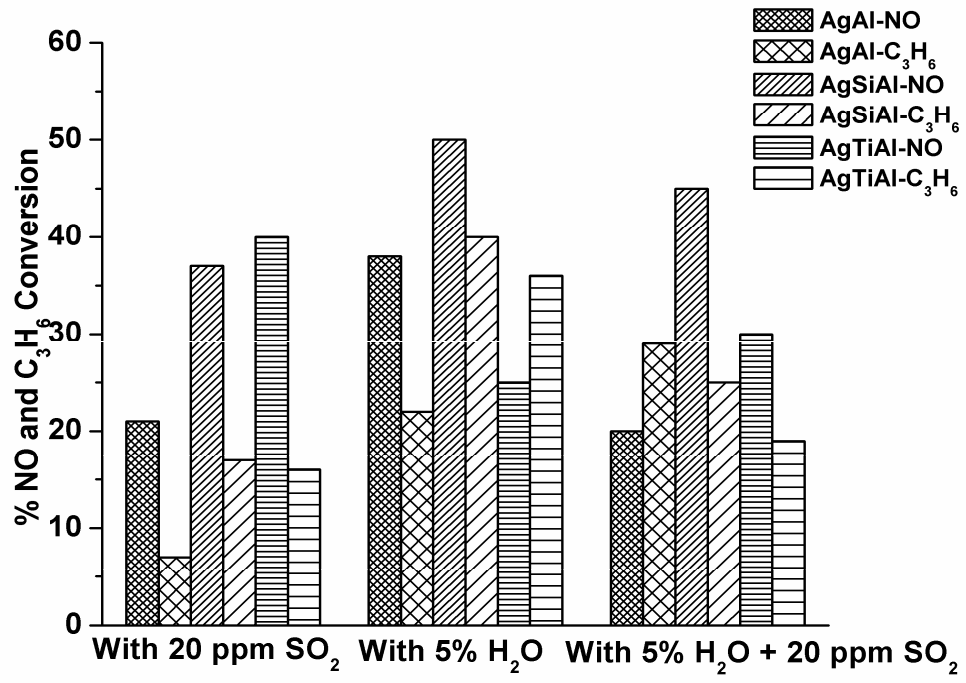

Figure 2.5 *Effect of SO_2 (dry conditions), H_2O and H_2O+SO_2 on conversion of NO_x and C_3H_6 on AgAl, AgSiAl and AgTiAl at 623 K. Reaction conditions: 1000 ppm NO, 2000 ppm C_3H_6, 10 % CO_2, 5 %O_2, 20 ppm SO_2, 5 % H_2O and He balance*

The corresponding conversions of propene are reported in Figure 2.5. Contrarily to previous measurements in the absence of water, CO is significantly formed irrespective of the catalyst composition. The CO formation in presence of water in case of AgAl, AlSiAl and AgTiAl was found to be 134, 425 and 265 ppm respectively confirmed by online GC. Conversion and specific rates for NO reduction to nitrogen have been tentatively estimated for further comparisons. Calculations reported in

Table 2.2 show a decrease in activity in the presence of water except on AgSiAl. In this latter case, a significant rate enhancement in NO conversion is observed. The simultaneous introduction of water and SO_2 induces a significant deactivation except on AgSiAl. As indicated in Table 2.2, AgTiAl is more sulphur resistant than AgAl, however the most prominent observation is probably the remarkable behavior of AgSiAl with a higher conversion level than that observed in the absence of SO_2 and H_2O. Now regarding the selectivity behavior, SO_2 and H_2O addition induce a weak effect on the selectivity of AgTiAl and AgSiAl. On the other hand, a strong detrimental effect is noticeable on AgAl. Hence, such observations evidence significant changes in catalytic properties after Si and Ti-modification.

Table 2.2 *Influence of water and SO_2 on the specific rate of NO conversion to N_2 on modified-Ag catalysts. T (reaction) = 623 K, 1000 ppm NO, 2000 ppm C_3H_6 with $W/F_0 = 0.05$ g h L^{-1}.*

Catalyst	**Reaction Conditions**	**NO conversion**	**Specific rate (mol $h^{-1}g^{-1}$)**
AgAl	A	0.44	3.6×10^{-4}
	B	0.21	1.7×10^{-4}
	C	0.38	3.1×10^{-4}
	D	0.20	1.6×10^{-4}
AgSiAl	A	0.36	3.0×10^{-4}
	B	0.37	3.0×10^{-4}
	C	0.50	4.1×10^{-4}
	D	0.45	3.7×10^{-4}
AgTiAl	A	0.38	3.1×10^{-4}
	B	0.40	3.1×10^{-4}
	C	0.25	2.1×10^{-4}
	D	0.30	2.5×10^{-4}

A: in the absence of water and SO_2

B: in the presence of 20 ppm SO_2

C: in the presence of 5 vol. % H_2O

D: in the presence of 5 vol. % H_2O and 20 ppm SO_2

Earlier investigations on various $DeNO_x$ catalysts have discussed a loss of catalytic activity due to H_2O and SO_2 by detailed characterizations of the deactivated catalyst

[27-29]. The loss due to H_2O was attributed to competitive adsorption of H_2O and NO whereas the loss due to SO_2 was attributed to sulphate formation. In the SCR of NO_x, when H_2O is present in the feed, it may compete with NO for adsorption on identical reaction sites. The reduction of available adsorption sites for NO by H_2O is one of the main causes for the deactivation of SCR catalyst [27]. Hence, the addition of Si and Ti would weaken the usual inhibiting effect of water. Such an explanation could be still valid for SO_2, which exhibits a weak inhibiting effect. The strengthening of the acidic properties would weaken the interaction between SO_2 and Al_2O_3.

The beneficial effect of water has also been observed for the reduction of NO by heavy hydrocarbons by Shimizu *et al.* [30]. These authors have tentatively explained their results on the basis of *in situ* IR measurements which suggest a significant reduction of carbonaceous deposits which can cause a poisoning effect. As a matter of fact, He *et. al*. [31] also reported a promoting effect of water for the C_3H_6-SCR. They observed a rate enhancement in NO and propene conversion but did not find similar effect for the single oxidation of propene by oxygen. However still such an effect is not correctly understood and could possibly involve direct interactions between hydrocarbons and NO_x to explain this beneficial effect. Ag-ZSM5, Ag/SiO_2-Al_2O_3 and Ag/SiO_2 are reported to catalyze partial oxidation of methane in presence of oxygen which has been studied using *in-situ* FTIR under dry conditions [32]. Ranney et al have reported beneficial effect of water on propylene partial oxidation using Ag catalyst; Ag (110) surface [33]. In the absence of water complete oxidation of propylene is observed on Ag (110) where as in presence of water partial oxidation is favored. It is noticeable that water addition in the feed in our experiments is accompanied with the parallel formation of CO (AgAl 134 ppm, AlSiAl 425 ppm and AgTiAl 265 ppm). In the present case the increase in the propylene conversion as well as NO_x conversion on AgSiAl could be attributed to partial oxidation of propylene to CO, CO_2 and hydrogen by comparison with the literature reports. However the exact reaction pathway for the formation of CO and hydrogen in presence of water under the experimental conditions of present study is not very clear. Though CO formation has been detected using online GC analysis, the corresponding hydrogen could not be detected due to reactive nature of hydrogen at reaction temperature (623 K). Satokawa *et al.* [34, 35] has reported positive effect of hydrogen on NO conversion using Ag/Al_2O_3 catalyst and light hydrocarbons as reductant at lower temperature. Hence,

the formed hydrogen in presence of water on AgAl, AgSiAl and AgTiAl is expected to react with NO under reaction conditions thereby unable to detect H_2 by GC.

(d) FT-IR study of spent catalysts

To study the nature of species formed during SCR in presence of 20 ppm SO_2, which are responsible for catalyst poisoning, the FTIR of the used catalyst was examined (Figure 2.6). Since the measurements were made in ambient air, the absorption band at 1640 cm^{-1}, due to bending vibration of adsorbed water, was seen over all the samples. The spectrum of AgAl (Figure 2.6a) shows an intense band at 1384 cm^{-1} and a broad hump at 1135 cm^{-1} which are assigned to asymmetric and symmetric stretching vibration of O=S=O of sulphate species on Al_2O_3 [19].

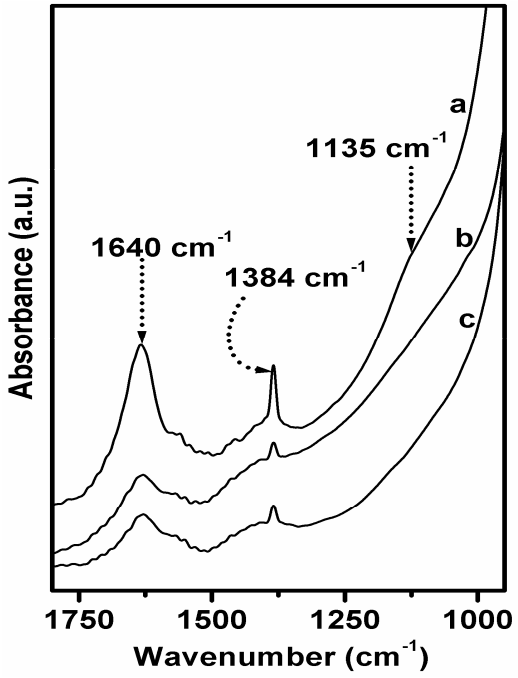

Figure 2.6 *FT-IR spectra of (a) AgAl, (b) AgSiAl and (c) AgTiAl after use in the SCR of NO_x with 20 ppm SO_2. Reaction conditions: 1000 ppm NO, 2000 ppm C_3H_6, 10% CO_2, 5%O_2, 20 ppm SO_2, He balance, Temp. 623 K*

The appearance of these peaks indicates the formation of aluminum sulfate species on the support. In contrast, a much less intense peak at 1384 cm^{-1} is observed in case of used AgSiAl (Figure 2.6b) and AgTiAl (Figure 2.6c). It is reported that the sulfates formed on Al_2O_3 are thermally more stable and decompose at temperature

~1073-1193 K [15] to yield the oxide whereas those formed on SiO_2 [17] or TiO_2 [18] are relatively less stable. These results show that sulphate species formed on AgSiAl and AgTiAl, get easily desorbed from the surface thus preventing the sulphation of the Al_2O_3 support and thereby preserving the catalytic activity in presence of SO_2.

(e) In-situ DRIFTS study

In order to examine the cause of catalyst deactivation in presence of SO_2, and to study the mechanism of deactivation, *in situ* FTIR studies were carried out in the absence of water. Since the deactivation due to SO_2 was more prominent at 623 K the *in-situ* DRIFTS analysis was carried out at this temperature. Two sets of experiments were carried out for each catalyst. In the first experiment, standard SCR gas mixture (1000 ppm NO + 2000 ppm C_3H_6 + 10% CO_2 + 5% O_2) was passed over the catalyst at 623 K and the species formed were monitored as a function of time. In second experiment along with standard SCR mixture, 20 ppm SO_2 was introduced in the feed at 623 K and the formation of different species was monitored as a function of time. The *in situ* IR results of SCR in presence of 20 ppm SO_2 on AgAl, AgSiAl and AgTiAl are shown in Figure 2.7, 2.8 and 2.9 respectively. For reference the spectrum in absence of SO_2 (exposed to 1000 ppm NO + 2000 ppm C_3H_6+ 10% CO_2 + 5% O_2 for 60 min) for AgAl [Figure 2.7A (i)], AgSiAl [Figure 2.8A (i)] and AgTiAl [Figure 2.9A (i)] is also included. Based on previous literature data [24, 36, 37], IR bands assigned to monodentate nitrate (1250, 1550 cm^{-1}), bidentate nitrate (1305, 1590 cm^{-1}), acetate species (1460, 1585 cm^{-1}), formate species (1595, 1390, 1380cm^{-1}), enolic (1637 cm^{-1}) and NCO species (Ag-NCO 2235 cm^{-1} and Al-NCO-2259 cm^{-1}) are summarized in Table 2.3. For all three catalysts in absence of SO_2 [Figure 2.7 A (i)] the characteristic infrared bands due to acetates (1574, 1445 and 1471 cm^{-1}), formates (1390 and 1377 cm^{-1}) and adsorbed nitrates (1638, 1591 and 1304 cm^{-1}) [30] are observed along with surface isocyanate species, Ag-NCO and Al-NCO (2226 and 2258 cm^{-1} for AgAl; 2229 and 2261 cm^{-1} for AgSiAl & 2226 and 2255 cm^{-1} for AgTiAl) [36] as well as surface enolic species (H_2C=CH-O-M) (1644 cm^{-1}) [24].

Meunier *et al.* [36] have studied SCR using propene on Ag/Al_2O_3 by *in situ* FTIR. Two broad absorption ranges with an apparent maximum at 1560 and 1300 cm^{-1} after exposure to NO+O_2 are reported. These observations are in qualitative

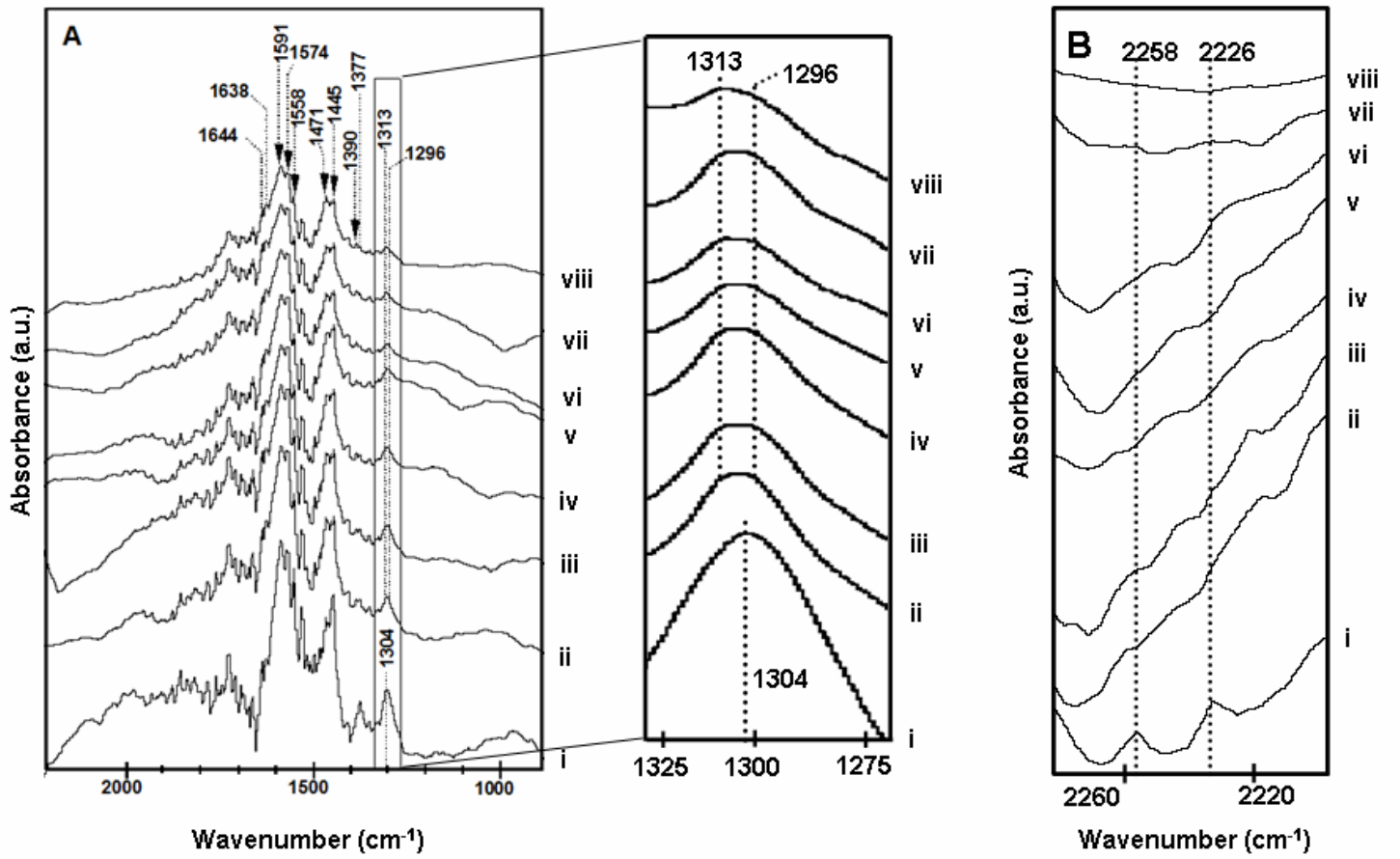

Figure 2.7 *Dynamic changes of in situ DRIFTS spectra over AgAl during the SCR of NO in presence of SO_2 at 623 K. (i) NO + C_3H_6–60 min, (ii) NO + C_3H_6 + SO_2–10, (iii) 30, (iv) 60, (v) 120, (vi) 180 min (vii) 240 and (viii) 300 min. Gas composition: 1000 ppm NO, 2000 ppm C_3H_6, 5% O_2, 10% CO_2, 20 ppm SO_2, He balance*

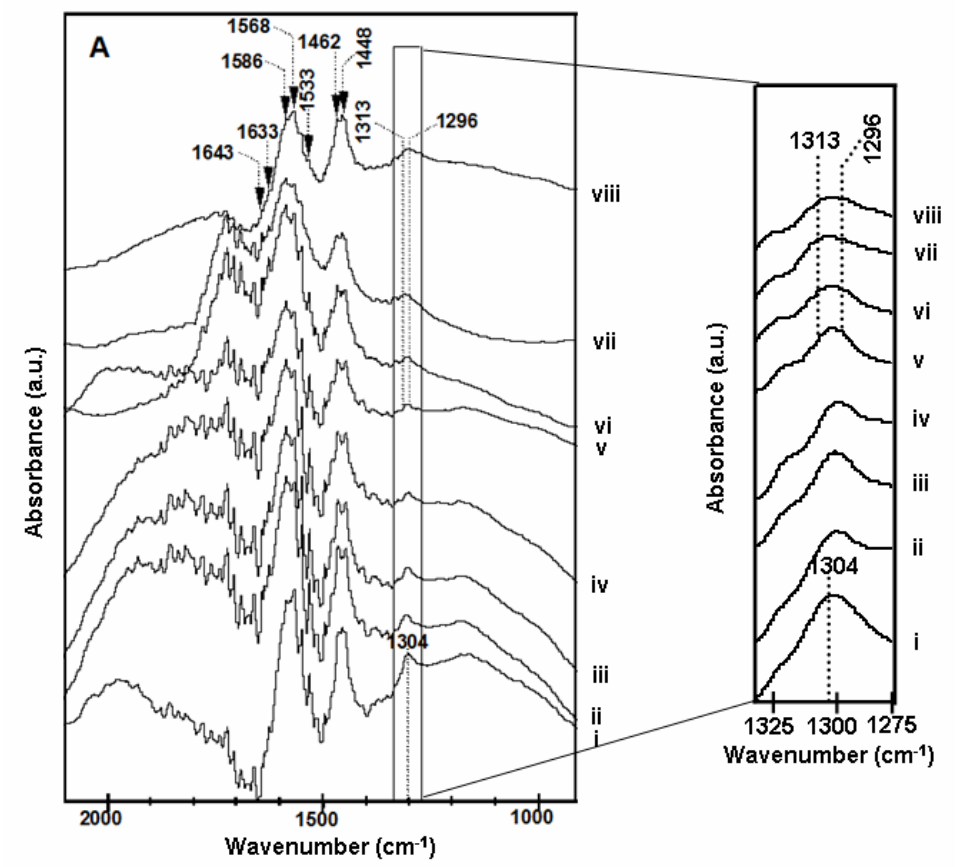

Figure 2.8 *Dynamic changes of in situ DRIFTS spectra over AgSiAl during the SCR of NO in presence of SO_2 at 623 K. (i) NO + C_3H_6–60 min, (ii) NO + C_3H_6 + SO_2–10, (iii) 30, (iv) 60, (v) 120, (vi) 180 min (vii) 240 and (viii) 300 min. Gas composition: 1000 ppm NO, 2000 ppm C_3H_6, 5% O_2, 10% CO_2, 20 ppm SO_2, He balance*

agreement with that reported in Figures 2.7A (i), 2.8A (i) and 2.9A (i) and would correspond to the formation of bidentate nitrates species on alumina. A distinct observation is related to the IR band at 1445 cm^{-1} with a shoulder at 1474 cm^{-1} (Figure 2.7A) which would result from the direct interaction between propene and $NO+O_2$ with the formation of oxygenates from the partial oxidation of propene. Those IR bands could characterize the presence of carboxylate species according to previous assignments [36]. Weak contributions evident at 1644 and 1377 cm^{-1}, could also highlight the presence of organo-nitrite, oxime and organo-nitro compounds. Weak IR bands are also observed near 2226 cm^{-1} previously assigned to -NCO species. Such tentative assignments seem to agree with those reported by Li *et al.* [23] who

investigated the reduction of NO by propene on Ag/TiO_2-Al_2O_3 and Ag/Al_2O_3. These authors suggested the formation of monodentate, bidentate and bridge nitrate, acetate species, formate species and isocyanate species.

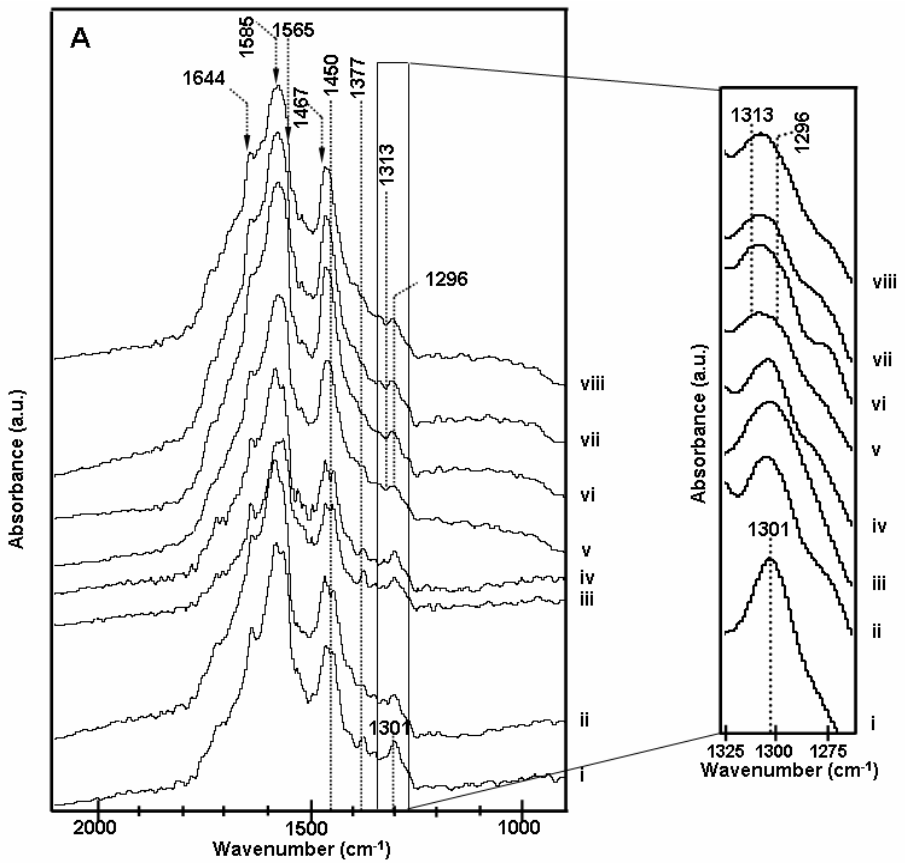

Figure 2.9 *Dynamic changes of in situ DRIFTS spectra over AgTiAl during the SCR of NO in presence of SO_2 at 623 K. (i) NO + C_3H_6–60 min, (ii) NO + C_3H_6 + SO_2–10, (iii) 30, (iv) 60, (v) 120, (vi) 180 min (vii) 240 and (viii) 300 min. Gas composition: 1000 ppm NO, 2000 ppm C_3H_6, 5% O_2, 10% CO_2, 20 ppm SO_2, He balance*

The influence of SO_2 on the formation of suggested reaction intermediates on the catalyst surface was examined. IR spectra recorded on AgAl in the course of the NO+C_3H_6+O_2 reactions with 20 ppm SO_2 are presented in Figure 2.7A (ii-viii). After exposure to 20 ppm SO_2 very weak signal for silver sulphate species starts appearing after 30 min at 1313 cm^{-1} which appears as broadening of the 1304 peak. The broadening of the peak at 1304 cm^{-1} becomes more evident from 30 min to 300 min and the peak broadens with maxima shifted to 1313 and 1296 cm^{-1}. It suggests the formation of silver sulphate species on the catalyst surface leading to deactivation due

to sulphur poisoning. After exposure to SO_2 the previously discussed IR bands ascribed to acetates, formates and nitrates do not disappear. On the other hand the IR bands associated with Ag-NCO at 2226 and Al-NCO at 2258 cm^{-1} gradually decreases in intensity from 10 min to 300 min. In parallel, the broad bands at 1558 cm^{-1} and 1445 cm^{-1} intensify which correspond to the development of nitrates species as well as adsorbed C-containing intermediates. This result indicates the sulfation of Ag phase in case of AgAl in presence of 20 ppm SO_2.

Table 2.3 *Assignments of IR bands formed on AgAl, AgSiAl and AgTiAl during in- situ studies*

Wavenumber (cm^{-1})	**Surface species**	**Vibrations**	**Observed wavenumber (cm^{-1})**	**References**
1585	Carboxylate COO^-	ν^a_{OCO}	1586	[36]
1460		ν^s_{OCO}	1456 and 1471	
1595	Formate $HCOO^-$	ν^a_{OCO}	1591	[36]
1380		ν^s_{OCO}	1377	
1390		δ_{CH}	1390	
1550	Monodentate nitrate NO_3^-	$\nu_{N=O}$	1558	[36]
1250		ν^a_{ONO}	Not detected	
1590	Bidentate nitrate NO_3^-	$\nu_{N=O}$	1595	[36]
1305		ν^a_{ONO}	1304, 1301	[36]
1560	Ad-NO_x		1558	[36]
1313	Ag_2SO_4		1313	[8]
1384	$Al(SO_4)_3$		Not detected	[8]
1637	H_2C=CH-O-M		1644	[37]
2230	Ag-NCO		2226, 2229	[24]
2260	Al-NCO		2255, 2258, 2261	[24]

(s= symmetric, a= asymmetric and δ=bending)

In case of AgSiAl (Figure 2.8) and AgTiAl (Figure 2.9) exposure to 20 ppm SO_2 shows formation of Ag-sulphate at 1313 cm^{-1} only after 120 min (Figure 2.8A-v

and 9A-v inset). The delayed formation of silver sulphate in case of AgSiAl and AgTiAl proves the improved sulphur tolerance of both the catalysts. It is noticeable that the decrease in intensity of the IR band assigned to Ag-NCO and Al-NCO on AgSiAl and AgTiAl is not significant compared to AgAl which can be correlated to a lesser deactivation on AgSiAl and AgTiAl than on AgAl due to SO_2 poisoning. The sulphation of Al_2O_3 generally evidenced by the presence of a 1384 cm^{-1} IR band (Al-sulfate) is not significantly observed even after 300 min exposure to SO_2, in case of all the catalysts which may be due to low concentration of SO_2 in the feed gas. Nevertheless, it must be mentioned here that the intensities of the IR bands for all adsorbed species in the absence of 20 ppm SO_2 (acetates, nitrates, etc) do not significantly change after SO_2 addition except for AgAl after 300 min SO_2 exposure.. This is because the adsorption of NO is known to take place on basic sites and in presence of SO_2 in the feed; there is a site competition between SO_2 and NO_x molecules [38]. Additionally, it is also worthwhile to note that the higher amount of nitrates, acetates on AgAlSi and AgTiAl correspond to a more extensive accumulation of isocyanate species both on Ag and alumina which seems to be well in agreement with previous mechanistic proposals where those adsorbates are supposed to be reactive intermediate for the formation of nitrogen [23].

In this present study, the increased sulphur tolerance of AgSiAl and AgTiAl can be explained on the basis of two factors: acidity of the support and the related extent of interaction between S-containing species and alumina and/or Ag species. The amount of SO_2 deposited onto the support is dependent on the acidity of the support and SO_2 being acidic increase in the acidity of the support results in decrease in the amount of SO_2 adsorbed. The addition of SiO_2 or TiO_2 to AgAl has led to increase in the acidity of the support as mentioned in section 3.3 [29, 39, 40]. This increase in acidity has enhanced the SO_2 desorption from the support, thereby reducing the extent of sulphation of the catalytically active phases i.e. Ag and Al_2O_3 and maintaining the high catalytic activity even in presence of SO_2. Secondly, the sulphates of SiO_2 [17] and TiO_2 [18] are known to be thermally less stable than the sulphates of Al_2O_3 [18]. This means that even if the SiO_2 and TiO_2 sites are sulphated, these would desorb more easily from the catalyst support than $Al_2(SO_4)_3$. It is well reported in the literature that role of Ag in Ag/Al_2O_3 system is the partial oxidation of C_3H_6 to form surface enolic species which in turn react with the adsorbed nitrates to form -NCO species, an important intermediate in the SCR of NO_x with C_3H_6 whereas

that of Al_2O_3 is to reduce NO_x to N_2 [10]. It may be concluded from the *in situ* DRIFTS results that over AgSiAl and AgTiAl the increase in the catalyst acidity suppressed the sulphur poisoning of Ag and Al_2O_3 sites up to certain extent and the lower stability of the sulphates of SiO_2 and TiO_2 could facilitate the fast desorption of sulphate species from the support thus retaining the activity of the catalysts even in the presence of SO_2.

2.4. Conclusions

The alumina support in case of Ag/Al_2O_3 has been modified for improving sulphur tolerance for SCR of NO_x using propene as reductant. Alumina doping with 1% SiO_2 or 1% TiO_2 has shown a remarkable improvement in the sulphur tolerance. The *in situ* FTIR study has shown that the deactivation of the catalyst is due to the formation of sulphates of Ag and Al_2O_3, which is minimized in presence of SiO_2 or TiO_2. The improved sulphur tolerance is due to the increase in the acidity of the catalyst thus decreasing the sulphate formation as well as lower stability of the sulphates of SiO_2 and TiO_2.

2.5. References

1. A. Obuchi, A. Ohi, M. Nakamura, A. Ogata, K. Mizuno, H. Ohuchi, *Appl. Catal. B* 2 (**1993**) 71.
2. R. Burch, J. P. Breen, F. C. Meunier, *Appl. Catal. B* 39 (**2002**) 283.
3. W. Held, A. Koenig, T. Richier, L. Puppe, SAE Paper 900496 (**1990**) 219.
4. M. Iwamoto, H. Yahiro, S. Shundo, Y. Yu-u, N. Mizuno, Shokubai (Catalyst) 32 (**1990**) 430.
5. A. Martinez-Arias, M. Fernandez-Garcia, A. Iglesias-Juez, J. A.Anderson, J. C. Conesa, J. Soria, *Appl. Catal. B* 28 (**2000**) 29.
6. H. Hamada, *Catal. Today* 22 (**1994**) 21.
7 K. Eränen, F. Klingstedt, K. Arve, L-E. Lindfors, D.Y. Murzin, *J. Catal*. 227 (**2004**) 328.
8. F. C. Meunier, J. R. H. Ross, *Appl. Catal. B* 24 (**2000**) 23.
9. H. W. Jen, *Catal. Today* 42 (**1998**) 37.
10. P. W. Park, C. L. Boyer, *Appl. Catal. B* 59 (**2005**) 27.
11. A. Abe, N. Aoyama, S. Sumiya, N. Kakuta, K. Yoshida, *Catal. Lett*. 51 (**1998**) 5.
12. S. Sumiya, M. Saito, H. He, Q.C. Feng, N. Takezawa, K. Yoshida, *Catal. Lett*. 50 (**1998**) 87.
13. T. N. Angelidis, S. Christoforou, A. Bongiovanni, N. Kruse, *Appl. Catal. B* 39 (**2002**) 197.
14. T. J. Lee, In-Sik Nam, S-W. Ham, Y-S. Baek, K-H. Shin, *Appl. Catal. B* 41 (**2003**) 115.
15. J. Wang, H. He, Q. Feng, Y. Yu, K. Yoshida, *Catal. Today* 93-95 (**2004**) 783.
16. J. Wang, H. He, S. Xie, Y. Yu, *Catal. Commun*. 6 (**2005**) 195.
17. B. A. Morrow, R. A. Mcfarlane, M. Lion, J. C. Lavalley, *J. Catal*. 107 (**1987**) 232.
18. O. Saur, M. Bensitel, A. B. M. Saad, J.-C. Lavally, C. P. Tripp, B. A. Morrow, *J. Catal.* 99 (**1986**) 104.
19. M. Haneda, Y. Kintaichi, H. Hamada, *Appl. Catal. B* 31 (**2001**) 251.
20. S. Rajagopal, J. A. Marzari, R. Miranda, *J. Catal*. 151 (**1995**) 192.
21. M. F. Williams, B. Fonfé, C. Sievers, A. Abraham, J. A. van Bokhoven, A. Jentys, J. A. R. van Veen, J. A. Lercher, *J. Catal*. 251 (**2007**) 485.

22. M. R. Basila, T. R. Kantner, K. H. Rhee, *J. Phys. Chem*. 68 (**1964)** 3197.
23. J. Li, Y. Zhu, R. Ke, J. Hao, *Appl. Catal. B* 80 (**2008**) 202.
24. S. Kameoka, T. Chafik, Y.Ukisu, T. Miyadera, *Catal. Lett*. 55 (**1998**) 211.
25. H. Imagawa, T. Tanaka, N. Takahashi, S. Matsunaga, A. Suda, H. Shinjoh, *Appl. Catal. B* 86 (**2008**) 63.
26. J. P. Breen, R. Burch, C. Hardacre, C. J. Hill, B. Krutzsch, B. Bandl-Konrad, E. Jobson, L. Cider, P. G. Blakeman, L. J. Peace, M. V. Twigg, M. Preis, M. Gottschling, *Appl. Catal. B* 70 (**2007**) 36.
27. Y. Li, P. J. Battavio, J. N. Armor, *J.Catal*. 142 (**1993**) 561.
28. M. H. Kim, In-Sik. Nam, Y. G. Kim, *Appl. Catal. B* 12 (**1997**) 125.
29. S. Matsumoto, Y. Ikeda, H. Suzuki, M. Ogai, N. Miyoshi, *Appl. Catal. B* 25 (**2000**) 115.
30. K. Shimizu, A. Satsuma, T. Hattori, *Appl. Catal. B* 25 (**2000**) 239.
31. H. He, Y. Yu, *Catal. Today* 100 (**2005**) 37.
32. Y. Kuroda, T. Mori, H. Sugiyama, Y. Uozumi, K. Ikeda, A. Itadani, M. Nagao, *J. Colloid Interface Sci.* 333 **(2009)** 294.
33. J. T. Ranney, S. R. Bare, J. L. Gland, *Catal. Lett.* 48 **(1997)** 25.
34. S. Satokawa, *Chem. Lett.* 29 **(2000)** 294.
35. S. Satokawa, J. Shibata, K. Shimizu, A. Satsuma, T. Hattori, *Appl. Catal. B* 42 (**2003**) 179.
36. F. C. Meunier, J. P. Breen, V. Zuzaniuk, M. Olsson, J. R. H. Ross, *J. Catal*. 187 (**1999**) 493.
37. H. He, J. Wang, Q. Feng, *Appl. Catal. B* 46 (**2003**) 365.
38. R. Burch, E. Halpin, J.A. Sullivan, *Appl. Catal B* 17 (**1998**) 115.
39. J. Valvon, M. Henker, K. –P. Wendlandt, *React. Kinet. Catal. Lett*. 38 (**1989**) 265.
40. H. Hirata, I. Hachisuka, Y. Ikeda, S. Tsuji, S. Matsumoto, *Top. Catal*. 16-17 (**2001**) 145.

Chapter 3: Effect of Magnesia Modification on the Low Temperature Catalytic Activity and Sulphur Tolerance of Ag/Al_2O_3 System

A series of magnesium incorporated silver alumina samples were prepared and tested for the SCR of NO_x using propene under lean conditions. Addition of magnesium improved the low temperature catalytic activity and the sulphur tolerance of silver alumina system. The improvement in low temperature activity was correlated to decreased acidity upon addition of magnesium. FTIR study showed that the deactivation in the presence of SO_2 was due to the sulphation of silver and aluminum sites in Ag/Al_2O_3 catalyst whereas, its formation is suppressed in the case of magnesium doped Ag/Al_2O_3.

Chapter 3: Effect of Magnesia Modification on the Low Temperature Catalytic Activity and Sulphur Tolerance of Ag/Al_2O_3 System

1.1. Introduction

Lean burn engines emit less CO_2 by virtue of complete combustion of fuel in the presence of excess of oxygen compared to their stoichiometric spark ignited gasoline counterparts and hence are becoming more popular. The three way catalysts which simultaneously convert NO_x, CO and HCs into N_2, CO_2 and H_2O from the exhaust of stoichiometric spark ignited gasoline engines are not capable of reducing NO_x from the exhaust of lean burn engines because of the presence of large excess of oxygen [1]. Thus, the removal of NO_x from the exhaust of lean-burn engines is a major challenge because it requires using the limited reductant to selectively react with NO rather than O_2. Therefore worldwide lot of efforts have been taken both academically and industrially to develop suitable technologies/catalysts for the reduction of NO_x under lean conditions. There are mainly two catalytic technologies for the removal of NO_x under lean conditions viz; the NO_x storage reduction (NSR) developed by Toyota [2, 3] and hydrocarbon selective catalytic reduction (HC-SCR) [4]. Though NSR technology has been commercialized in Japan where low sulphur content fuel is available, the major drawback of this catalyst is its sensitivity to deactivation by sulphur poisoning. In the presence of SO_x, the NO_x adsorption sites are occupied by sulphur species causing a decrease in the number of available sites for NO_x adsorption eventually leading to catalyst deactivation. In this context, HC-SCR seems to be a promising method for the removal of NO_x under lean conditions since this method exploits unburned hydrocarbons already contained in the exhaust gas stream. Many catalytic formulations have been evaluated for the HC-SCR of NO_x in presence of excess of O_2 [5] and can be classified into three categories: ion-exchanged zeolite catalysts, metal oxide catalysts, and supported precious metal catalysts. Although metal exchanged zeolite catalysts exhibit high activity for the reduction of NO these have the disadvantage of insufficient hydrothermal stability under realistic exhaust compositions. Precious metal-based catalysts (PGM), especially Pt based catalysts such as Pt/Al_2O_3 exhibit the best low temperature activity (lower than

300 °C) [6] and are more resistant to water vapor and SO_x poisoning. But these have two major disadvantages: low selectivity towards N_2 (substantial amount of N_2O is formed) and narrow temperature window of operation for NO reduction [5, 7]. Metal oxide-based catalysts, for example Al_2O_3, TiO_2, ZrO_2, MgO and these oxides promoted by, e.g. Co, Ni, Cu, Fe, Sn, Ga, In, Ag compounds have been reported to be active for HC-SCR [8-10]. Amongst these, Ag/Al_2O_3 is thought to be the most promising candidate for practical use since it exhibits high activity for NO reduction, high selectivity towards N_2 and moderate tolerance to SO_x and water vapor, especially at higher temperatures [5, 11]. However the major drawback of this system is the negligible activity and poor SO_2 tolerance at low temperatures (573-673 K). The low activity in this temperature region is due to poor activation of the reductant on the alumina supported catalyst whereas the activity loss in the presence of SO_2 is due to the sulphation of active sites (Ag and Al_2O_3). Many authors have investigated the influence of SO_2 on the catalytic activity in details and mechanistic studies have proven that the deactivation is caused due to the formation of silver and aluminum sulphate species [5 and references therein, 12, 13]. Thus improvement in the low temperature activity and SO_2 tolerance in the temperature range 573 -673 K is still a major challenge for HC-SCR.

One way of improving the low temperature activity and the SO_2 tolerance is by modification of the support with a promoter. Magnesia seems to be a promising promoter for these applications for two reasons:

(i) It has been reported in the literature that the modification of alumina support with magnesia has enhanced the conversion of NO to N_2 [14]. The presence of magnesia modified the surface acid sites of alumina supports leading to the promotion of the SCR activity.

(ii) Magnesium oxide is used as a catalyst support for chemisorption of SO_2 [15] whereas magnesium aluminate spienel is used as a sulphur transfer catalyst [16] in fluidized catalytic cracking (FCC) processes.

Based on these considerations magnesia was used in the present study to modify the alumina support so as to improve the low temperature catalytic activity and SO_2 tolerance of $AgAl_2O_3$ system in the SCR of NO_x with C_3H_6. The aim was to investigate the influence of MgO component on the catalytic activity and sulphur tolerance of Ag/Al_2O_3 system in NO reduction with C_3H_6.

3.2. Experimental Section

3.2.1. Materials

Commercially available boehmite (AlOOH) was used as a precursor of γ-Al_2O_3. Magnesium nitrate $Mg(NO_3)_2$. $6H_2O$ and silver nitrate ($AgNO_3$) purchased from Merck were of analytical grade and used without further purification.

3.2.2. Catalyst Preparation

The series of Ag-Mg/Al_2O_3 catalysts were prepared with 2% Ag loading and varying the Mg content from 5.5 wt% to 17 wt% by impregnation method. In a typical preparation of the catalyst containing 5.5 wt % Mg, 6.11 g of $Mg(NO_3)_2$.6 H_2O was dissolved in distilled water. To this solution boehmite (13.89 g) was added under constant stirring. The solution was evaporated and the sample dried overnight at 373 K and then calcined at 773 K for 6 h. To this calcined sample aqueous silver nitrate solution (0.214g) was added, stirred on a hot plate and dried overnight at 373 K followed by calcination in air at 873 K for 6 h. The final sample was labeled as Ag5.5MgAl, where 5.5 denotes the amount of Mg in wt%. The above procedure was repeated for the preparation of the samples with magnesium content 7, 11, and 17 wt% Mg. For comparison, alumina-supported silver catalyst (2 wt% Ag, labeled as AgAl) was prepared by impregnation method with aqueous silver nitrate solution. The sample was dried overnight at 373 K and calcined in air at 773 K for 6 h.

3.2.3. Catalysts characterization

(a) Powder X-ray diffraction studies

The powder X-ray diffraction data was collected on a Rigaku Miniflex diffractometer equipped with a Ni filtered Cu Kα radiation (λ = 1.5406 Å, 30 kV, 15 mA) radiation. The data was collected in the 2θ range 20-80° with a step size of 0.02° and scan rate of 4° min^{-1}.

(b) Nitrogen adsorption studies

The BET surface area of the calcined samples was determined by N_2 sorption at 77 K using NOVA 1200 (Quanta Chrome) equipment. Prior to N_2 adsorption, the

material was evacuated at 573 K under vacuum. The specific surface area, S_{BET}, was determined according to the BET equation.

(c) NH_3 temperature programmed desorption (TPD) studies

The NH_3 temperature programmed desorption (TPD) experiments were performed using a Micromeritics Autochem 2910 instrument. A weighed amount of the sample ($\approx$100 mg) was placed in a quartz reactor, pretreated in a flow of He gas at 773 K for 1 h (ramp rate of 10 K min^{-1}) and cooled to 373 K. The catalyst was then exposed to a gas mixture of NH_3 (5% NH_3-95% He, 50 ml min^{-1}) at 373 K, followed by evacuation at 373 K for 3 h. The temperature was raised to 973 K at a heating rate of 10 K min^{-1}. Then, the measurement was made from 373 K with a heating rate of 5 K min^{-1} in flowing He as a carrier gas at a flow rate of 60 ml min^{-1} until ammonia was desorbed completely. A thermal conductivity detector (TCD) was employed at the outlet of the reactor to measure the volume of ammonia consumed during reduction of the samples.

(d) In situ Diffuse Reflectance FT-IR studies (DRIFTS)

The diffuse reflectance FT-IR measurements were carried out under a flow of He in a high temperature cell (Spectra-Tech) fitted with a Zn-Se window (Shimadzu 8000 FTIR spectrophotometer). The temperature in the cell was varied from 303 to 698 K. About (30 mg) of finely crushed sample was placed in a sample holder and pretreated at 698 K for 2 h in He flow to remove adsorbed moisture. The spectrum of neat catalyst was recorded (400 scans with resolution 4 cm^{-1}) at 623 K prior to the experiment under He flow. The reported spectra are difference spectra of adsorbed species and neat catalyst.

3.2.4. Catalytic activity measurement

The SCR of NO by propene was carried out at atmospheric pressure in a tubular down flow reactor (inner diameter 4 mm). A mechanical mixture of catalyst powder (500 mg, particle size < 180 μm) and commercial silica gel (2.0 gm, particle size 125-250 μm) was placed in the reactor and a thermocouple was inserted in the center of the catalyst bed to measure the temperature. Prior to the reaction the catalyst was activated at 773 K for 1 h in 10% O_2/He flow. The typical reactant gas mixture

consisting of NO (1000 ppm), C_3H_6 (2000 ppm) CO_2 (10%), O_2 (5%), 20 ppm SO_2 gas (when added) and balance He were fed from independent mass flow controllers. The online analysis of the effluent gases was carried out by monitoring the relative masses m/z = 30 (NO), 28 (N_2), 44 (N_2O, CO_2), 41 (C_3H_6) and 46 (NO_2) as function of time using a quadropole mass spectrometer (Hiden Analytical HPR 20), a chemiluminescence's $NO/NO_2/NO_x$ analyzer (42C HL, Thermo Environmental) and a micro GC (Agilent 3000A) equipped with a molecular sieve 5Å column. The reaction was carried out at a gas hourly space velocity (GHSV) of 20000 h^{-1} (W/F =0.05 g h L^{-1}). In these studies NO and C_3H_6 conversions were calculated as follows:

$$\text{NO conversion (\%)} = \frac{[NO_x]_{inlet} - [NO_x]_{outlet}}{[NO_x]_{inlet}} \times 100$$

$$C_3H_6 \text{ conversion (\%)} = \frac{[C_3H_6]_{inlet} - [C_3H_6]_{outlet}}{[C_3H_6]_{inlet}} \times 100$$

3.3. Results and Discussion

3.3.1. Structural and Textural properties

Table 3.1 shows the BET surface area of γ-Al_2O_3, AgAl and AgMgAl samples prepared in this study. Addition of Ag to the γ-Al_2O_3 support has led to the decrease in the surface area. In the case of Mg modified silver alumina catalysts, the increase in the loading of Mg from 5.5 wt% to 17 wt% has resulted in the decrease of surface area from 169 m^2 g^{-1} to 111 m^2 g^{-1}. This is due to the blocking of the pores of γ-Al_2O_3 after impregnation of the support with metal oxides. Figure 3.1 shows the XRD patterns of the series of catalysts prepared. For comparison, the XRD pattern of γ-Al_2O_3 is also shown. Incorporation of Ag in all the samples did not show any separate phase of bulk metallic Ag or Ag_2O species indicating high dispersion of Ag on the support as well as amorphous nature due to low silver loading (2 wt% Ag).

Table 3.1 *Specific surface area and total acidity of the catalysts*

Samples	**Surface area (m^2g^{-1})**	**Total acidity of support (mmol g^{-1})**

γ- Al_2O_3	237	0.714
AgAl	216	0.615
Ag5.5MgAl	169	0.550
Ag7MgAl	166	0.527
Ag11MgAl	157	0.483
Ag17MgAl	111	0.412

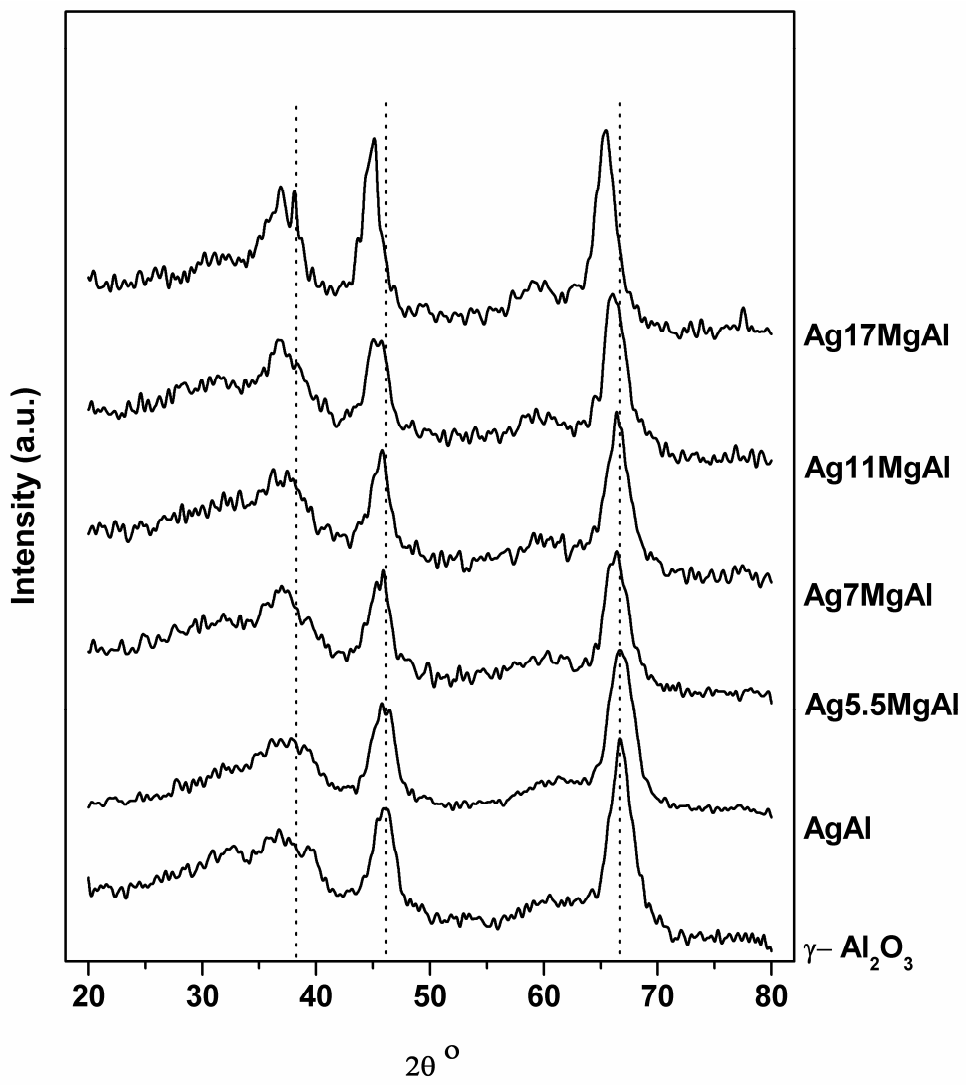

Figure 3.1 *X-ray diffraction pattern of fresh γ-Al_2O_3 and the different magnesium modified Ag/Al_2O_3 samples*

For AgAl sample, only the diffraction lines assignable to γ-Al_2O_3 phase located at 2θ = 36.7, 46.0 and 66.90° (JCPDS: 29-0063) were observed. In case of Mg modified samples, similar trend was seen upto 7 wt% Mg loading. Further increase in the Mg loading (11 and 17 wt%) has resulted in the shift in the peaks at 46.0 and 66.90° to

45.10 and 65.35° indicating the formation of magnesium aluminate ($MgAl_2O_4$) phase (JCPDS: 47-0254).

3.3.2. NH_3 TPD studies

The total acidity of the samples measured by temperature programmed desorption of NH_3 is shown in Table 3.1. Pure γ-Al_2O_3 showed the highest acidity (0.714 mmol g^{-1}) amongst all the samples. Addition of 2 % Ag onto the support led to the decrease in the total acidity of the support. This result can be corroborated with the BET surface area results, which showed decrease in the surface area due to blocking of the alumina pores upon incorporation of Ag. The acidity further decreased in case of Mg loaded samples. The acidity decreased with increasing Mg loading from 0.550 mmol g^{-1} for Ag5.5MgAl to 0.412 mmol g^{-1} of support for Ag17MgAl (Table 3.1). From the above results it is seen that the total acidity decreased with the incorporation of magnesia into alumina.

3.3.3. Catalytic activity study

The catalytic activity of AgAl and AgMgAl with different Mg content in the SCR of NO using propene was examined in the absence and presence of SO_2. Over the temperature range studied N_2 was the only product formed and no undesirable products (NO_2 and N_2O) were formed

(a) Catalytic performance of AgMgAl in the absence of SO_2

Figure 3.2 shows the temperature dependent study of NO and C_3H_6 conversion over AgAl and AgMgAl samples in the 573 to 673 K range. As seen from Figure 3.2A, the NO conversion began at 573 K and increased with increase in the temperature for all the samples. It can be seen that the modification of the alumina support with a small amount of Mg improves the low temperature activity compared to AgAl. Ag5.5MgAl showed 78% NO conversion as compared to 44% NO conversion over AgAl at 623 K (Figure 3.2A). Amongst the Mg modified catalysts prepared, Ag7MgAl showed maximum activity with 98% NO conversion at 623 K. Further increase in Mg loading had a detrimental effect on NO conversion. The catalyst containing 11 wt% (Ag11MgAl) and 17 wt% (Ag17MgAl) Mg loading showed 61% and 59% NO conversion respectively at 623 K (Figure 3.2A). Similar enhancement in NO reduction activity upon addition of Mg has been previously

reported [12]. In their study, the influence of different weight percentages of Mg (1, 2.5, 5, 7 and 10 wt%) over Ag (3 wt%) impregnated alumina catalyst in the NO reduction activity was studied.

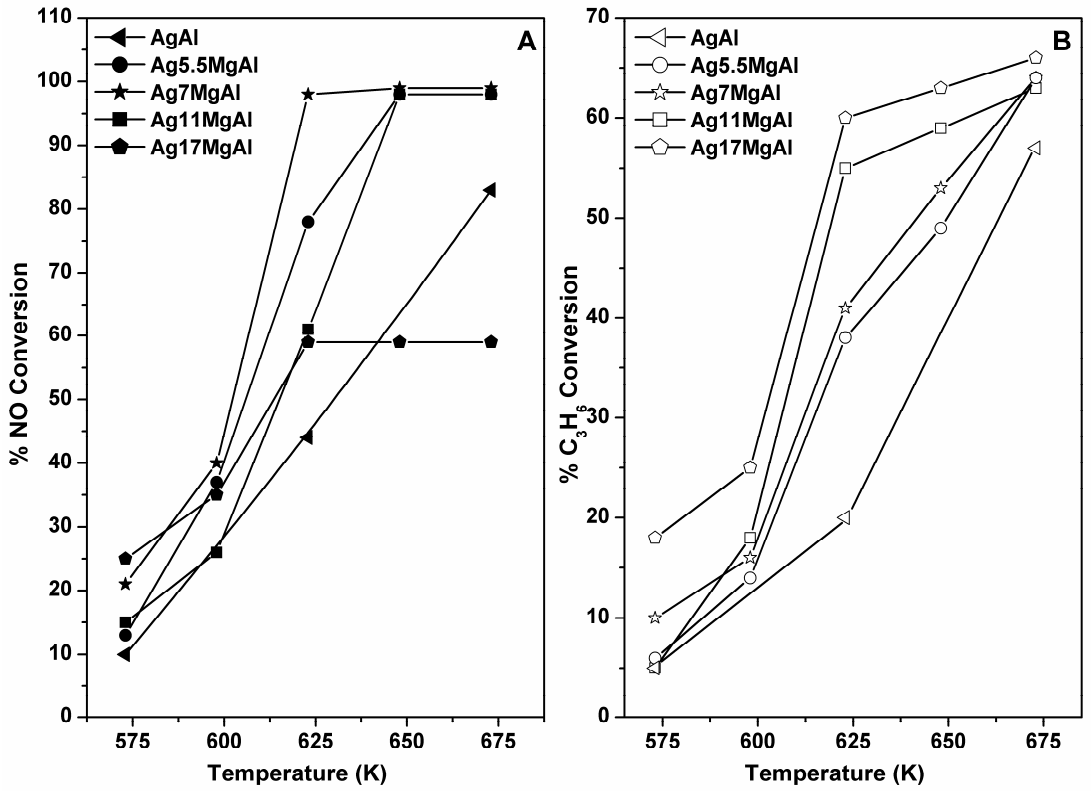

Figure 3.2 *NO conversion (A) and C_3H_6 conversion (B) over AgAl and AgMgAl samples as a function of temperature. Reaction conditions: 1000 ppm NO, 2000 ppm C_3H_6, 5% O_2, 10% CO_2, He balance, GHSV= 20000 h^{-1}*

With increase in the Mg content from 1 to 5 wt% progressive increase in the reduction of NO to N_2 was observed however further increase in Mg content has resulted in decreased NO conversion. Among the series of catalysts prepared the best catalytic activity was displayed by the catalyst containing 5 wt% Mg (Mg(5)SA) whereas the least activity was shown by the catalyst containing the highest amount (10 wt%) of Mg (Mg(10)SA). The high catalytic activity over Mg(5)SA was attributed to the presence of high percentage of magnesium aluminate ($MgAl_2O_4$) phase (confirmed by XRD and XPS studies). They concluded that the formation of $MgAl_2O_4$ in the catalyst Mg(5)SA enhanced the dispersion and stabilization of silver phases and also resulted in optimal high surface availability of Ag^0 and Ag^+ species which in turn

promoted the NO reduction. In case of the catalyst Mg(10)SA the poor activity was ascribed to the presence of different phases of Mg viz; MgO and $MgAl_2O_4$. It was concluded that the presence of MgO and $MgAl_2O_4$ in Mg(10)SA led to agglomeration of silver particles. The poor dispersion of silver promoted the non-selective oxidation of C_3H_6 instead of NO reduction which resulted in low activity. These results show that there is an optimal amount of Mg that is needed to enhance the catalytic activity and that the presence of higher amount of Mg would lead to decreased activity. Our data can be discussed in view of these results. First it needs to be emphasized here that the whole series of samples containing Mg prepared in this study gave better NO conversion in the whole temperature range studied as compared to AgAl. Even the catalyst containing the highest amount of Mg (Ag17MgAl) gave better NO conversion (59%) as compared to AgAl (44%) at 623 K. As discussed above, in the present study Ag7MgAl gave the best NO conversion at 623 K amongst all the catalysts studied. Although formation of $MgAl_2O_4$ phase was not detected in this catalyst, it can be said from the discussion above that the addition of optimal amount of Mg (7 wt% in this study) to silver alumina system may have resulted in better dispersion and stabilization of silver along with high surface availability of Ag^0 and Ag^+ species [12]. As for the decrease in NO conversion with increasing Mg content over Ag17MgAl (59%) and Ag11MgAl (61%) as compared to Ag7MgAl (98%) and Ag5.5MgAl (78%) at 623 K it may be attributed to the decrease in the number of active sites by Mg, which is less active than Al_2O_3 [18]. Park *et al* have already reported that in the SCR of NO_x the role of Al_2O_3 in Ag/Al_2O_3 system is to reduce NO_x to N_2 [19]. For Ag11MgAl and Ag17MgAl high Mg loading probably leads to blocking of the alumina surface, which consequently results in decreased NO reduction activity.

The improvement in the NO reduction activity upon addition of Mg can be explained on the basis of activation of C_3H_6. The importance of surface acid–base property in NO reduction has been emphasized by many researchers [14, 20-22]. It is well-known that activation of C_3H_6 takes place on Brønsted acid sites [23]. Haneda *et al* [23] have reported that the creation of Brønsted acid sites in the presence of 90 ppm SO_2 over Ga_2O_3-Al_2O_3 accelerated the C_3H_6 oxidation step. Similarly, Masters and Chadwick [24] reported that the activation of methanol is promoted on Brønsted acid sites created by SO_2 adsorption on γ-Al_2O_3. Our group in a recently published paper has reported improved SO_2 tolerance of Ag/Al_2O_3 system after incorporation of 1 wt% of SiO_2 or TiO_2 [25]. However the enhanced SO_2 tolerance, which was

attributed to the strengthening of Lewis acid sites (LAS) on the incorporation of above-mentioned additives, was accompanied by a slight decrease in the NO reduction activity. The reaction conditions used were similar to those in the present study. In the absence of water AgAl gave 44% NO and 20% C_3H_6 conversion at 623 K. Upon modification of the support by incorporation of 1 wt% SiO_2 (AgSiAl) or 1 wt% TiO_2 (AgTiAl) the NO conversion slightly decreased to 36% and 38% respectively. Similar trend was observed in case of propene conversion with 17% on AgSiAl and least propene conversion on AgTiAl (13% at 623 K). In the present case the improvement in the low temperature activity in NO reduction over Mg modified sample can be explained on the basis of decrease in the total acidity of the support, which in turn has resulted in low temperature activation of C_3H_6. Alumina which is often used as a support for SCR of NO_x has strong acid as well as strong basic sites. The addition of magnesia to the alumina system is known to neutralize the acidity of alumina [26-27]. The total acidity and acid strength of magnesia alumina mixed oxide support was measured by microcalorimetric method by Aberuagba *et al* [28]. It was found that the total acidity decreased with the incorporation of magnesia into alumina. The strong acid sites which were noticeable in pure alumina were completely neutralized with the incorporation of 50% magnesia. At higher loadings of magnesia where the strong acid sites were absent, medium and weak acid sites were predominant. Klisińska *et al* [29] studied the effect of additives on V_2O_5/SiO_2 (VSiA) and V_2O_5/MgO (VMgA) catalysts in the oxidative dehydrogenation of propane and ethane. They reported that the additives did not affect markedly the catalyst structure, but modify their acido-basic properties and reducibility. The pyridine sorption measurements showed that these two systems differ in type of the acid sites, the VMgA series exhibiting less LAS, slightly lower amounts of strong sites and lower strength of sites as compared with VSiA, and no Brønsted acid sites. Similar results were reported by Hong *et al* [30] who reported that the modification of the alumina support with magnesia resulted in stable activity of the supported vanadium-antimony oxide catalysts for the dehydrogenation of ethylbenzene to styrene. They correlated the enhanced catalytic activity to the reduced acid sites of VSb/MgAl (magnesia modified alumina supported vanadium-antimony)) catalysts compared to the un-modified VSb/Al (alumina supported vanadium-antimony) catalyst. From the above discussion it is clear that though magnesia incorporation did not result in the generation of Brønsted acid sites, however it led to the weakening of Lewis acid sites.

In the present case these observations can be correlated with our results. From the NH_3 TPD data (Table 3.1) it is clear that the total acidity of the support has decreased with increasing amount of Mg. This decreased acidity has helped in the activation of C_3H_6 over Mg incorporated samples, which in turn has improved the NO reduction activity.

Figure 3.2B shows the propene conversion over AgAl and AgMgAl samples as a function of temperature. AgAl showed 20% C_3H_6 conversion at 623 K. Addition of 5.5 wt% Mg resulted in higher C_3H_6 conversion (38%) as compared to AgAl. Amongst the Mg incorporated samples, Ag5.5MgAl showed the lowest C_3H_6 conversion (38%) whereas Ag17MgAl showed highest C_3H_6 conversion (60 %) at 623 K. However the NO conversion over Ag17MgAl at this temperature was much less as compared to Ag5.5MgAl (Figure 3.2). From this result it can be said that increasing the Mg content favors the unselective oxidation of C_3H_6 rather than the selective reduction of NO. Similar results were reported by Kumar *et al* [12] who correlated this behaviour to the presence of MgO phase and bigger silver particles in their sample. Previous reports on Ag/Al_2O_3 catalysts [17] revealed that the presence of larger silver particles at higher loadings resulted in low NO reduction and complete oxidation of C_3H_6. As for the selectivity behavior, addition of Mg has improved the selectivity of C_3H_6 towards NO reduction. Over all the catalysts prepared in this study the C_3H_6 conversion remained below 65% even when NO reduction was almost 100%. Generally, in the presence of excess of oxygen with increase in the temperature the unselective oxidation of C_3H_6 is favored which leads to low NO reduction. In the present case however this trend was not observed which shows that the addition of Mg has led to selective use of C_3H_6 in NO reduction.

(b) Catalytic performance of AgAl and Ag7MgAl in the presence of SO_2

The effect of SO_2 addition under dry conditions on the catalytic activity as a function of time-on-stream was monitored at 623 K based on the preliminary results which showed that Ag7MgAl showed maximum NO conversion at this temperature. First the catalyst was exposed to a reaction mixture containing 1000 ppm NO + 2000 ppm C_3H_6 + 5% O_2 + 10 % CO_2 for 60 min. After the measurement of steady state NO conversion in the absence of SO_2, 20 ppm SO_2 was added to the feed gas and NO conversion measured. The effect on NO conversion after the addition of 20 ppm SO_2 on the catalytic activity of AgAl and Ag7MgAl is shown in Figure 3.3.

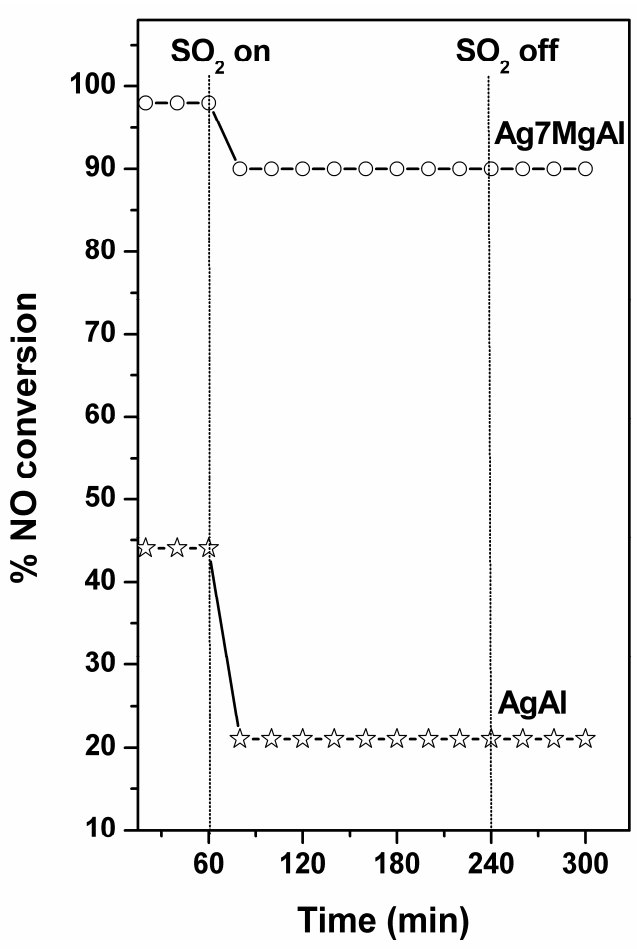

Figure 3.3 C*omparative study of SO_2 tolerance of AgAl and Ag7MgAl as a function of time. Reaction conditions: 1000 ppm NO, 2000 ppm C_3H_6, 5%* O_2, 10*% CO_2, 20 ppm SO_2, He balance, GHSV= 20000 h^{-1}, Temp. 623 K*

In the absence of SO_2, AgAl showed 44% NO conversion which decreases to 21% in the presence of 20 ppm SO_2. On the other hand, upon exposure to 20 ppm SO_2 the NO conversion over Ag7MgAl decreased marginally form 98% to 90%. From these results, it is evident that SO_2 has considerable negative impact on the catalytic activity of AgAl whereas on Ag7MgAl the effect is not that profound. However it must be noted here that over both the catalyst, even after removal of SO_2 from the feed gas the catalytic activity was not regained to its original value indicating that the deactivation caused was irreversible.

3.3.4. In situ DRIFTS study

In order to examine the cause of catalyst deactivation in presence of SO_2, and to study the mechanism of deactivation, *in situ* FTIR studies were carried out in the absence of water. Since the deactivation due to SO_2 was more prominent at 623 K the *in-situ* DRIFTS analysis was carried out at this temperature. Two sets of experiments were carried out for each catalyst. In the first experiment, standard SCR gas mixture (1000 ppm NO + 2000 ppm C_3H_6 + 10 % CO_2 + 5% O_2) was passed over the catalyst at 623 K and the species formed were monitored as a function of time. In second experiment along with standard SCR mixture, 20 ppm SO_2 was introduced in the feed at 623 K and the formation of different species was monitored as a function of time and the results are shown in Figure 3.4 and 3.5 respectively. For reference the spectrum in absence of SO_2 (exposed to 1000 ppm NO + 2000 ppm C_3H_6+ 10 % CO_2 + 5% O_2 for 60 min) for AgAl [Figure 3.4A (i)] and Ag7MgAl [Figure 3.5A (i)] is also included. Based on previous literature data [17, 31-32], IR bands assigned to monodentate nitrate (1250, 1550 cm^{-1}), bidentate nitrate (1305, 1590 cm^{-1}), acetate species (1460, 1585 cm^{-1}), formate species (1595, 1390, 1380cm^{-1}), enolic (1637 cm^{-1}) and NCO species (Ag-NCO 2235 cm^{-1} and Al-NCO-2259 cm^{-1}) are summarized in Table 3.2. For AgAl catalysts in absence of SO_2 [Figure 3.5 A (i)] the characteristic infrared bands due to acetates (1574, 1445 and 1471 cm^{-1}), formates (1390 and 1377 cm^{-1}) and adsorbed nitrates (1638, 1591 and 1304 cm^{-1}) [33] are observed along with surface isocyanate species, Ag-NCO and Al-NCO (2226 and 2258 cm^{-1}) [17] as well as surface enolic species (H_2C=CH-O-M) (1644 cm^{-1}) [31]. Under identical reaction conditions, for Ag7MgAl catalysts these bands are observed at 1584, 1468 and 1445 cm^{-1} (acetate species), 1301 cm^{-1} (bidentate nitrate) and 1625 cm^{-1} (enolic species).

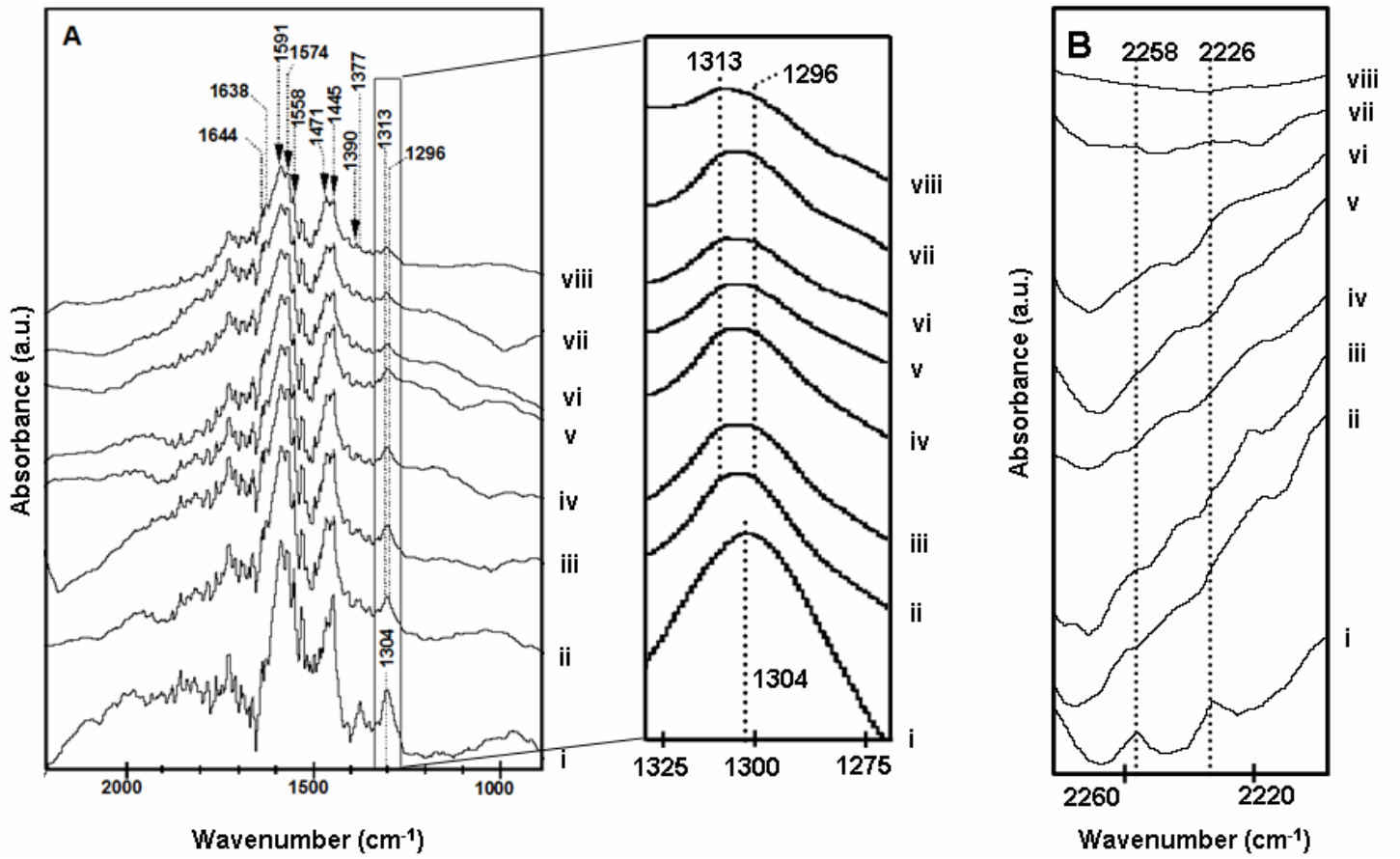

Figure 3.4 *Dynamic changes of in situ DRIFTS spectra over AgAl during the SCR of NO_x in presence of SO_2 at 623 K. (i) NO + C_3H_6–60 min, (ii) NO + C_3H_6 + SO_2–10, (iii) 30, (iv) 60, (v) 120, (vi) 180 min (vii) 240 and (viii) 300 min. Gas composition: 1000 ppm NO, 2000 ppm C_3H_6, 5 %O_2, 10 % CO_2, 20 ppm SO_2, He balance*

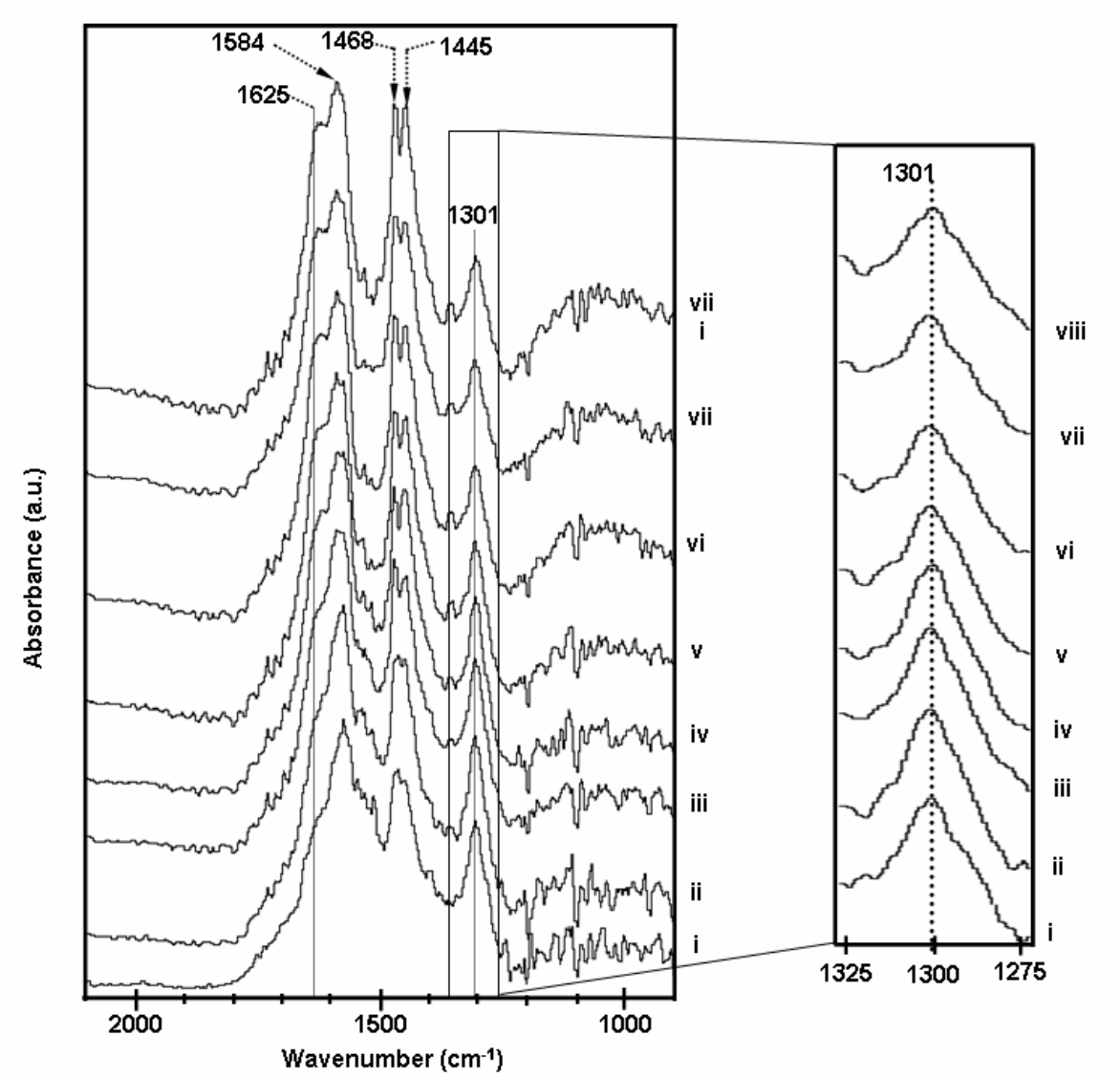

Figure 3.5 *Dynamic changes of in situ DRIFTS spectra over Ag7MgAl during the SCR of NO in presence of SO_2 at 623 K. (i) NO + C_3H_6–60 min, (ii) NO + C_3H_6 + SO_2–10, (iii) 30, (iv) 60, (v) 120, (vi) 180 min (vii) 240 and (viii) 300 min. Gas composition: 1000 ppm NO, 2000 ppm C_3H_6, 5 %O_2, 10 % CO_2, 20 ppm SO_2, He balance*

Meunier *et al.* [17] have studied SCR using propene on Ag/Al_2O_3 by *in situ* FTIR. Two broad absorption ranges with apparent maxima at 1560 and 1300 cm^{-1} after exposure to $NO+O_2$ are reported. These observations are in qualitative agreement with that reported in Figure. 3.4 A (i) and 3.5 A (i) and would correspond to the formation of bidentate nitrates species on alumina. A distinct observation is

related to the IR band at 1445 cm^{-1} with a shoulder at 1474 cm^{-1} (Figure 3.4 A) which would result from the direct interaction between propene and $NO+O_2$ with the formation of oxygenates from the partial oxidation of propene. Those IR bands could characterize the presence of carboxylate species according to previous assignments [17]. Weak contributions evident at 1644 and 1377 cm^{-1} could also highlight the presence of organo-nitrite, oxime and organo-nitro compounds. Weak IR bands are also observed near 2226 cm^{-1} previously assigned to -NCO species. Such tentative assignments seem to agree with those reported by Li *et al.* [34] who investigated the reduction of NO by propene on Ag/TiO_2-Al_2O_3 and Ag/Al_2O_3. These authors suggested the formation of monodentate, bidentate and bridge nitrate, acetate species, formate species and isocyanate species.

Table 3.2 *Assignments of IR bands formed on AgAl and Ag7MgAl during in situ studies*

Wavenumber (cm^{-1})	**Surface species**	**Vibrations**	**Observed Wavenumber (cm^{-1})**	**References**
1585	carboxylate COO^-	ν^a_{OCO}	1586	[17]
1460		ν^s_{OCO}	1456 and 1471	
1595	formate $HCOO^-$	ν^a_{OCO}	1591	[17]
1380		ν^s_{OCO}	1377	
1390		δ_{CH}	1390	
1550	monodentate nitrate NO_3^-	$\nu_{N=O}$	1558	[17]
1250		ν^a_{ONO}	Not detected	
1590	bidentate nitrate NO_3^-	$\nu_{N=O}$	1595	[17]
1305		ν^a_{ONO}	1304, 1301	[17]
1560	Ad-NO_x		1558	[17]
1313	Ag_2SO_4		1313	[35]
1384	$Al(SO_4)_3$		Not detected	[35]
1637	H_2C=CH-O-M		1644	[32]
2230	Ag-NCO		2226	[31]
2260	Al-NCO		2258	[31]

(s= symmetric, a= asymmetric and δ=bending)

The influence of SO_2 on the formation of suggested reaction intermediates on the catalyst surface was examined. IR spectra recorded on AgAl in the course of the $NO+C_3H_6+O_2$ reactions with 20 ppm SO_2 are presented in Figure 3.4 A (ii-viii). After exposure to 20 ppm SO_2 very weak signal for silver sulphate species started appearing after 30 min at 1313 cm^{-1} which appeared as broadening of the 1304 peak. The broadening of the peak at 1304 cm^{-1} became more evident from 30 min to 300 min and the peak broadened with maxima shifted to 1313 and 1296 cm^{-1}. It suggests the formation of silver sulphate species on the catalyst surface leading to deactivation due to sulphur poisoning. After exposure to SO_2 the previously discussed IR bands ascribed to acetates, formates and nitrates did not disappear. On the other hand the IR bands associated with Ag-NCO at 2226 and Al-NCO at 2258 cm^{-1} gradually decreased in intensity from 10 min to 300 min. In parallel the broad bands at 1558 and 1445 cm^{-1} intensified which correspond to the development of nitrates species as well as adsorbed C-containing intermediates. These result indicated the sulfation of Ag phase in case of AgAl in presence of 20 ppm SO_2.

In case of Ag7MgAl (Figure 3.5) exposure to 20 ppm SO_2 did not show formation of Ag-sulphate at 1313 cm^{-1} upto 300 min (Figure 3.5A ii-viii inset). The absence of formation of silver sulphate in case of Ag7MgAl proved the improved sulphur tolerance of this catalyst. It is noticeable that the decrease in intensity of the IR band assigned to Ag-NCO and Al-NCO on Ag7MgAl was not significant compared to AgAl which can be correlated to a lesser deactivation on Ag7MgAl than on AgAl due to SO_2 poisoning. The sulfation of Al_2O_3 generally evidenced by the presence of a 1384 cm^{-1} IR band (Al-sulfate) was not significantly observed even after 300 min exposure to SO_2, in case of both the catalysts which may be due to low concentration of SO_2 in the feed gas.

3.4. Conclusion

The effect of magnesia addition to Ag/Al_2O_3 catalysts for the SCR of NO has been investigated. In the series containing varying Mg loadings (5.5 to 17 wt% Mg), catalyst containing 7% Mg (Ag7MgAl) showed maximum activity with 98% NO conversion at 623 K whereas catalyst containing 17% Mg (Ag17MgAl) loading showed the least NO conversion under identical conditions. The increase in the catalytic activity upon addition of Mg was correlated with the decrease in the total acidity of the support. The presence of Mg helped in the low temperature activation of

C_3H_6, which in turn resulted in higher NO conversion. The order of activity for the catalysts was Ag7MgAl > Ag5.5MgAl > Ag11MgAl > Ag17MgAl. The sample with best activity (Ag7MgAl) was tested for sulfur tolerance under dry conditions. In the presence of 20 ppm SO_2 in the feed, the NO conversion decreased to 90% at 623 K. The *in situ* FTIR study has shown that the deactivation in the case of Ag/Al_2O_3 catalyst is due to the sulphation of active sites (Ag). In the presence of Mg, the formation of sulphates of Ag is inhibited and therefore the activity maintained. In conclusion, the addition of magnesia was found to improve the catalytic activity of Ag/Al_2O_3 in the reduction of NO to N_2 in the temperature range 598-673 K. The presence of magnesia has significantly improved the sulfur tolerance of this system.

3.5. References

1. R.A. van Santen, P.W.N.M. van Leeuwen, J.A. Moulijn, B.A. Averill, *Catalysis: An Integrated Approach, 2nd* edition, Elsevier, Amsterdam, **1999**.
2. N. Miyoshi, S. Matsumoto, K. Katoh, T. Tanaka, J. Harada, N. Takahashi, K. Yokota, M. Sugiura, K. Kasahara, *SAE Technical Paper 950809* **(1995)**.
3. M. Takeuchi, S. Matsumoto, *Top Catal.* 28 **(2004)** 151.
4. W. Held, A. Konig, T. Richter, L. Pupper, *SAE Paper 900496* **(1990).**
5. R. Burch, J. P. Breen, F.C. Meunier, *Appl. Catal. B* 39 **(2002)** 283.
6. Z. Liu, S.I. Woo, *Catal. Rev.* 48 **(2006)** 43
7. V.I. Pârvulescu, P. Grange, B. Delmon, *Catal. Today* 46 **(1998)** 233.
8. H. Hamada, Y. Kintaichi, M. Sasaki, T. Ito, *Appl. Catal.* 75 **(1991)** L1.
9. Y. Kintaichi, H. Hamada, M. Tabata, T. Yoshinari, M. Sasaki, T. Ito, *Catal. Lett.* 6 **(1990)** 239.
10. K. A. Bethke, D. Alt, M. C. Kung, *Catal. Lett.* 25 **(1994)** 37.
11. D.E. Sparks, P.M. Patterson, G. Jacobs, N. Dogimont, A. Tackett, M. Crocker, *Appl. Catal. B* 65 **(2006)** 44.
12. P. Anil Kumar, M. Pratap Reddy, B. Hyun-Sook, H. Heon Phil *Catal Lett.* 131 **(2009)** 85.
13. Y. Shi, H. Pan, Y. Zhang, W. Li, *Catal. Comm.* 9 **(2008)** 796.
14. K. Shimizu, M. Hashimoto, J. Shibata, T. Hattori, A. Satsuma *Catal. Today* 126 **(2007)** 266.
15. K.J. Klabunde, J. Stark, O. Koper, C. Mohs, D.G. Park, S. Decker, Y. Jiang, I. Lagadic, D. Zhang, *J. Phys. Chem.* 100 **(1996)** 12142.
16. M. Waqif, O. Saur, J.C. Lavalley Y. Wang, B.A. Morrow *Appl. Catal.* 71 **(1991)** 319.
17. F.C. Meunier, J.P. Breen, V. Zuzaniuk, M. Olsson, J.R.H. Ross, *J. Catal.* 187 **(1999)** 493.
18. N. Okazaki, T. Sasaki, Y. Katoh, A. Tada, *J. Jpn. Petrol. Inst.* 45 **(2002)** 288.
19. P.W. Park, C.L. Boyer, *Appl. Catal. B* 59 **(2005)** 27.
20. A. Satsuma, K. Yamada, T. Mori, M. Niwa, T. Hattori, Y.Murakami, *Catal. Lett.* 31 **(1995)** 367.
21. H. Hamada, Y. Kintaichi, M. Sasaki, T. Ito, M. Tabata, *Appl. Catal.* 64 **(1990)** L1.

22. Y. Li, J.N. Armor, *J. Catal.* 145 **(1994)** 1.
23. M. Haneda, Y. Kintaichi, H. Hamada, *Appl. Catal. B* 31 **(2001)** 251.
24. S.G. Masters, D. Chadwick, *Catal. Lett.* 57 **(1999)** 155.
25. N. Jagtap, S.B. Umbarkar, P. Miquel, P. Granger, M.K. Dongare, *Appl. Catal. B* 90 **(2009)** 416.
26. C.T. Fishel, R.J. Davis, *Catal. Lett.* 25 **(1994)** 87.

Chapter 4: NO Reduction under Diesel Exhaust Conditions over Au/Al_2O_3

NO reduction under diesel exhaust conditions was carried out over Au/Al_2O_3 prepared by deposition-precipitation method and compared with the catalytic activity of Ag/Al_2O_3 sample.

Chapter 4: NO Reduction under Diesel Exhaust Conditions over Au/Al_2O_3

1.1. Introduction

Lean burn automobile engines are becoming increasingly popular than the stoichiometric gasoline engines because of their high fuel efficiencies resulting in lower CO/CO_2 emissions. The present three-way catalytic converter is ineffective under lean burn conditions for the reduction of NO_x due to excess oxygen and lesser CO and hydrocarbon in the exhausts of these engines [1]. Various approaches and catalytic compositions are being investigated to reduce the NO_x from lean burn engines. In this context, NO_x storage and reduction (NSR) developed by Toyota [2, 3] and selective catalytic reduction of NO_x by urea (urea SCR) and hydrocarbon (HC-SCR) are being investigated as promising processes for NO_x abatement [4, 5]. HC-SCR seems to be more promising because of its merits over the other two approaches. Amongst the various catalytic formulations reported silver on alumina show promising activity for the selective reduction of NO_x to N_2 by hydrocarbons under lean burn conditions especially in the presence of hydrogen [5]. However deactivation of the catalyst due to SO_2 in the exhaust gases is one of the major limitations of this catalyst system for its practical applications and improvement in sulfur tolerance has been achieved upto certain extent by modifying the alumina support [6]. Silver on alumina catalyst system is extensively studied for effect of various parameters on NO_x conversion and selectivity for N_2 as well as *in situ* studies for understanding the mechanism. Hence mechanism of very high catalytic activity as well as deactivation of catalyst in presence of SO_2 is very well understood in case of Ag/Al_2O_3.

Supported gold-based catalysts [7-14] are also one more set of catalysts which have been investigated for HC-SCR of NO_x. Ueda *et al* have carried out a study of gold supported on various metal oxides for HC-SCR and reported Au/Al_2O_3 to be the most active in the reduction of NO_x to N_2 in the presence of moisture and oxygen among all studied Au systems [10, 11]. Recently, Ilieva *et al* have reported reduction of NO_x by CO with 100% selectivity to N_2 at 200 °C over gold supported on ceria-alumina mixed catalysts [15, 16]. However the catalytic activity of Au/Al_2O_3 is low

compared to Ag/Al_2O_3 catalyst for SCR of NO_x using hydrocarbons as well as the Au system is not investigated in much greater details compared to Ag/Al_2O_3 system.

All the previous reports on Au/Al_2O_3 for SCR of NO_x, use lower alkanes or alkenes [11-13] or CO as the reductant [15, 16]. However simultaneous use of CO, H_2 and a higher hydrocarbon like decane, which are present in the exhausts of a diesel engine has not been reported so far. In this chapter, we have investigated the catalytic activity of Au/Al_2O_3 (1% Au) for HC-SCR of NO_x under real diesel engine exhaust conditions and compared the results with that of Ag/Al_2O_3 system. The effect of addition of H_2 in the feed on the activity of these catalysts was also studied. Detailed *in-situ* FTIR experiments were performed using hydrocarbon and hydrogen to examine the surface species formed during the course of the reaction to understand the mechanistic aspects of SCR of NO_x over Au/Al_2O_3 catalyst and the results are reported.

3.2. Experimental Section

3.2.2. Catalyst Preparation

γ-Al_2O_3 was obtained by sol-gel procedure. Aluminium sec-butoxide and 2-butanol was mixed and stirred at 85 °C till a homogenous solution was formed. Water was added in a molar ratio of $1Al/6C_4H_9OH/10H_2O$, giving a gel that was dried at 120 °C overnight. Before calcination, gold was deposited on alumina precursor using the deposition precipitation method with urea. Urea solution was thermostated at 80 °C and the solution of $HAuCl_4$. xH_2O was added. Al_2O_3 precursor powder was introduced in the solution after 5 min under stirring at 80 °C. The obtained sample was dried at 80 ° C followed by a washing step using water. After subsequent drying at 80°C, the sample (1 wt% Au/Al_2O_3) was calcined in air at 500 °C for 12 h.

For comparison, silver-based catalyst was prepared by wet impregnation using $AgNO_3$ as the precursor on the same alumina support. Final catalyst (2 wt % Ag/Al_2O_3) was obtained after successive drying overnight at 80 °C followed by calcination at 500 °C for 12 h.

4.2.2. Catalytic activity measurements

Temperature-programmed experiments were performed in a fixed-bed flow reactor. The reaction mixture consisted of 300 ppm NO, 300 ppm CO, 300 pm C_3H_6, 100 ppm $C_{10}H_{22}$, 2000 ppm H_2, 10% O_2, 10% CO_2, 5% H_2O and balance He. The

catalyst (300 mg) was used in a powder form (40-80 μm). The total flow rate of the gas mixture was set at 250 mL min^{-1} to obtain a gas hourly space velocity of 50000 h^{-1}. The effluent gas was analyzed using an online mass spectrometer (Omnistar GSD 301) and a micro GC (Varian CP 4900) equipped with a thermal conductivity detector. The reactants and products were separated on a molecular sieve 5Å (NO, N_2, O_2, H_2 and CO) and a Porapaq Q column (N_2O, C_3H_6). $C_{10}H_{22}$ was monitored on the mass spectrometer. Prior to the reaction, the catalyst was activated in He at 500 °C for 1 h.

3.2.3. Catalysts characterization

IR spectra of the adsorbed species were recorded using a FTIR spectrometer (Thermo Nicolet 460 Protégé, MCT detector) equipped with a DRIFT cell (Harrick). Prior to each experiment, 30 mg of the sample was heated in He flow at 385 °C with a heating rate of 10 °C min^{-1}. The sample was then cooled down to 128 °C (in the case of experiments with H_2) or 150 °C (experiments without H_2) under He flow and then heated again under the reaction mixture containing 467 ppm NO, 958 ppm CO, 958 ppm C_3H_6 and 173 ppm $C_{10}H_{22}$, 2000 ppm H_2 (when present), 5% O_2 with He. The ratio W/F^0 was also adjusted to 0.072 g s cm^{-3}.

X-ray photoelectron spectroscopy (XPS) was used to carry out the surface characterization of the fresh and used catalyst. XPS experiments were performed using a Vacuum Generators Escalab 220XL spectrometer equipped with a monochromatized aluminum source. The pressure in the analysis chamber was maintained at 10^{-10} Torr. Binding energy (B.E.) values were referenced to the binding energy of the C 1s core level (285.1 eV) for charge correction.

3.3. Results and discussion

3.3.1. HC-SCR of NO over 1 wt% Au/Al_2O_3 and 2 wt% Ag/Al_2O_3

The activated catalysts were exposed to reaction mixture in a fixed bed reactor using 300 ppm NO, 300 ppm CO, 300 ppm C_3H_6, 100 ppm $C_{10}H_{22}$, 2000 ppm H_2, 10% O_2, 10% CO_2, 5% H_2O and balance He. Figure 4.1(A) compares the NO reduction to N_2 and N_2O as a function of temperature over 1 wt% Au/Al_2O_3 and 2 wt% Ag/Al_2O_3.

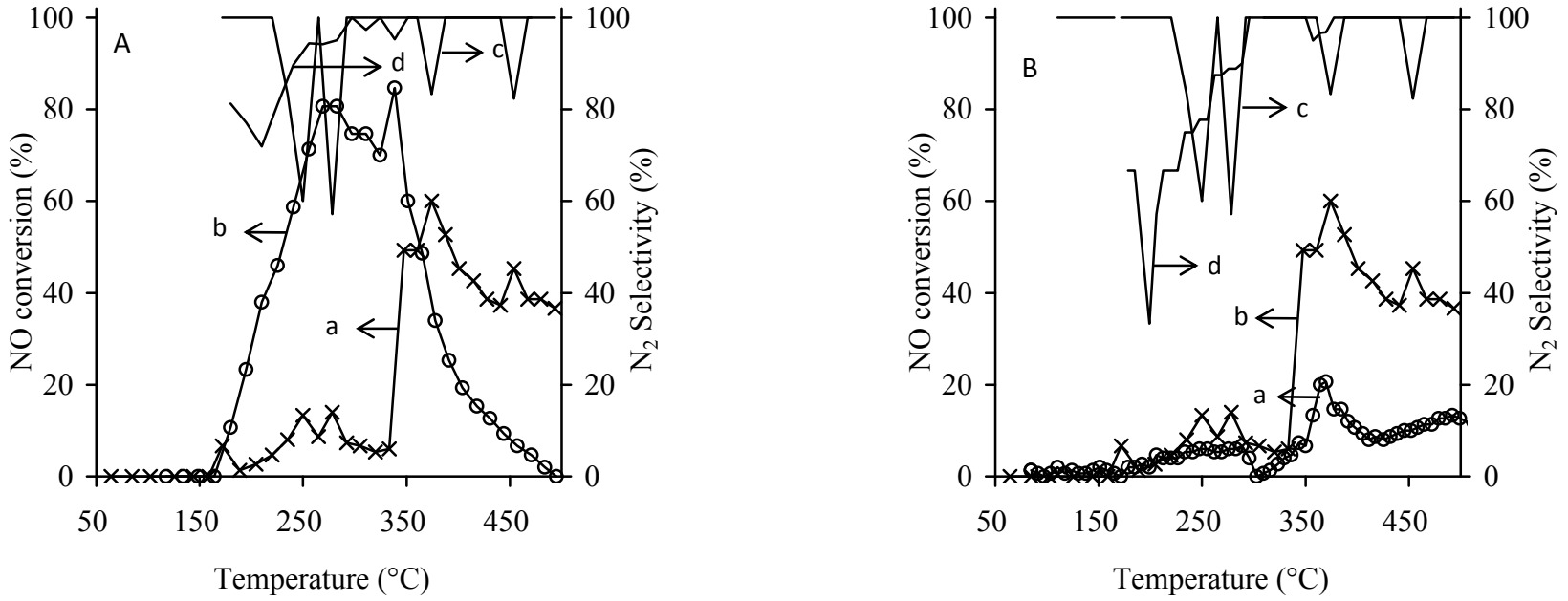

Figure 4.1 *Comparison of (A) NO conversion and N_2 selectivity over 1 wt% Au/Al_2O_3 (a and c) and 2 wt% Ag/Al_2O_3 (b and d) as a function of temperature in the presence of H_2. (B) Comparison of NO conversion and N_2 selectivity over 1wt% Au/Al_2O_3 in the absence (a and d) and presence (b and c) of H_2 (Reaction conditions: 300 ppm NO, 300 ppm CO, 300 pm C_3H_6, 100 ppm $C_{10}H_{22}$, 0 or 2000 ppm H_2, 10% O_2, 10% CO_2, 5% H_2O and balance He. GHSV = 50000 h^{-1})*

Two temperature domains could be distinguished for NO reduction on Au/Al_2O_3. The first temperature domain (185-325 °C) showed a low conversion level (max. 14% conversion around 250-275 °C) and N_2 selectivity higher than 55%. In the second temperature domain (350-500 °C) a maximum of 60% NO conversion at 375 °C was observed and complete selectivity towards N_2 was evidenced as previously reported over Au/Al_2O_3 [7]. A classical behavior is reported in Figure 4.1(A) for Ag/Al_2O_3. NO conversion began at 170 °C and 75-85% of conversion was obtained in the temperature range of 250-350 °C. At the same time the selectivity to N_2 formation progressively increased with temperature till it reached 100%.

The conversion of all the reductants (H_2, CO, C_3H_6 and $C_{10}H_{22}$) was followed during temperature-programmed experiments and temperatures corresponding to 50% of conversion are reported in Table 4.1. H_2 and CO were activated on Au/Al_2O_3 at low temperature with T_{50} around 200 °C whereas no significant simultaneous reduction of NO arose in this temperature range. It indicated that H_2 and CO are unselectively oxidized to H_2O and CO_2. By contrast, the activation of propylene and decane began above 300 °C when the simultaneous reduction of NO to N_2 was seen. After 340 °C the NO conversion decreased progressively due to complete consumption of the reductants. The activation of reductants followed the sequence T_{50} $C_{10}H_{22}$ < T_{50} H_2 < T_{50} C_3H_6 < T_{50} CO on Ag/Al_2O_3. Clearly, decane combined with hydrogen addition seems to be the most efficient reductant for the HC-SCR on both catalytic systems. Figure 4.1(B) compares the activity of Au/Al_2O_3 in the presence and in the absence of hydrogen, i. e. in the presence of CO, propylene and decane as reductants. The conversion level of NO previously observed above 350 °C decreased from 60% to 20% when hydrogen was not present in the feed. However the selectivity remained almost complete for N_2 in this temperature range (350-500 °C) as observed in the presence of H_2.

Table 4.1 *Temperature corresponding to 50% conversion of reductants on Au/Al_2O_3 and Ag/Al_2O_3 catalysts*

Catalyst	T_{50} CO (°C)	T_{50} H_2 (°C)	T_{50} C_3H_6 (°C)	T_{50} $C_{10}H_{22}$ (°C)
1%Au/Al_2O_3	195	200	335	350
2%Ag/Al_2O_3	385	240	325	170

4.3.2. In-situ Infrared studies

a) Infrared spectra over Au/Al_2O_3 under $NO+CO+C_3H_6+O_2$

In order to identify the different species formed on the surface of the Au/Al_2O_3 catalyst during HC-SCR reactions, the catalyst placed in a DRIFT cell was first exposed after activation to 467 ppm NO, 958 ppm CO, 958 ppm C_3H_6 and 5% O_2 with He as balance. Figure 4.2 presents the IR spectra during the temperature-programmed sequence under reaction mixture. At 150 °C, the signal at 1652 cm^{-1} (spectrum a) revealed the presence of adsorbed water on the surface of the solid (Figure 4.2A). Further increase in temperature led to the appearance of IR bands located at 1587, 1460, 1392, 1375 cm^{-1} (Figure 4.2A) and at 2999 and 2909 cm^{-1} (Figure 4.2B). Finally, at 388 °C, a shoulder around 1555 cm^{-1} developed. The evolution of intensity was extracted as function of temperature for all bands and is presented in Figure 4.3. As observed, the evolution of bands located at 1375, 1392, 1587, 2909 and 2999 cm^{-1} follows the same trend with an increase of intensity until 355 °C and a progressive attenuation of their intensity above this temperature. Clearly these bands arise from unique adsorbed species assigned to formate species in agreement with previous IR studies (Table 4.2). At higher temperature, both signals at 1460 and 1555 cm^{-1} increased. Several assignments could be proposed for these bands. The formation of carbonate with ν_s(COO) and ν_{as}(COO) modes respectively could arise from propylene oxidation on the surface of the catalyst. However the evolution of intensity of the signal around 1555 cm^{-1} doesn't match exactly with the one at 1460 cm^{-1} band. This can reflect the presence of additional signal around 1555 cm^{-1} assigned to linear nitrite. Previous IR studies ascribe bands around 1460-1555 cm^{-1} to acetate adsorbed on alumina but the absence of signals corresponding to methyl group is not in agreement with this assignment.

b) Effect of addition of decane

Decane was added to previous feed and IR spectra were recorded as a function of temperature (Figure 4.4). The global feature of IR spectra remained similar to that without the addition of $C_{10}H_{22}$. IR spectra evidenced the development of band located at 1375, 1392, 1587, 2909 and 2999 cm^{-1} at intermediate temperature previously assigned to formate species. The development of carbonate species and nitrite species associated with signals at 1460 and 1555 cm^{-1} arise at high temperature (Figure 4.4A).

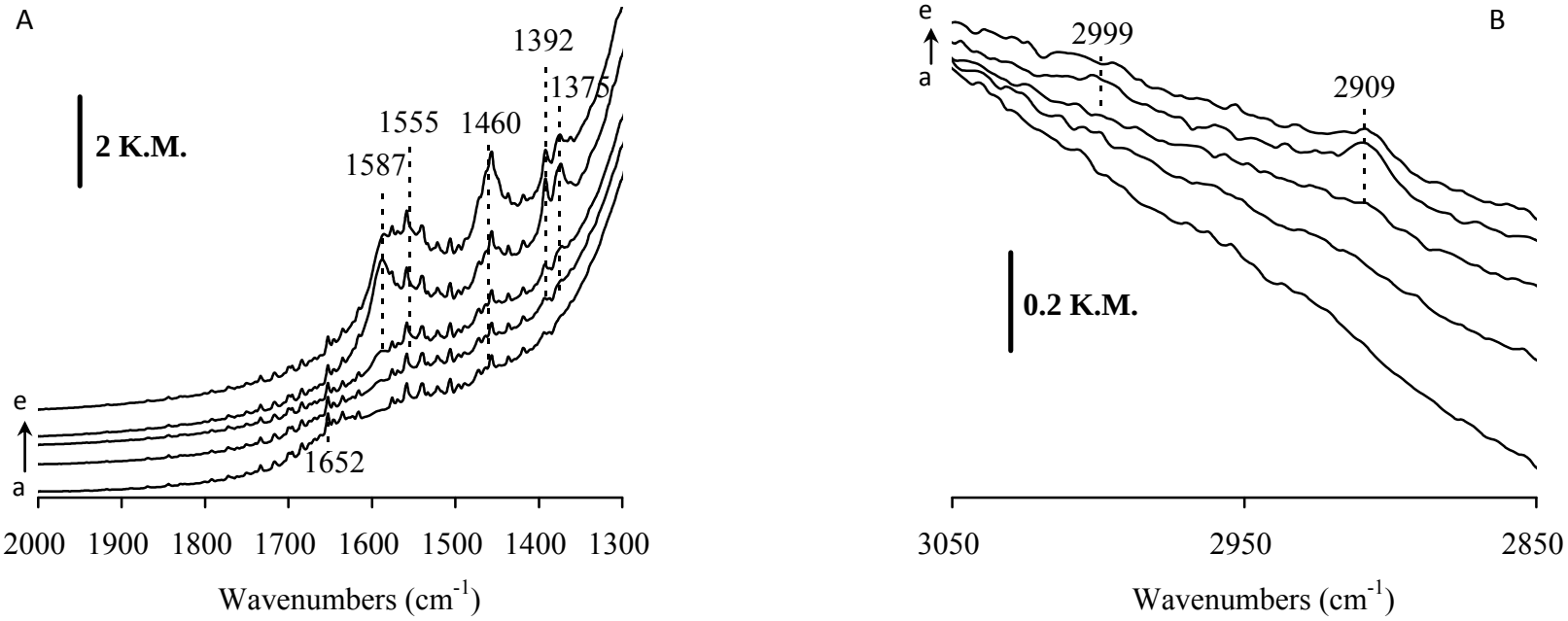

Figure 4.2 *IR spectra of 1 wt% Au/Al_2O_3 in temperature programmed conditions with $NO+CO+C_3H_6+O_2+He$ in the (A) 2000-1300 cm^{-1} and (B) 3050-2850 cm^{-1} region. (a) 150 °C, (b) 185 °C, (c) 256 °C, (d) 343 °C and (e) 388 °C.*

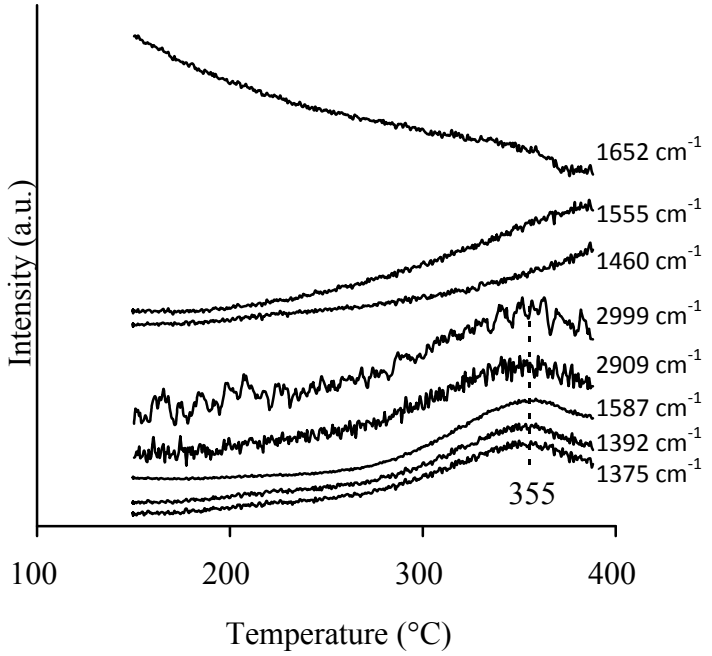

Figure 4.3 *Evolution of IR bands intensity on 1 wt% Au/Al_2O_3 during temperature-programmed reaction with $NO+CO+C_3H_6+O_2+He$*

At low temperature, the presence of new IR bands at 2960, 2929 and 2860 cm^{-1} could reflect the adsorption of decane on the surface of the catalyst (Figure 4.4B). The evolution of intensities as function of temperature is reported in Figure 4.5. At low temperature, decane accumulates on the surface of the catalyst and desorbs/reacts with increase in the temperature. Formate species concentration reached maximum at 360 °C whereas carbonate species accumulated above 360 °C. Neither isocyanate nor cyanide species could be detected at any temperature under these conditions.

c) Effect of addition of hydrogen and decane

Simultaneous addition of decane and hydrogen to initial feed was used for the characterisation of Au/Al_2O_3 during NO reduction with hydrocarbons. IR spectra and the evolution of intensity *vs.* temperature are presented in Figure 4.6 and Figure 4.7 respectively. By contrast to previous experiments, strong changes are mainly observed at low temperature (spectrum A) with the appearance of new bands at 2196, 1719,

Table 4.2 *Assignment of IR bands*

Catalyst	**Assignments**	**Vibrational modes**	**Wavenumbers /cm^{-1}**	
			Literature [reference]	**This study**
Al_2O_3	Formate	$\nu_{(s)OCO}$	1380 [17]	1375
		$\nu_{(s)OCO}$	1595 [17]	1587
		$\nu_{(as)OCO}$	1395 [17]	1392
		δ_{CH}	2905 [17]	2909
		ν_{CH}	2970 [17]	2999
		$\nu_{(a)OCO}+\delta_{CH}$		
Cu/SiO_2	Cu^0-NCO	ν_{NCO}	2230-2240 [18]	
	Cu^{2+}-NCO		2180-2185 [18]	
Au/SiO_2	Au-NCO	ν_{NCO}	2180-2186 [19]	2196
Ag/Al_2O_3	Al^{3+}-CN	ν_{CN}	2155 [20]	2180-2196
	Ag-CN		2127 [20]	2128-2152
Au/SiO_2	Au-NO^-	ν_{NO}	1733 [19]	1719
Co/ZrO_2	NO_2^- (bridging nitro)	$\nu_{(as)NO2}$	1545-1530 [21]	1555
Ag/Al_2O_3	NO_3^- (nitrate B)	$\nu_{N=O}$	1580 [22]	1624
		$\nu_{(as)NO2}$	1305 [22]	1308
Ag/Al_2O_3	Free carboxylate	$\nu_{(as)OCO}$	1575 [22]	1555
	COO^-/acetate	$\nu_{(s)OCO}$	1465 [22]	1457

1624, 1587 and 1308 cm^{-1} in addition to decane-related signals (2962, 2927 and 2857 cm^{-1}). The intensity of bands assigned to decane adsorption decreased progressively with increase in temperature. Signals at 1719, 1624, 1587 and 1308 cm^{-1} also disappeared until 250-350 °C. The adsorption of NO on gold particles (Au-NO or Au-NO^-) is evidenced with band at 1719 cm^{-1} in the presence of hydrogen. Addition of hydrogen could prevent the superficial oxidation of gold particles. The evolution of other bands with temperature was complex but intense signals at 1624cm^{-1} and 1305 cm^{-1} with similar evolution could be isolated and assigned to a nitrate species with

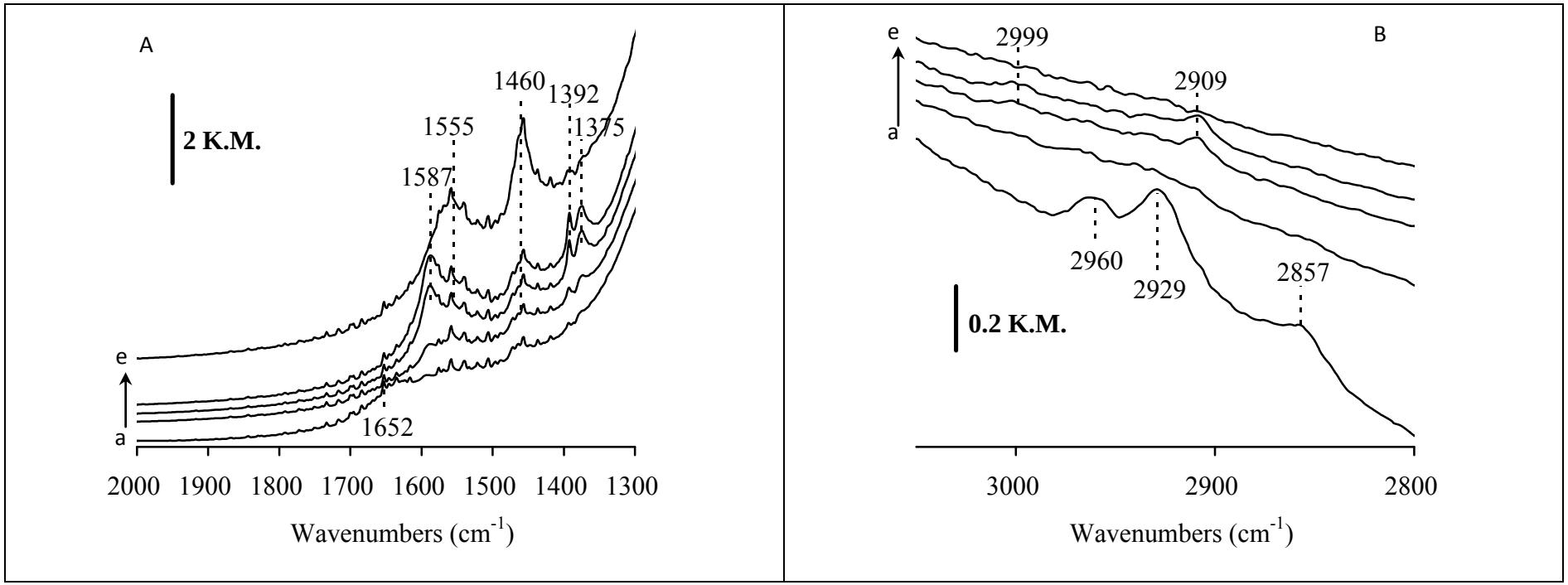

Figure 4.4 *IR spectra of 1 wt% Au/Al_2O_3 under temperature programmed conditions with $NO+CO+C_3H_6+C_{10}H_{22}+O_2+He$ in the (A) 2000-1300 cm^{-1} and (B) 3000-2800 cm^{-1} region. (a) 150 °C, (b) 250 °C, (c) 325 °C, (d) 363 °C, (e) 441 °C*

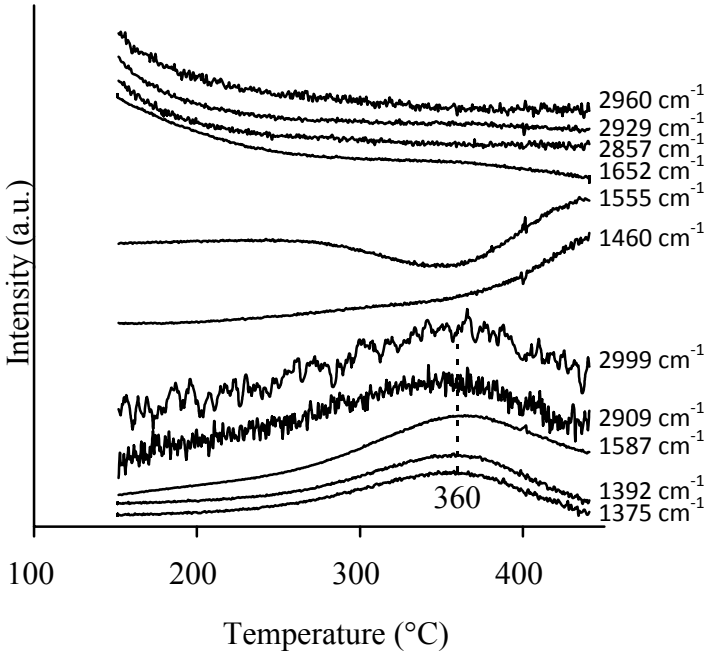

Figure 4.5 *Evolution of IR bands on 1 wt% Au/Al_2O_3 during temperature-programmed reaction with $NO+CO+C_3H_6+C_{10}+O_2+He$*

$\nu_{(N=O)}$ and $\nu_{as\ (ON-O)}$ vibration modes respectively. Additional signal of nitrite at 1587 cm^{-1} was observed. The increase in temperature led to the consumption of nitrate/nitrite adsorbed species as well as nitrosyl species with complete disappearance of corresponding IR signals around 300 °C.

In the 2250-2000 cm^{-1} region new bands at 2196 and 2152 cm^{-1} were observed between 130 °C and 270 °C (Figure 4.6C). Bion *et al* [20] reported on Ag/Al_2O_3 the presence of isocyanate and cyanide species at 2255-2228 cm^{-1} (Al-NCO) and 2155-2127 cm^{-1} (Ag^+-CN and/or Al-CN). The band at 2195 cm^{-1} can be ascribed to Au-CN species whereas the one at 2152 cm^{-1} to Al-CN. The intensity of the band at 2152 cm^{-1} decreased with increasing temperature. The band at 2195 cm^{-1} shifted to 2180 cm^{-1} with increasing temperature along with increase in the intensity. Additional band at 2128 cm^{-1} corresponding to cyanide species is observed at 409 °C. The presence of isocyanate with corresponding signal at 2250 cm^{-1} could be suggested at high temperature. This in turn implies the transformation of –CN species to –NCO species

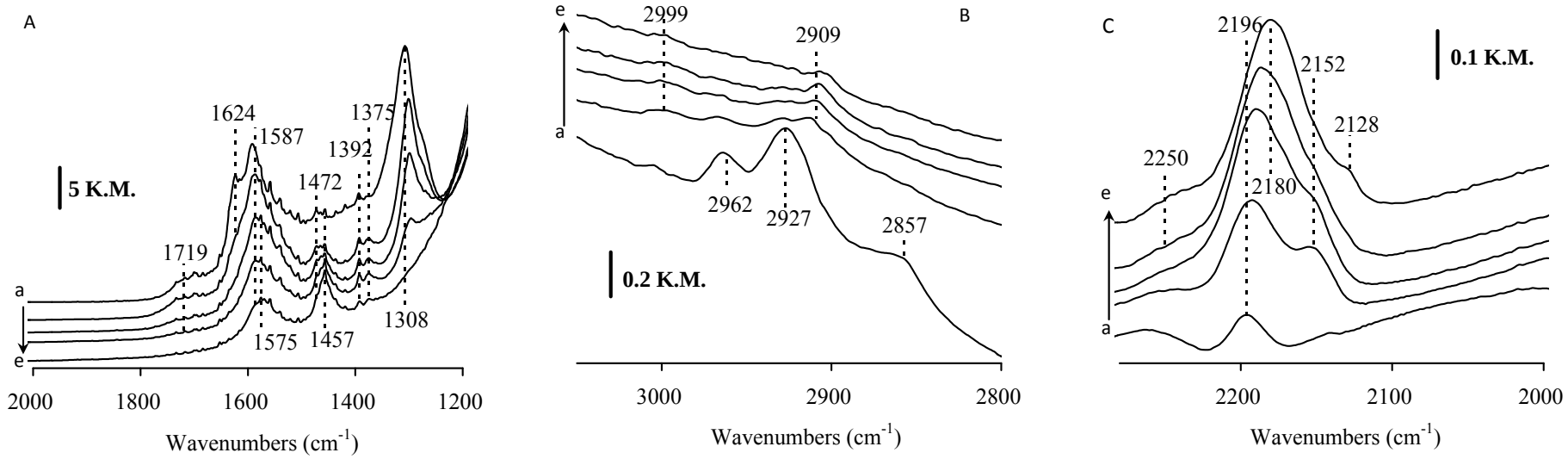

Figure 4.6 *IR spectra of 1 wt% Au/Al_2O_3 in temperature programmed conditions with $NO+CO+C_3H_6+C_{10}H_{22}+O_2+H_2+He$ in the (A) 2000-1200 cm^{-1}, (B) 3000-2800 cm^{-1} and (c) 2300- 2000 cm^{-1} region. (a) 130 °C, (b) 269 °C, (c) 330 °C, (d) 363 °C, (e) 409 °C*

with increasing temperature. It is noteworthy that the formation of cyanide and/or isocyanate species was evidenced only in the presence of hydrogen in the feed. At high temperature, spectral features assigned to formate species develop until 300 °C before diminishing. Above 400 °C signals of carbonate species and nitrite species at 1457 and 1575 cm^{-1} predominate.

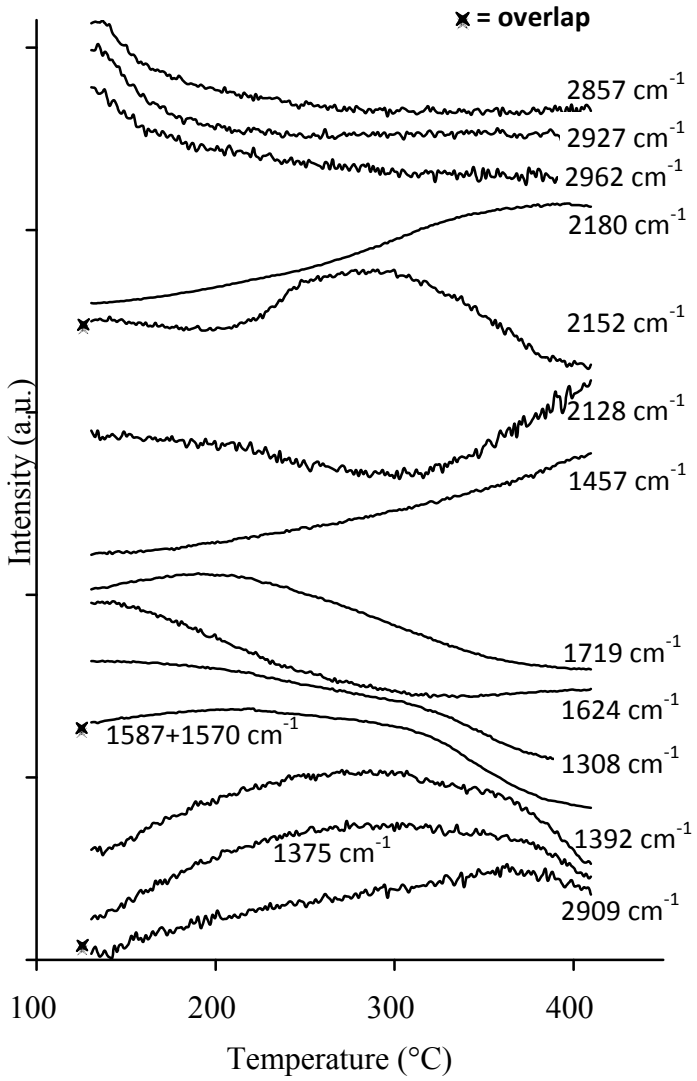

Figure 4.7 *Evolution of IR bands intensity on 1 wt% Au/Al_2O_3 during temperature-programmed reaction with $NO+CO+C_3H_6+C_{10}+H_2+O_2+He$*

4.3.3. Ex-situ XPS measurements

Surface analysis was performed using XPS measurements. Figure 4.8 shows the Au 3f photopeak before and after catalytic tests. On the fresh catalyst, the binding

energy value of Au $3f_{7/2}$ is 84 eV, which is characteristic of metallic oxidation state of gold nanoparticles. After reaction under lean condition in the presence of decane (spectrum (b)) or in the presence of decane and hydrogen (spectrum (c)), the B.E. values do not vary significantly that confirms the preservation of metallic character of gold nanoparticles even at high temperature in presence of excess oxygen.

The surface concentration of Au was estimated from XPS measurements (Table 4.3). As observed, the surface concentration was not significantly affected after reaction. The stabilization of gold particles on alumina is evidenced and the vaporization of part of gold is not observed even after reaction at 500 °C. These results have clearly demonstrated that Au/Al_2O_3 catalysts exhibit high catalytic activity for the reduction of NO with propene, decane and hydrogen in the presence of oxygen and moisture. The catalyst was the most active above 350 °C with a complete selectivity for N_2. Ueda *et al* [9] have carried out a study of gold supported on

Figure 4.8 *Au 3f photopeak of Au/Al_2O_3 (a) fresh catalyst; (b) after reaction under $NO+CO+C_3H_6+C_{10}H_{22}+O_2+He$; (c) after reaction under $NO+CO+C_3H_6+C_{10}+H_2+O_2+He$*

Table 4.3 *Semi quantitative analysis by XPS of Au/Al_2O_3*

Treatment	B.E. Au $3f_{7/2}$ /eV	FWHM* /eV	Atomic ratio Au/Al
Calcined	83.8	1.37	0.02
After reaction under NO+CO+C3+C10	84.1	1.48	0.02
After reaction under NO+CO+C3+C10+H2	84.2	1.42	0.02

* FWHM: Full Width at Half-Maximum

different metal oxides (α-Fe_2O_3, ZnO, MgO, TiO_2 and Al_2O_3) prepared by deposition-precipitation and coprecipitation methods with different gold loading (0.17-1.2 wt%). The reaction gas mixture consisted of 1000 ppm NO, 500 ppm C_3H_6, 5% O_2, 1.8% H_2O and balance He and the space velocity used was 20000 h^{-1}. Amongst the different supports the highest NO conversion to N_2 (38%) was obtained on Au/Al_2O_3 with a metal loading of 0.82 wt% at 400 °C prepared by deposition precipitation method. Compared to the above data, the activity of 1 wt% Au/Al_2O_3 in the absence of H_2 (Figure 4.1B) in this study was almost half (20% around 380 °C). This may be due to a more complicated gas composition and higher space velocity used so as to represent conditions that prevail in actual diesel exhaust. The addition of hydrogen to the feed gas strongly enhanced NO reduction to N_2 when combined with propene and decane. Similar positive effect of hydrogen is well known in the case of supported silver catalyst [5]. However temperatures range of Au catalyst is observed at higher temperature than the one of silver-based catalyst as illustrated in Figure 4.1. The beneficial effect of H_2 on NO_x reduction over supported gold catalysts is already known. Ueda *et al* in a comparative study of NO_x reduction with propane, propene, ethane and ethene in the presence of oxygen and moisture reported that the H_2 addition significantly improved the conversion of NO to N_2 in the low temperature region [11]. In our case however no beneficial effects of H_2 on the reduction of NO were observed in the low temperature region. This maybe because of the presence of CO in the reaction feed, which inhibits the reaction between H_2 and NO_x at low temperature. Macleod and Lambert reported that in the lean NO_x reduction with CO + H_2 over Pt/Al_2O_3, the surface of the catalyst was poisoned by CO due to strong

adsorption and subsequent coverage by CO which in turn increases the temperature required to initiate the reaction between NO_x and H_2 [23]. However, no CO adsorption on gold could be evidenced during our IR experiments. In another study, in order to understand the effects of H_2 on the SCR of NO_x under diesel exhausts conditions, Abu-Jrai *et al* [24] carried out H_2-SCR over 1 wt% Pt/Al_2O_3 followed by simultaneous addition of CO and hydrocarbon. They reported that in the presence of H_2 alone the NO_x reduction activity peaked at 140 °C whereas in the presence of CO and hydrocarbon the maximum temperature peak shifted to higher temperatures (200-250 °C). It is clear from the above discussion that the presence of CO could be detrimental to the NO_x reduction activity in the low temperature region through the accumulation of inhibiting species (carbonate, isocyanate…) and suppresses the beneficial effects of H_2. The role of adsorbed species in the NO reduction in lean conditions is not clear on supported gold catalyst.

In the absence of decane and hydrogen, formate species and carbonate/nitrite species are observed. NO adsorption on gold is not evidenced under these conditions. Lee and Schwank previously claimed that NO does not adsorb on Au/SiO_2 and on Au/MgO [24]. Propylene adsorption and oxidation through formate intermediate could illustrate the reaction with oxygen and/or NO in lean conditions. The role of formate species is of debate but is mostly considered as spectator species on alumina support [26]. In the present study, the formation of formate and the evolution of its intensity are not promoted by hydrogen that lead to the conclusion that formate are not directly involved in the reduction of NO. In the case of silver-based catalyst, isocyanate species were proposed to have a role in the $DeNO_x$ process [20]. The formation of silver cyanide is followed by its transformation into adsorbed Al^{3+} NCO species that is hydrolysed into ammonia. Then, ammonia further reacts stoichiometrically with NO leading to high N_2 selectivity. This reaction scheme could be discussed in the case of gold-based catalysts. In the presence of hydrogen, cyanide species interacting with Au or Al are observed. The presence of isocyanate species adsorbed on gold could be alternately proposed with the band at 2195 cm^{-1} as proposed by Solymosi *et al* [19] but the assignment is still under debate. Hydrolysis of those species could promote nitrogen formation as proposed by Bion *et al* [20]. The presence of cyanide and/or isocyanate could also reflect the indirect role of hydrogen, i.e. to prevent oxygen accumulation on the surface of gold nanoparticles. In case of Au/Al_2O_3, the role of

hydrogen in the reaction mechanism is probably similar to that reported on silver-based catalyst. Previous studies stated that the oxidation of H_2 by O_2 arise more readily on gold catalysts than the NO_2+H_2 reaction [11]. The observation of nitrosyl adsorbed on metal nanoparticles of gold is an indirect indication of the role of hydrogen to prevent oxygen accumulation on the surface of nanoparticles.

4.4. Conclusion

The alumina supported gold catalyst has shown good activity and selectivity for reduction of NO to N_2 under lean conditions. NO reduction to N_2 is observed at higher temperature as compared to Ag/Al_2O_3 catalyst under the same reaction conditions. Hydrogen did not show any promotional effect on the reduction of NO in the low temperature region. By contrast, hydrogen addition promotes NO reduction at high temperatures. FTIR studies showed that the addition of hydrogen has prevented the accumulation of oxygen on the surface of the catalyst and has increased the formation of surface adsorbed species.

4.5. References

1. R. Burch, J. P. Breen, F. C. Meunier, *Appl. Catal. B* 39 **(2002)** 283.
2. N. Miyoshi, S. Masumoto, K. Katoh, T. Tanaka, J. Harada, *SAE Technical paper, No. 950809* **(1995)**.
3. K. Katoh, T. Kihara, T. Asanuma, M. Gotoh, N. Shibagaki, *Toyota Technical Review* 44 **(1994)** 27.
4. M. Koebel, M. Elsener, M. Kleemann, *Catal. Today* 59 **(2000)** 335.
5. J. P. Breen, R. Burch, C. Hardacre, C. J. Hill, B. Krutzsch, B. Bandl-Konrad, E. Jobson, L. Cider, P. G. Blakeman, L. J. Peace, M. V. Twigg, M. Preis, M. Gottschling, *Appl. Catal. B* 70 **(2007)** 36.
6. N. Jagtap, S. B. Umbarkar, P. Miquel, P. Granger, M. K. Dongare, *Appl. Catal. B* 90 **(2009)** 416.
7. E. Seker, E. Gulari, *Appl. Catal. A* 232 **(2002)** 203.
8. E. Seker, E. Gulari, R.H. Hammerle, C. Lambert, J. Leerat, S. Osuwan, *Appl. Catal. A* 226 **(2002)** 183.
9. A. Ueda, T. Oshima, M. Haruta, *Appl. Catal. B* 12 **(1997)** 81.
10. A. Ueda, M. Haruta, *Appl. Catal. B* 18 **(1998)** 115.
11. A. Ueda, M. Haruta, *Gold Bull.* 32 **(1999)** 3.
12. L. Q. Nguyen, C. Salim, H. Hinode, *Appl. Catal. A* 347 **(2008)** 94.
13. D. Niakolas, Ch. Andronikou, Ch. Papadopoulou, H. Matralis, *Catal. Today* 112 **(2006)** 184.
14. A. C. Gluhoi, S. D. Lin, B. E. Nieuwenhuys, *Catal. Today* 90 **(2004)** 175.
15. L. Ilieva, G. Pantaleo, I. Ivanov, A.M. Venezia, D. Andreeva, *Appl. Catal. B* 65 **(2006)** 101.
16. L. Ilieva, G. Pantaleo, J.W. Sobczak, I. Ivanov, A.M. Venezia, D. Andreeva, *Appl. Catal. B* 76 **(2007)** 107.
17. G. Busca, J. Lamotte, J.-C. Lavalley, V. Lorenzelli, *J. Am. Chem. Soc.* 109 **(1987)** 5197.
18. F. Solymosi, T. Bansagi, *J. Catal.* 156 **(1995)** 75.
19. F. Solymosi, T. Bansagi, T. Zakar, *Phys. Chem. Chem. Phys*. 5 **(2003)** 4724.
20. N. Bion, J. Saussey, M. Masaaki, M. Daturi, *J. Catal*. 217 **(2003)** 47.
21. M. Kancheva, A.S. Vakkasoglu, *J. Catal.* 223 **(2004)** 352.

22. F. C. Meunier, V. Zuzaniuk, J. P. Breen, M. Olsson, J. R. H. Ross, *Catal. Today* 59 **(2000)** 287.
23. N. Macleod, R. M. Lambert, Appl. Catal. B 35 (2002) 269-279.
24. A. Abu-Jari, A. Tsolakis, *Int. J. Hydrogen Energy* 32 **(2007)** 2073.
25. J. Y. Lee, J. Schwank, *J. Catal.* 102 **(1986)** 207.
26. E. Iojoiu, P. Gélin, H. Praliaud, M. Primet, *Appl. Catal. A* 263 **(2004)** 39.

Chapter 5: Summary and Conclusions

This chapter delivers the overall summary of the results and highlights the key findings.

Chapter 5: Summary and Conclusions

This chapter gives a brief summary of the results discussed in previous chapters and the overall conclusions derived from the work.

Chapter 1: Introduction

Chapter 1 provides a general introduction to the field of catalysis followed by a brief background about the emission and sources of NO_x, its effect on the environment and the various emission legislation norms introduced for its control. It also gives information about the various emission control strategies that are used for the reduction of NO_x. The different lean-NO_x control technologies used for the abatement of NO_x are also discussed in this chapter. The use of "three-way catalysts" in stoichiometric engines and their ineffectiveness in the reduction of NO_x in gasoline and diesel engines, which work under lean-burn condition is also discussed. Finally the scope and objective of the present thesis work with a clear emphasis on the selective catalytic reduction of NO_x with hydrocarbons as reductant is highlighted.

Chapter 2: Support Modification to Improve the Sulphur Tolerance of Ag/Al_2O_3 for SCR of NO_x with Propene under Lean-Burn Conditions

Silver (2 wt%) was supported on alumina by wet impregnation method. The alumina support was doped with 1 and 2 wt % SiO_2 or TiO_2 and tested for the SCR of NO under lean conditions. The catalysts containing optimum amount of SiO_2 or TiO_2 were tested for SO_2 tolerance in the presence/absence of water in the feed. The catalysts were characterized by different physico-chemical techniques before and after the reaction. In the presence of SO_2 in the feed the catalytic activity of Ag/Al_2O_3 decreased drastically whereas that of SiO_2 or TiO_2 doped catalysts remained unchanged. BET surface area and EDAX data of the catalysts showed sulfur accumulation on Ag/Al_2O_3 after the catalytic tests. No accumulation of sulfur was observed on the SiO_2 or TiO_2 doped catalysts. FTIR spectra of the spent catalysts were recorded in order to find out the cause of deactivation. On Ag/Al_2O_3 the bands at 1384 cm^{-1} and a broad hump at 1135 cm^{-1} were detected which were assigned to asymmetric and symmetric stretching vibration of O=S=O of sulphate species on

Al_2O_3. These bands were less intense in the case of SiO_2 and TiO_2 doped catalysts. In order to examine the cause of catalyst deactivation in presence of SO_2, and to study the mechanism of deactivation, *in situ* FTIR studies were carried out in the absence of water. The *in situ* FTIR study has shown that, in the case of Ag/Al_2O_3, the deactivation of the catalyst is due to the formation of sulphates of silver and aluminum which is minimized in presence of SiO_2 or TiO_2.The most significant observation of this study was the increase in the catalytic activity of SiO_2 doped sample when water was added to the feed. The increase in the activity was attributed to partial oxidation of propylene to CO, CO_2 and hydrogen by comparison with the literature reports. It was noticeable that water addition in the feed in these experiments was accompanied with the parallel formation of CO. However the exact reaction pathway for the formation of CO and hydrogen in presence of water under the experimental conditions of present study is not very clear.

Chapter 3: Effect of Magnesia Modification on the Low Temperature Catalytic Activity and Sulphur Tolerance of Ag/Al_2O_3 System

A series of $Ag\text{-}Mg/Al_2O_3$ catalysts were prepared with 2% Ag loading by impregnation method. The Mg content was varied from 5.5 wt% to 17 wt%. These samples were tested for the selective catalytic reduction of NO with propene under lean conditions in presence and absence of SO_2 under dry conditions and the catalytic activity was compared with that of Ag/Al_2O_3. The addition of magnesium showed beneficial effect on NO reduction activity. In the series containing varying Mg loadings (5.5 to 17 wt% Mg), catalyst containing 7% Mg showed maximum activity with 98% NO conversion at 350 ºC whereas catalyst containing 17% Mg loading showed minimum activity with 59% NO conversion under identical conditions. The increase in the catalytic activity upon addition of Mg was correlated with the decrease in the total acidity of the support. The presence of Mg helped in the low temperature activation of C_3H_6, which in turn resulted in higher NO conversion. The order of activity for the catalysts was $Ag7\%Mg/Al_2O_3 > Ag5.5Mg/Al_2O_3 > Ag11\%Mg/Al_2O_3 > Ag17\%Mg/Al_2O_3 > Ag/Al_2O_3$ at 623 K. The sample with best activity ($Ag7\%Mg/Al_2O_3$) was tested for sulfur tolerance under dry conditions as a function of time. In the presence of 20 ppm SO_2 in the feed, the NO conversion decreased marginally to 90% at 350 °C. The *in situ* FTIR study has shown that the deactivation

in the case of Ag/Al_2O_3 catalyst is due to the sulphation of active sites (Ag). In the presence of Mg, the sulphation of silver sites is prevented and therefore the activity maintained.

Chapter 4: NO Reduction under Diesel Exhaust Conditions over Au/Al_2O_3

Au/Al_2O_3 was prepared by deposition-precipitation method and NO reduction was carried out under diesel exhaust conditions and the catalytic activity was compared with Ag/Al_2O_3 sample. In this study the reaction feed was more complicated as compared to the previous chapters. The reaction feed consisted of 300 ppm NO, 300 ppm CO, 300 ppm C_3H_6, 100 ppm $C_{10}H_{22}$, 2000 ppm H_2 (when present), 10% O_2, 10% CO_2, 5% H_2O and balance He. The effect of presence of H_2 in the feed on the catalytic activity as a function of temperature was also studied. Addition of H_2 to the feed had a beneficial effect on the NO reduction activity. In the absence of H_2, Au/Al_2O_3 catalyst showed ~ 20% NO conversion and 100% selectivity for N_2 in the temperature range 300-350 °C. When H_2 was added to the reaction mixture the NO reduction increased to ~ 60% and the selectivity to N_2 remained unaffected. At higher temperatures, in the presence/absence of H_2 the NO conversion decreased due to competitive oxidative reactions of the reductants. Infrared experiments were carried out to study the effect of addition of decane and H_2 to the feed on the nature of adsorbed species formed on the catalyst surface. In the absence of $C_{10}H_{22}$ and H_2, only formate and nitrite species were detected on the catalyst surface. Upon addition of $C_{10}H_{22}$ alone, the global feature of the IR spectra remained the same except that adsorption of decane was evidenced at low temperature. Simultaneous addition of $C_{10}H_{22}$ and H_2 led to strong changes in the IR spectra. The adsorption of NO on Au nanoparticles and the formation of Au-CN and Al-CN species was enhanced in the presence of H_2. With increase in the temperature the –CN species were transformed into –NCO species, which is an important intermediate in the SCR of NO to N_2.

In conclusion the objective of the thesis which was to improve the low temperature catalytic activity, the hydrothermal stability and the sulphur tolerance of Ag/Al_2O_3 system in NO reduction was achieved by modification of the alumina support with SiO_2, TiO_2 and MgO. The mechanistic aspects of these improvements have been investigated by *in-situ* FTIR study to follow the reaction pathways.

Similarly Au/Al_2O_3, a less studied catalyst system for the SCR of NO_x has also been investigated in detail under lean condition. This catalyst system showed promising results in the presence of H_2. Detailed in-situ FTIR study of the adsorption and co-adsorption of the different gas components at different temperatures was done to find out the nature of the adsorbed species formed on this catalyst system.

Publications from the thesis

1. **Neelam Jagtap**, Shubhangi B. Umbarkar, Pierre Miquel, Pascal Granger, Mohan K. Dongare "*Support modification to improve the sulphur tolerance of Ag/Al2O3 for SCR of NOx with propene under lean-burn conditions"* Applied Catalysis B: Environmental 90 (2009) 416–425.
2. Pierre Miquel, Christophe Dujardin, Pascal Granger, **Neelam Jagtap**, Shubhangi B. Umbarkar, Mohan K. Dongare "*NO Reduction under Diesel Exhaust Conditions over Au/Al_2O_3 prepared by Deposition-Precipitation Method*" Communicated to Journal Molecular Catalysis A: Chemical (2009).
3. **Neelam Jagtap**, Rajni K Barangule, Shubhangi B. Umbarkar, Mohan K. Dongare "Effect of Magnesia Modification on the Low Temperature Catalytic Activity and Sulphur Tolerance of Ag/Al_2O_3 System" Applied Catalysis B: Environmental (to be submitted).

Other publications

1. Veda Ramaswamy, **N.B. Jagtap**, S. Vijayanand, D. S. Bhange, P. S. Awati *"Photocatalytic Decomposition of Methylene Blue on Nanocrystalline Titania Prepared by Different Methods"* Materials Research Bulletin 43 (2008) 1145-1152.
2. **Neelam Jagtap** and Veda Ramaswamy *"Oxidation of aniline over titania pillared montmorillonite clays"* Applied Clay Science 33 (2006) 89-98.
3. **Neelam Jagtap** and Veda Ramaswamy *"Encapsulation of Co Phthalocyanine in Alumina-Pillared Clays and their Characterization"* Clays and Clay Minerals, 54 (2006) 54-61.
4. **Neelam Jagtap**, Mahesh Bhagwat, Preeti Awati, Veda Ramaswamy *"Characterization of nanocrystalline anatase titania: an in situ HTXRD study"* Thermochimica Acta 427 (2005) 37-41.

Presentations at symposia

1. *Poster presentation in North American Catalysis Society, Philadelphia, USA, May 2005. Topic: "*Liquid phase oxidation of Benzyl alcohol to Benzaldehyde on Cobalt Phthalocyanine Encapsulated on Alumina Pillared Clays*".*
2. *Poster presentation in the 17th National Symposium on Catalysis held at Bhavnagar, Gujarat, India, January 2005. Topic: "*Oxidation of Aniline over Titania Pillared Montmorillonite Clay*".*
3. *Poster presentation in the 16th National Symposium on Catalysis and First Indo-German Conference on Catalysis, IICT, Hyderabad, India, February 2003. Topic: "*Encapsulation and Characterization of Cobalt Phthalocyanine on Alumina Pillared Clay*".*